

ETTEFAGH, KEIVAN A., Ph. D. Inhibiting Antimicrobial Resistance in *Staphylococcus aureus* Using Natural Products. (2013)  
Directed by Dr. Nadja Cech. 136 pp.

Since the treatment of infections with antibiotics, *Staphylococcus aureus* has developed resistance to antimicrobial agents. Methicillin-resistant *S aureus* (MRSA) contributes significantly to the healthcare burden of both hospital and community infections. Investigation into the resistance mechanism and their inhibition has the potential to increase the effectiveness in treating infection. It is hypothesized that the diversity of compounds and efficacy found in complex natural product extracts would lead to active leads that inhibit bacterial resistance. Using synergistic activity testing as a guide to a fractionation process, 3 flavonoids (8-desmethyl-sideroxylin, sideroxylin, and 6-desmethyl-sideroxlyn) were identified as synergists within a *Hydrastis canadensis* extract. These compounds were further characterized as efflux pump inhibitors using fluorescence in real-time and under confocal microscopy. In addition to disrupting efflux, the ability of *S. aureus* to cause disease was investigated. By detecting auto-inducing peptide I (AIP I), a direct product in the activation of this pathway, inhibition via natural products could be determined. Disruption in the intercellular communication via the Agr quorum sensing pathway in MRSA was observed in a *Penicillium* fungus and in *H. canadensis*. This quorum sensing inhibition (quorum quenching) limits virulence and toxin production making it easier for the host to manage infection.

INHIBITING ANTIMICROBIAL RESISTANCE IN *STAPHYLOCOCCUS AUREUS* USING  
NATURAL PRODUCTS

by

Keivan A. Ettefagh

A Dissertation Submitted to  
the Faculty of the Graduate School at  
The University of North Carolina at Greensboro  
in Partial Fulfillment  
of the Requirements for the Degree  
Doctor of Philosophy

Greensboro  
2013

Approved by

---

Committee Chair

To my daughter Sarah, my joy and my life

APPROVAL PAGE

This dissertation has been approved by the following committee of the Faculty of  
The Graduate School at the University of North Carolina at Greensboro

Committee Chair

\_\_\_\_\_

Committee Members

\_\_\_\_\_

\_\_\_\_\_

\_\_\_\_\_

\_\_\_\_\_  
Date of Acceptance by Committee

\_\_\_\_\_  
Date of Final Oral Examination

## TABLE OF CONTENTS

CHAPTER	Page
I. REVIEW OF LITERATURE OF <i>STAPHYLOCOCCUS AUREUS</i> AND ITS MECHANISMS OF RESISTANCE .....	1
1.1. Pathogenesis of <i>S. aureus</i> .....	2
1.2. History of MRSA as a nosocomial pathogen.....	3
1.3. <i>S. aureus</i> : A present-problem.....	5
1.4. Resistance mechanisms and epidemiology of <i>S. aureus</i> .....	7
1.5. The role of multidrug efflux pumps in resistance .....	10
1.6. Chromosomal multidrug efflux pumps.....	11
1.7. Assessing efflux activity.....	14
1.8. Quorum sensing in <i>S. aureus</i> .....	16
1.9. Natural products as a possible source to combat bacterial resistance.....	16
1.10. Research objective .....	18
II. SYNERGY-GUIDED FRACTIONATION TO IDENTIFY ANTIMICROBIAL POTENTIATORS FROM A COMPLEX <i>HYDRASTIS CANADENSIS</i> EXTRACT.....	20
2.1. Abstract .....	20
2.2. Introduction.....	22
2.3. Experimental .....	26
2.3.1. <i>S. aureus</i> preparation.....	26
2.3.2. Plant material, extract preparation and LC-MS .....	28
2.3.3. Checkerboard assay with <i>S. aureus</i> NCTC 8325-4 .....	30
2.4. Results and discussion .....	32
2.4.1. Characterization of <i>S. aureus</i> wild-type NCTC 8325-4 .....	32
2.4.2. Detection and quantification of berberine in extracts of <i>Hydrastis canadensis</i> .....	34
2.4.3. Synergy assessment of both root and aerial of commercially prepared extracts .....	38
2.4.4. Synergism within extracts and fractions of <i>Hydrastis canadensis</i> in synergy-guided fractionation approach. ....	41
2.5. Conclusion .....	47

III. MECHANISM OF ACTION OF SYNERGISTS FROM <i>HYDRASTIS CANADENSIS</i> .....	50
3.1. Abstract .....	50
3.2. Introduction.....	51
3.2.1. Multi-Drug-Resistant pumps in <i>S. aureus</i> .....	51
3.2.2. <i>Hydrastis canadensis</i> as a possible efflux pump inhibitor .....	53
3.2.3. <i>Hydrastis canadensis</i> an inhibitor of MDR pumps in the liver.....	53
3.2.4. Ethidium bromide based assay for efflux pump inhibition.....	56
3.3. Experimental .....	56
3.3.1. Confocal microscopy to measure efflux pump inhibition.....	56
3.3.2. Quantization of relative fluorescence.....	57
3.4. Results and discussion .....	58
3.4.1. NorA knockout (SA-K1758) and NorA complemented (SA-K2708) growth curve.....	58
3.4.2. Confocal microscopy with mutant strains of <i>Staphylococcus aureus</i> . .....	62
3.4.3. Quantification of efflux inhibition.....	76
3.5. Conclusion .....	82
IV. A NEW METHOD TO IDENTIFY NATURAL PRODUCT QUORUM QUENCHERS: MASS SPECTROMETRY-BASED MEASUREMENTS OF AUTOINDUCING PEPTIDE PRODUCTION .....	84
4.1. Abstract .....	84
4.2. Introduction.....	86
4.3. Methods .....	90
4.3.1. Detection and quantification of AIP I in MRSA (AH1263) in a time-course study.....	90
4.3.2. AIP inhibition assay in 96-well plate from fractionated natural products .....	91
4.3.3. Large scale extraction separation. ....	92
4.4. Results and discussion .....	94
4.4.1. Time-course production of AIP I by MRSA- AH1263.....	94
4.4.2. Method development AIP I inhibition assay in 96-well plate using a <i>Penicillium</i> fungus.....	100
4.4.3. AIP I Inhibition assay with <i>Hydrastis canadensis</i> after 96-well plate separation .....	106
4.4.4. Large scale bioactivity guided fractionation of <i>Hydrastis canadensis</i> .....	119

4.5. Conclusion .....	121
REFERENCES.....	125

## CHAPTER I

### REVIEW OF LITERATURE OF *STAPHYLOCOCCUS AUREUS* AND ITS MECHANISMS OF RESISTANCE

Staph infections are a significant source of morbidity, mortality, and health care costs in our society. In 2007, the Centers for Disease Control and Prevention estimated the direct cost of hospital-acquired infections in the United States was close to \$45 billion and expected to rise. Of these infections over 20% were from methicillin-resistant strains of *Staphylococcus aureus*.<sup>1</sup> The incidence of resistant strains of *S. aureus* has risen significantly in the past 50 years, paralleling the development of novel antibiotics.<sup>2</sup> Since the development of penicillin in the 1940s, strains of *S. aureus* have developed ever-evolving defense mechanisms to disable, inactivate, and expel nearly every commercially available antibacterial. Therefore, novel strategies, including combination of antibiotics and adjunctive therapies are needed to treat these increasingly resistant infections.



## 1.1 Pathogenesis of *S. aureus*

*S. aureus* is a Gram-positive bacterium that is naturally resistant to desiccation and does not produce spores like many other Gram-positive species. *S. aureus* can survive in a variety of conditions including human skin and favors a saline environment. In fact, approximately 30% of the general population's normal skin flora includes *S. aureus*.<sup>3</sup> *S. aureus* may be transmitted via direct contact with contaminated skin or via a contaminated surface.<sup>4</sup> Once inoculated beneath the human epidermis, *S. aureus* can become a formidable human pathogen.<sup>5</sup> Enzymes within the bacteria catalyze the conversion of soluble fibrinogen to insoluble fibrin, which causes the blood around the bacterium to clot in order to create a physical barrier to protect the bacterium from host defense.<sup>6</sup>

In addition to the production of physical barriers to block host defense mechanisms, *S. aureus* produces a series of virulence factors that facilitate toxin production and promote its pathogenesis. The extracellular toxins consist of alpha-, beta-, gamma- and delta-hemolysin, general enterotoxins, and toxic shock syndrome toxin 1. Toxic shock syndrome causes hypotension, shock, organ failure, and fever. The other toxins can cause necrotizing pneumonia in children through the disruption of eukaryotic cell membranes.<sup>7</sup>

## 1.2 History of MRSA as a nosocomial pathogen

Studies have shown the appearance of resistant *S. aureus* has come in four large distinct waves as a response to the increased implementation of certain antibiotics of the time. The first wave was penicillin resistant and came as a result of the overuse of the drug as a treatment of infections in hospitals in the 1940s. The second wave appeared in response to methicillin producing the MRSA strains in the early 1960s. The third wave was a new MRSA strain that spread worldwide in the 1970s significantly increasing the overall healthcare burden of *Staphylococcus* infections. The final wave began in the 1990s and consists of the transference of hospital-acquired *Staphylococcus* infections to the community causing significant outbreaks in specific areas. This community acquired MRSA strain (CA-MRSA) added a significant burden to the healthcare system due to its wide spread prevalence and resistance to typical antibiotic treatment. Although initially susceptible to most antibiotics, CA-MRSA has continued to increase its resistance and is expected to become more difficult to treat within the next decade.<sup>8 9 10</sup>

Hospital-acquired Gram-positive infections became a significant problem beginning in the 1940, and were first thought to be isolated incidents.<sup>11</sup> However, by the 1950s, the prevalence of staphylococcal infections had increased to the point that outbreaks were widely reported in the medical press.<sup>12</sup> Penicillin resistance was reported as early as 1955, thus encouraging the development of novel antibiotics.<sup>13</sup>

Methicillin, a synthetic penicillin derivative, was introduced in the 1950s to target penicillin resistant strains of bacteria; however, resistance to methicillin was recorded by the end of the decade.<sup>14</sup> Furthermore, these strains of methicillin-resistant *S. aureus* (MRSA) were also resistant to cephalosporins, cloxacillin, and dicloxacillin. Nevertheless, prevalence of these MRSA strains remained low, and the majority of *S. aureus* strains remained susceptible to antibiotics through the 1970's.<sup>15</sup> MRSA did not receive significant press and remained obscure until several well publicized outbreaks occurred in the 1980s and 1990s.<sup>8</sup>

Initial medical reports of MRSA infections suggested that MRSA was a weakly virulent pathogen and posed no greater threat to health than other hospital-acquired infections. MRSA was labeled as weakly pathogenic, and few resources were devoted to development of new treatment strategies given the low abundance of reported cases.<sup>16</sup> More recently, however, there have been numerous reports in the literature of bacterial infection from MRSA; all highlighting one theme: the inability of standard infection-prevention precautions to control outbreaks of MRSA despite its relatively low virulence.<sup>17 18 19</sup>

Beginning in the 1990s, there were widespread international hospital-based outbreaks of MRSA infections leading to increased attention from the scientific and medical communities. It became apparent that increasing resistance patterns among *S.*

*aureus* strains had resulted from repeated exposure of *S. aureus* to broad-spectrum antibiotics allowing for hyper-mutation and selection of the most resistant organism.<sup>20</sup> Thus, the term 'MRSA' was developed to refer to a heterogeneous group of bacteria with multiple different mechanisms for antimicrobial resistance including antibiotic expulsion and inactivation.<sup>21</sup> In addition, the growing diversity of MRSA strains facilitated the sharing of resistance producing genes through plasmid exchange which allowed for the evolution of even more virulent and sturdy strains of MRSA. Further studies of these MRSA strains including those performed by Casewell and Hill showed the emergent strains to be highly virulent. Casewell and Hill showed that under the right conditions MRSA could achieve full pathogenic potential, leading to severe systemic infection as opposed to colonization as was first thought.<sup>22</sup>

### **1.3 *S. aureus*: A present-problem**

Presently, *S. aureus* is one of the leading causes of hospital acquired infections, with MRSA infection specifically growing each year. In fact, *S. aureus* is the primary source of hospital-acquired respiratory tract infections and infections in sites in which surgery was performed. It is also the second leading cause for nosocomial pneumonia and cardiovascular infections.<sup>23</sup> Due to the increasing resistance to treatment, MRSA infections have become extremely difficult to treat.

Across the United States, hospital-acquired MRSA has become a significant problem, especially in long-term care facilities and intensive care units.<sup>24 25 26</sup> In the year 2000, 43.2% (125,969) of all *S. aureus* infections were determined to be methicillin-resistant.<sup>27</sup> From 1999-2005 the number of infections caused by *S. aureus* increased 62% from 294,570 to 477,927.<sup>28</sup> In the same study, the number of MRSA-related hospitalizations more than doubled (127,036 – 278,203), and the incidence of MRSA surgical site infections and MRSA pneumonia more than tripled.<sup>29</sup> Since 2005 the MRSA infections have continued to rise with total infections increasing to 463,017 in 2009 - almost doubling within 4 years.<sup>30</sup> Additionally, CA-MRSA has become increasingly prevalent amongst groups living in close quarters such as day care facilities, military barracks, and college campuses.<sup>25</sup> From 2005 to 2009 the number of incidents of CA-MRSA infections have more than doubled 70,432 to 152,000. Unlike hospital-acquired MRSA, CA-MRSA has caused more episodic localized outbreaks in various communities. These outbreaks have been more difficult to eradicate due to the colonization of larger populations, which has significantly increased the cost of treating CA-MRSA.<sup>31</sup>

The direct cost of *S. aureus* infections acquired in the hospital has been estimated to be > \$6 billion.<sup>32</sup> Drug-resistant infections pose an even greater cost when compared to general susceptible infections. These resistant infections prolong illness, increase mortality, and increase direct health care cost by 30-100%.<sup>33</sup> MRSA infections, when compared to methicillin sensitive *S. aureus* (MSSA), can increase the direct cost of

treatment of a single infection \$3,000 - \$35,000. Without taking into account the indirect costs of infection, MRSA alone cost the healthcare system an estimated \$830 million - \$9.7 billion in 2005.<sup>34</sup>

#### **1.4 Resistance mechanisms and epidemiology of *S. aureus***

Resistance in *S. aureus* results from many different factors. Mutations in common resistance genes can have a profound impact on antimicrobial uptake, degradation, augmentation, and export. Also, the exchange of genetic information between microorganisms can spread the expression of resistant genes throughout a population of bacteria. Furthermore, certain environmental conditions, especially those found in hospital settings, can facilitate the spread of resistant organisms. Exposure to various antibiotics preferentially selects for resistant bacteria which are able to survive and reproduce. Thus, treatment with broad spectrum antibiotics can indirectly facilitate the spread of resistant clones across a large human population.<sup>35</sup>

As *S. aureus* replicates, uncorrected base substitutions of the copied DNA occur randomly at a frequency of  $10^{-9}$  to  $10^{-10}$  per gene, leading to a possible expression or deletion of individual genes.<sup>36</sup> This allows the bacteria to express new proteins which may exhibit antibacterial resistance. Expression of these proteins can result in breakdown or augmentation of antibiotics, up-regulation of efflux systems, or down-regulation of uptake pathways.<sup>37</sup>

Scientists initially posited that bacteria would develop resistance solely from mutation events at the chromosomal level, and thus mutations would be a rare event.<sup>38</sup> However, it was determined that some mutations in preexisting resistance genes enhanced resistance. These genes, when activated are not specific to a certain antibiotic, but provide a generic defense to toxic compounds by turning on a series of defense-related proteins which expands the range of resistance. As a result, a minor mutation could lead to an up-regulation of a protein responsible for the activation of a series of preexisting defense mechanisms and render a bacterium resistant to multiple antibiotics from a single gene mutation. For example,  $\beta$ -lactamases that initially only provided resistance to penicillin and ampicillin, and through a mutation, became capable of hydrolyzing not only basic penicillins but also extended-spectrum cephalosporins and monobactams.<sup>39</sup> This type of mutation has been shown to increase the resistance of bacteria in a single hospital during a period of 2 years by 50% as compared to theoretical resistance calculated via general mutation statistics.<sup>40</sup>

In the 1980s, scientists discovered *S. aureus* had the ability to exchange genetic information across different species of bacteria.<sup>41</sup> Like other Gram-positive bacteria, transduction and transformation are the primary forms of genetic exchange in *S. aureus*.<sup>42</sup> For example, *S. aureus* and *Staphylococcus epidermis* have been shown to share aminoglycoside resistance across species.<sup>43</sup> Although resistance genes were determined to be transferred amongst different species of bacteria, expression is not

always maintained, and the case in which resistance is not expressed is not fully understood.<sup>44</sup> However, the bacteria can acquire resistance genes from other organisms, including the natural bacterial flora of the gut, and the potential of cross-species transfer of resistance mechanisms could lead to a more rapid development of resistance in *S. aureus*.

One strategy to combat the ever increasing resistance of the staphylococci bacteria is the development of new drugs. However, resistance mechanisms often appear soon after widespread administration of a new antibiotic. For example, when vancomycin was developed, it was used frequently to treat MRSA infections. The heavy use of this antibiotic created a selective pressure, environmental conditions promoting resistance to develop in a bacterium, which encouraged the development and spread of resistance to the drug in the 1990s.<sup>45</sup> Vancomycin was used in hospitals, long-term care facilities, agricultural sites, and day-cares, which all increased the selective pressure. Whether resistance was acquired due to a spontaneous mutation or the exchange of genetic information across species is unknown; however, the level of resistance has been shown to be directly correlated to the intensity of use of an antibiotic.<sup>46</sup> Normally, vancomycin has a minimum inhibitory concentration (MIC) against *S. aureus* of 1-4 µg/mL; however, a subpopulation of *S. aureus* has become resistant to vancomycin up to concentrations of 8 µg/mL.<sup>47</sup> Thus, new antimicrobial strategies, such as drug



combination or directly attacking resistance mechanisms, are needed in treatment of resistant *S. aureus* infections other than increasing antibiotic use.

### **1.5 The role of multidrug efflux pumps in resistance**

A significant way *S. aureus* becomes resistant to antimicrobial agents is through the expression of multi-resistant phenotypes, which impart resistance to multiple antibiotic classes. One such multi-resistant phenotype is the expression of multi-drug resistant (MDR) efflux pumps, transmembrane proteins that actively transport metabolites outside the cell. Efflux pumps have the potential to remove a variety of antimicrobial agents.<sup>48</sup> Although efflux-mediated resistances have been overlooked in the past, recently there has been an increased interest due to their ability to provide broad-spectrum resistance in *S. aureus*. It is hypothesized that inhibition of MDR efflux pumps in *S. aureus*, would lead to increased efficacy of antimicrobial compounds at lower concentrations. By limiting the diversity of resistant mechanisms through the inhibition of efflux pumps in *S. aureus*, more treatment options for infections would be available.<sup>49</sup>

Efflux pumps in bacteria play a physiological role in removing toxic metabolites produced by the cells, exporting of virulence factors during pathogenesis, and responding to cell stress. The expulsion of antimicrobial agents, therefore, is said to be a secondary mode of action of these pumps. Efflux pumps can exhibit specificity towards a particular antimicrobial agent or class of antimicrobial agents; however, they

can also have a broad range of antimicrobial compounds that they remove from the cell. Efflux pumps are able to act on a wide range of substrates which has enabled the bacteria to apply the efflux pump mechanism to a wide range of antimicrobial compounds. Furthermore, stress to the bacteria has been shown to increase the expression of these pumps allowing for increased resistance.<sup>50</sup>

### **1.6 Chromosomal multidrug efflux pumps**

There are five families of multidrug resistance (MDR) efflux pumps that are separated based on the energy requirement needed to actively efflux outside the bacterial cell. They are the major facilitator super-family (MFS); the small multidrug resistance family (SMR); the multidrug and toxic compound extrusion family (MATE); the resistance-nodulation-cell division super-family (RND); and the adenosine-triphosphate (ATP)-binding cassette (ABC) super-family. The MATE family uses a proton or sodium membrane gradient to drive the export of its substrates, whereas the MFS, SMR, RND use the proton motive force to drive efflux. As the name suggests, the ABC super-family uses ATP as the energy needed to actively transport its substrates outside the cell.<sup>51</sup>

The most studied chromosomally-encoded MDR pump in *S. aureus* is the NorA efflux pump, which is part of the MFS class of pumps. The NorA efflux pump accounts for the majority of broad spectrum resistance in *S. aureus* through its overexpression

and its ability to efflux multiple antimicrobial compounds. In fact the NorA efflux pump is overexpressed in almost all resistant strains of *S. aureus* isolated from blood infections.<sup>52</sup>

The *norA* gene consists of three alleles that have up to a 10% difference in sequence.<sup>53</sup> The *norA* gene is a 388 amino acid transmembrane protein containing 12 segments.<sup>54</sup> The NorA pump effluxes a variety of dissimilar compounds such as fluoroquinolones, dyes, and quaternary ammonium compounds.<sup>55</sup> The expression of the *norA* gene can be induced through activation of regulatory proteins or mutations in the *norA* promoter region.<sup>56</sup>

Like all of the efflux pumps belonging to the MFS, NorA uses a proton motive force via an H<sup>+</sup> anti-port mechanism to transport antimicrobial compounds outside the cell. By taking in 2 protons, the pump is able to export an intercellular substrate outside the cell against a concentration gradient. This mode of action was determined through using a proton motive force disrupter, carbonyl *m*-chlorophenylhydrazine (CCCP). CCCP disrupts the proton motive force by dissipating the proton gradient which has been shown to inhibit the efflux of norfoxacin and ethidium bromide via the NorA efflux pump.<sup>57</sup>

In *S. aureus* the NorB and the NorC efflux pump systems are structurally similar to the NorA system. NorB is a proton dependent pump of the MFS composed of 463

amino acids and 12 transmembrane segments with a 30% complementary sequence to that of NorA.<sup>58</sup> The antimicrobial substrates for NorB include all of the NorA substrates plus tetracycline and hydrophobic fluoroquinolones such as moxifloxacin and sparfloxacin.<sup>59</sup> The NorC pump is a 462 amino acid protein consisting of 12 transmembrane portions with a 61% complementation to NorB.<sup>60</sup> Overexpression of the *norC* gene can be induced when *S. aureus* is exposed to hypoxemic or acidic conditions such as those found in shock.<sup>61</sup> Substrates similar to the NorB pump as well as garenoxacin and rhodamine have been shown to be substrates of the NorC efflux pump.<sup>62</sup>

Recently, a new efflux pump was discovered in *S. aureus* that resulted from a *norA* mutation.<sup>63</sup> This new efflux pump, known as MepA, is the first MDR pump classified as part of the MATE family to be found in *S. aureus*. MepA consists of 451 amino acids with 12 transmembrane segments and its antimicrobial substrates include quaternary ammonium compounds, ethidium bromide, and some glycyclines.<sup>64</sup>

Another chromosomal MDR found in *S. aureus* is MdeA. This efflux pump consists of 479 amino acids with 14 transmembrane segments and is classified into the MFS. Activation of the MdeA gene leads to resistance against dequalinium, benzalkonium, ethidium bromide, virginiamycin, novobiocin, and fusidic acid with

fluroquinones being weak substrates. It has been shown expression of MdeA can be induced by a mutation on the MdeA promoter region.<sup>65</sup>

The SepA pump is another chromosomal MDR classified into the SMR family found in *S. aureus*. Some argue it belongs in a new type of family based on its dissimilarity in protein structure. It consists of 157 amino acids with 4 transmembrane segments which is characteristic of the SMR family; however, residues important for substrate specificity are located in completely different parts of the protein compared to the rest of this class. The SepA pump has not been studied in detail, but it has been shown to add low level resistance to antiseptic compounds in *S. aureus*.<sup>66</sup>

This dissertation will focus on the inhibition of the NorA efflux pump specifically. Although there have been many different types of efflux pumps identified in *S. aureus*, studies have shown inhibition of the NorA to significantly enhance the antimicrobial effects of many different compounds.<sup>105</sup> Providing the *S. aureus* with a broad range of resistance, overexpression of this pump has significantly lowered the efficacy of currently used drugs. Through its increased prevalence in clinical isolates of MRSA, inhibition research on this pump is relevant and needed.

### **1.7 Assessing efflux activity**

Measuring the decrease in the MIC of current antibiotics with the addition of potential efflux pump inhibitors (EPis) allows determination of whether certain

compounds disrupt the expulsion of antimicrobial agents outside the cell.<sup>67</sup> MIC is the concentration of an antimicrobial agent needed to inhibit the growth of the bacteria with lower values indicating more potent antimicrobial agents. The presence of known EPIs have been shown to lower the MIC values of many antimicrobial agents; however, this assay fails to describe whether an EPI inhibits a specific efflux pump or has a more general antimicrobial effect. One of the limitations of this approach in assessing inhibition of efflux in *S. aureus* is the diversity of MDR pumps. A particular inhibitor can have varying degrees of inhibition which complicates the mechanism of action at the cellular level.<sup>68</sup>

A different approach for identifying possible EPIs has been to use ethidium bromide, a fluorescent dye, which is a substrate for most MDR efflux pumps in *S. aureus*. By measuring extracellular concentrations of the dye both with and without the potential EPI one can determine the net effect of the candidate compound.<sup>69</sup> Also, ethidium bromide has been used in the cartwheel method, which measures the amount of ethidium bromide inside a cell after overnight incubation.<sup>70</sup> Ethidium bromide has also been reported to be used to measure efflux activity directly using real-time fluorometry, which will be its primary use in this dissertation.<sup>71</sup>

### **1.8 Quorum sensing in *S. aureus***

Quorum sensing, which allows adjacent organisms to communicate via intercellular signaling, is another potential target for novel compounds that disable the harmful effects of a bacterial infection. This form of communication across bacteria cells has been shown to be important in virulence of *S. aureus*. Virulence for a bacterial species includes the route of entry into the host, the number of bacteria present, the general effect on the host's defense mechanism, and the types of virulence factors produced. Virulence factors are typically proteins synthesized by enzymes triggering a cascade effect promoting toxin production and pathogenesis. These virulence factors are an intrinsic property to the quorum sensing pathway in *S. aureus*. By specifically inhibiting the production of virulence factors it is possible to disrupt the intercellular communication and limit the ability of the bacteria to cause disease. By decreasing virulence antimicrobial treatments become more effective at eradicating an infection, and thus prevent a population of bacteria to develop resistance.

### **1.9 Natural products as a possible source to combat bacterial resistance**

From poultices to teas to salves, a variety of natural products from plants, animals, and fungi have been used to treat ailments since before the development of modern medicine. In the past significant research went into the discovery of constituents within natural products that lead to a desired biological activity. Between

1981 and 2002, almost half (49%) of the 877 new small molecule drugs developed in the United States were either natural products, semi-synthetic natural product analogs, or synthetic compounds based on a natural-product structure.<sup>72</sup> Natural herbal remedies have been a major source bioactive compounds because they are considered to have stood the test of time, to have little toxicity, and to be relatively easily obtained at low costs.<sup>73</sup>

Since the 1990s pharmaceutical research into natural products has been on the decline. This decline can be attributed to both specific technologic advances in drug research and overall change of the economic climate of drug development. The advent of high-throughput screening assays has encouraged testing of synthetic known compounds as opposed to natural product extracts. Additionally, increases in molecular targets discovered from advances in molecular biology and genomics have shortened drug discovery timelines. Also, major drug companies have largely shifted away from antimicrobial compounds to focus on more lucrative chronic illnesses such as diabetes, heart disease, and cancer.<sup>74</sup> Nevertheless, recent trends into natural remedies coupled with the underwhelming production of new drug therapies from commercial pharmaceutical companies has sparked a renewed interest in the chemical diversity that can be found in natural products.<sup>75</sup>



It is important to note the decreased emphasis on natural product research in the past twenty years has not been due to a lack of potential drug targets. Research into the diversity of compounds found in antimicrobial natural product extracts has been revived as a result of the increased burden that MRSA and other resistant bacteria are having on the healthcare system. Specifically, extracts in which antimicrobial compounds have been isolated are being reevaluated in pursuit of possible synergistic effects of undiscovered constituents. The diversity of compounds in these extracts has the potential to be bioactive against new targets of resistance.<sup>76</sup>

#### **1.10 Research objective**

*S. aureus* resistance has dramatically increased due to rapid evolution in response to increased in antibiotic use and hyper-mutation. As resistance and virulence increases, the cost and burden on society increases as well. New strategies to combat this growing problem are needed to help relieve this global healthcare burden. Investigation of the biodiversity of secondary metabolites from natural products represents an exciting possible solution. By analyzing antimicrobial properties of historically used natural products and identifying possible synergists, it may be possible to find a new approach to address growing resistance. In this dissertation, different strategies are discussed and evaluated in vitro against various strains of *S. aureus* to demonstrate possible solutions to limit virulence and inhibit resistance mechanisms.

The overall goal is to illustrate possible strategies to combat antimicrobial resistant *S. aureus* through the use of secondary metabolites found in natural products.

## CHAPTER II

### SYNERGY-GUIDED FRACTIONATION TO IDENTIFY ANTIMICROBIAL POTENTIATORS FROM A COMPLEX *HYDRASTIS CANADENSIS* EXTRACT

#### 2.1 Abstract

**Rationale:** The objective of this study was to identify and characterize synergy within various *Hydrastis canadensis* root and leaf extracts by adapting a checkerboard assay traditionally used for single drug combinations. Using this new assay, we sought to determine whether commercial preparations of the leaf or the root portion of the plant had a greater synergistic effect. Also, we implemented synergy testing to guide the isolation of synergists from a large chloroform extract.

**Methods:** *S. aureus* NCTC 8325-4<sup>77</sup> was used and characterized by a growth curve.

*Hydrastis canadensis* plant samples were collected at Bearwallow Ginseng in Hendersonville, North Carolina. Pooled extracts were prepared using 100 g of root/rhizome material and 100 g of aerial portions in 50% ethanol extract. Berberine in the pooled ethanol extracts and a crude chloroform extract were quantified.

Combinations of the pooled ethanol extracts and the chloroform aerial extract were standardized based on the concentration of berberine and tested using a checkerboard

assay. Fractions from the crude chloroform extract were tested against the original chloroform extract to determine which extracts exhibited synergy. Subsequent fractions of the aerial chloroform were tested for synergistic activity and the most active fraction was fractionated into sub fractions and tested for synergistic activity.

**Results:** The pooled ethanol extract of the aerial portion of the plant exhibited synergy with a FIC Index value of 0.375 and crude chloroform extract, Fraction 3, and Sub Fraction 2 exhibited a synergistic effect when tested via the checkerboard assay with FIC Index values of 0.19, 0.13, and 0.03 respectively. The pooled ethanol extract of the root/rhizome and berberine alone exhibited an additive effect in the checkerboard assay with FIC Index values of 0.75 and 1.0 respectively. Fraction 3 and Sub Fraction 2 were characterized as potentiators by having no antimicrobial effect alone at their maximal concentrations that could be solubilized.

**Conclusions:** By standardizing a complex *Hydrastis canadensis* extract to a single known compound within the extract, synergy testing can be utilized. Through this methodology the root portion of the *Hydrastis canadensis* had a lower synergistic effect than the aerial portion of the plant which contained potentiators that could be identified via synergy-guided fractionation.

## 2.2 Introduction

Antimicrobial synergy is defined as a greater antimicrobial outcome observed for two drugs used in combination compared to the expected antimicrobial effect when each drug's individual efficacy is summed at the same concentration.<sup>78</sup> Thus, if Drug A and Drug B were tested for antimicrobial synergy and had a theoretical antimicrobial effect of 1 each, and if the overall effect of Drug A plus Drug B was greater than 2, then Drug A and Drug B would be synergist for the reason that  $1+1 > 2$ . Moreover, if Drug A theoretically had no individual antimicrobial effect alone, yet when combined with Drug B had a net efficacy greater than Drug B's individual efficacy, then Drug A would be characterized as a potentiator, a specific type of synergist which enhances the overall effect, but has no effect of its own.<sup>79</sup> In this case  $0 + 1 > 1$ . In determining synergistic effects in antimicrobial studies, efficacy can be measured through the minimum inhibitory concentrations (MICs) of the individual drugs and the combination of those drugs in a checkerboard assay.

Synergism between two compounds can be identified qualitatively and quantitatively assessed by varying the concentrations of the two compounds of interest and measuring their combined efficacy. Traditionally in an antimicrobial study, a checkerboard assay is used in which varying concentrations of Drug A and Drug B are used and percent activity assessed. Efficacy can then be plotted in an graph detailing the interaction between drugs called an isobologram, and based on the curvature; the effect of the combination of the drugs tested can be determined to be synergistic,

additive, or antagonistic as shown in Figure 1. Furthermore, by assessing the fractional inhibitory concentrations of each component, a quantitative value can be assigned to the individual efficacies of each drug. By summing the fractional inhibitory concentrations the fractional inhibitory concentration index (FIC index) can be calculated as shown in the below equation:

$$(Equation 1) \quad FIC \text{ Index} = FIC_A + FIC_B = \frac{[A]}{MIC_A} + \frac{[B]}{MIC_B}$$

If the calculated FIC Index is less than 0.5, then the interaction between drug A and B is characterized as a synergistic effect. If the value is between 0.5 and 1.0, the interaction is characterized as additive effect, and any value greater than 1.0 the interaction is characterized as antagonistic effect.<sup>80</sup>

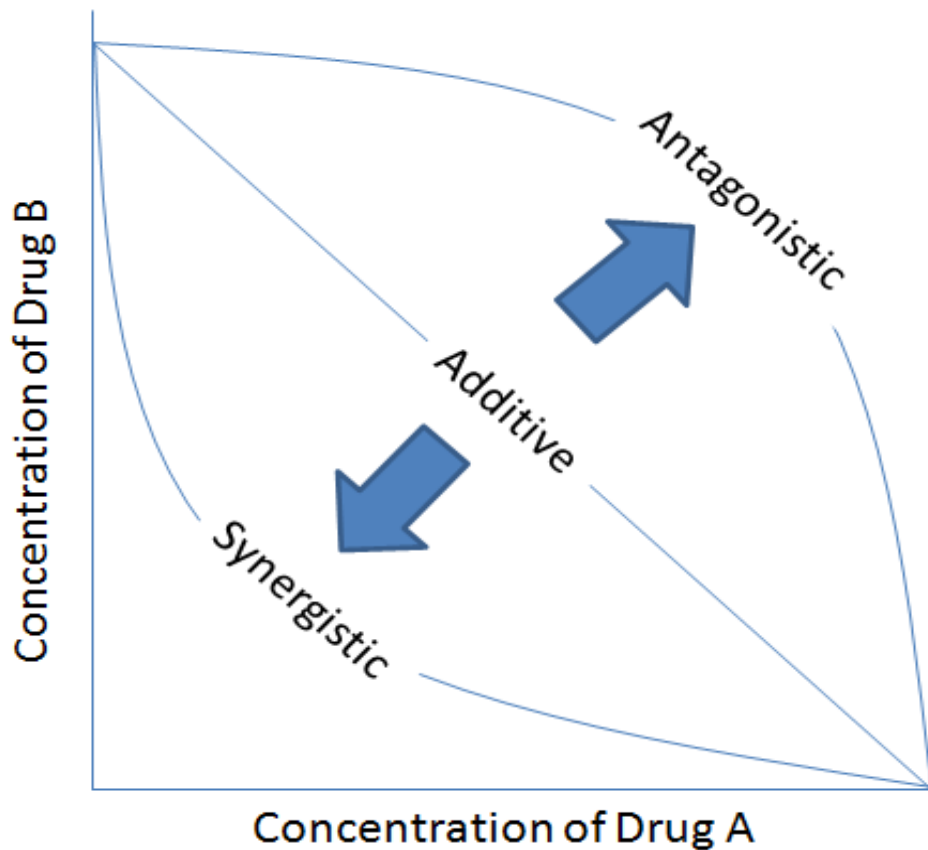


**Figure 1. Isobologram of two drugs to evaluate possible combination effects.**

In the area of alternative medicine, efficacy of complex extracts has been argued to be the result of the combined activity of multiple components working in synergy. It is hypothesized implementing a checkerboard assay on chloroform and an ethanol extract of *Hydrastis canadensis* can determine if synergistic activity exists between components of plant. Tinctures and salves of *Hydrastis canadensis*, commonly referred to as Goldenseal, have historically been used by Iroquois to treat ailments ranging from eyesores and skin infections, to dysentery and upset stomach.<sup>81 82 83</sup> More recently,

extracts from *H. canadensis* have been shown to have an antimicrobial effect against *S. aureus*. This antimicrobial effect has largely been attributed to the alkaloid found in the plant called berberine shown in Figure 2, which has been shown to intercalate with the DNA of the bacteria preventing basic cell function.<sup>84</sup> This compound has been shown to be effective at inhibiting the growth of Gram-positive and Gram-negative bacteria<sup>85</sup> Today, *Hydrastis canadensis* is used as a botanical medicine to combat inflammation and infection. The plant extracts are popular in the international market<sup>86 87</sup> and is ranked twelfth among the top selling botanical dietary supplements in the US<sup>88</sup>. Typically the roots are more commonly used medicinally because of their higher alkaloid content<sup>89</sup>, although *H. canadensis* leaves have also been used for medicinal purposes. Its antimicrobial properties have led to increased cultivation, which destroys the plant leading to a decrease on the *H. canadensis* population.

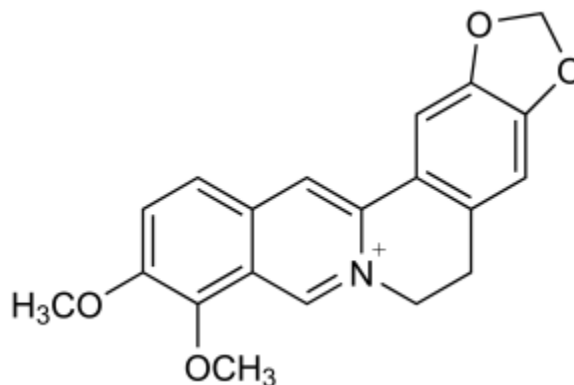


**Figure 2. Structure of the alkaloid berberine found in *Hydrastis canadensis*.**



The goals of the research described in this chapter are to apply the checkerboard assay to a complex extracts of *Hydrastis canadensis* to characterize the interaction of the complex extracts and berberine as synergistic, additive, or antagonistic, to further test different extracted portions of the plant (leaf and root), and to test fractions of the chloroform extract against the crude to guide the isolation process to indentify individual synergists. By standardizing the berberine within the extract, the extract can be treated as an individual component (Drug A) in the checkerboard assay, and it is then possible to observe the interactions between fractions of the extract and the extract itself to determine whether synergy exists between components of the plant.

## **2.3 Experimental**

### **2.3.1 *S. aureus* preparation**

A single colony of wild-type *S. aureus* (NCTC 8325-4) was incubated in 5.00 mL of Mueller-Hinton broth for a 24-hr period. After incubation, it was added to 50.0 mL Mueller-Hinton broth in a 150 mL Erlenmeyer flask to make a stock solution. The optical density at 600 nm (OD<sub>600</sub>) of the stock solution was measured using a Spectrometer 20 and was designated as the OD<sub>600</sub> at time T = 0. To measure colony forming units (CFU) of this original bacterial solution, a 100 µL aliquot of the original stock solution was diluted with 900 µL PBS in an Eppendorf tube, which resulted in a  $1.00 \times 10^{-1}$  dilution (A). After preparing solution A, the original stock solution was incubated at 37 °C while

shaking at 200 rpm. Then from solution **A**, a series of 10-fold dilutions were performed, giving  $1.0 \times 10^{-2}$  (**B**),  $1.0 \times 10^{-3}$  (**C**),  $1.0 \times 10^{-4}$  (**D**),  $1.0 \times 10^{-5}$  (**E**), and  $1.0 \times 10^{-6}$  (**F**) dilutions of the stock solution. Each dilution of the bacteria was grown in agar plate. A 100  $\mu\text{L}$  solution was spread evenly across an agar plate while spinning the Petri dish with a small rotating circular platform. The growth plate was prepared in duplicate for each dilution and incubated for 24 hr at  $37^{\circ}\text{C}$ . The colony forming units (CFU) in each plate were counted after 24 hrs. The average CFU was calculated from the duplicate plates prepared for each dilution at each time interval. All plates with 30 to 300 CFUs were considered measureable, and the CFU per mL for each plate was calculated by taking account the dilution factor via the following formula:

$$\text{CFU/mL} = (\text{CFU}/100 \mu\text{L}) \times \text{dilution factor} \times 1000,$$

where the average CFU (between 30 to 300 colonies) for every 100  $\mu\text{L}$  of the solution spread unto the agar plate is the CFU/100  $\mu\text{L}$ ; the dilution factor is the total number of unit volume used to make the final solution volume, i.e. Solution A is 10 times more dilute than the original stock solution while solution B is 10 times more dilute than solution A therefore the solution B should be multiplied by 100; and 1000 is the conversion factor from  $\mu\text{L}$  to mL. Multiple stock bacterial solutions were made and placed in cryopreservation to run checkerboard assays. Cryopreservation was accomplished by incubating a single colony of bacteria in 2.00 mL of Mueller-Hinton broth for a 24-hr period. After incubation, it was added to 20.0 mL Mueller-Hinton broth

in a 150 mL Erlenmeyer flask to make a stock solution and was shaken for 2 hr at 200 rpm at 37 °C. After 2 hrs, the bacterial solution is dispensed into sterile cryovials with glycerol (1:1 ratio).

To monitor the bacterial growth based on optical density, the original stock solution of bacteria was incubated at 37 °C while shaking at 200 rpm. The OD600 was measured at a 30-minute time interval for a 9-hr period. In addition, the growth plates were prepared concomitant with each OD600 measurement at every time point.

Based on the growth curve, log phase begins at 2.5 hrs of shaking at 200 rpm at 37 °C. At the log phase, the bacteria grow exponentially at which point a  $5.0 \times 10^5$  CFU/mL stock is made and added to checkerboard assay with the test samples combined with berberine. The growth of the bacteria in the plate after 18-hr incubation period is assessed using OD600 measurements.

### **2.3.2 Plant material, extract preparation and LC-MS**

*Hydrastis canadensis* L. (Ranunculaceae) was cultivated in its natural habitat (a hardwood forest in Hendersonville, NC, N 35° 24,277', W 082° 20.993', 702.4m elevation) and harvested in September of 2008. A voucher specimen was deposited at the Herbarium of the University of North Carolina at Chapel Hill (NCU583414) and identified by Dr. Alan S. Weakly.

The pooled ethanol extracts (50% ethanol: 50% nanopure water) were prepared using 100 g of powdered aerial portion (leaves and stems) or roots (including the

rhizomes) per 500 mL of solvent (1:5w:v) according to the standard procedures in the US dietary supplements industry.<sup>90</sup> Plant material was blended with solvent, macerated for 24 hrs and filtered under vacuum. Extracts were stored in amber bottles at room temperature. Berberine concentration was determined using liquid chromatography-mass spectrometry (LC-MS) using a mass spectrometer with electrospray source (LCQ Advantage Thermo) coupled to reversed phase HPLC (HP1100; Agilent). A C-18 column (50mm x 2.1 mm, 3  $\mu$ m particle size, 110 Å pore size, Prevail packing; Grace and 0.5  $\mu$ m precolumn filter, MacMod Analytical) was utilized to characterize the pooled ethanol extracts, using 0.2mL/min flow rate and 10  $\mu$ L injection volume. The following gradient was used to analyze the extracts, where A = 1% acetic acid in nanopure water and B = HPLC grade acetonitrile: 100-68% A from 0 to 5 min; 68% A from 5-20 min 0%A from 20 to 25 min, 100% B from 25 to 40 min. The detection was conducted in the positive ion mode with a scan range of 50-2000 *m/z*. Capillary temperature was 275 °C, sheath gas pressure was 20 (arbitrary units), and spray, capillary, and tube lense voltages were 4.5 kV, 3 V, and 60 V respectively.

A standard of berberine was prepared at a stock concentration of 1 mg/mL in methanol. Calibration curves over a concentration range of 0.005 to 100  $\mu$ M were created using the peak area of the selected berberine ion versus concentration. The ethanol extracts were diluted as necessary in 50:50 ethanol:water to yield berberine concentrations within the linear range of the calibration curve. Berberine was

identified in the extracts by fragmentation patterns and retention matching with the standards.

Pre-weighed air-dried leaves of goldenseal were homogenized using a commercial coffee grinder (Kitchen Aid). The ground leaves were percolated with methanol for at least 24 hr., at which time the solvent was removed and replaced with an equivalent volume of methanol. The residue-free methanol extract was collected and concentrated in vacuo using a rotary evaporator (Heidolph Laborota 4000 Efficient). The methanol extract was re-suspended in 9:1 methanol:water and then partitioned with hexane in a separatory funnel. The aqueous methanol layer was separated from the non-polar hexane layer and subsequently partitioned with 4:1 ratio of chloroform to methanol in water in a separatory funnel. The hexane layer was collected, dried in vacuo and was set aside for testing. The chloroform-methanol layer was washed with 1% saline solution to remove water-soluble tannins.

### **2.3.3 Checkerboard assay with *S. aureus* NCTC 8325-4**

Extracts were dried under nitrogen and redissolved in Müller Hinton broth containing 10% DMSO and filtered through a 0.45 µm PVDF filter. Broth microdilution MIC assays were performed according to Clinical and Laboratory Standards Institute (CLSI) guidelines.<sup>91</sup> All extracts were standardized to berberine and tested in combination with berberine with a checkerboard assay<sup>92</sup> over various concentrations ranging from 5 to 300 µg/mL standardized to the mass of berberine within the extract or

fraction. The fractionated chloroform extract (fraction 4 and sub-fraction 2) did not contain berberine and was tested from a range of its highest soluble concentration of 50  $\mu\text{g}/\text{mL}$  to its lowest concentration of 5  $\mu\text{g}/\text{mL}$ . A purified standard of berberine served as the positive control. The assay was performed in triplicate in 96-well plates with  $1 \times 10^5$  CFU/mL *S. aureus*, 2% final DMSO content, and a final well volume of 250  $\mu\text{L}$ . The negative (vehicle control consisted of 2% DMSO in Müller Hinton broth. MIC values were determined at the point at which there was no significant difference between the OD600 of the vehicle control and the treatment. A duplicate 96-well plate was made with the varying treatments (berberine, extract, or fraction) without the addition of bacteria and the OD600 was subtracted from the relevant assay wells to minimize interference. FIC values were calculated according to equation 1, where B is the compounds, extracts, or fractions tested in combination with A which is berberine.  $\text{MIC}_A$  is defined as the minimum inhibitory concentration of A alone, and  $\text{MIC}_B$  is defined as the minimum inhibitory concentration of B alone, and [B] is defined as the MIC of B in the presence of A, and [A] is defined as the MIC of A in the presence of B.

Fractions 4 and 5 separated from the chloroform aerial extract were tested in combination with the chloroform aerial extract to test for synergy within the plant fractions. MIC and FIC values were determined by constructing isobolograms from the checkerboard assay. The negative and positive controls were the same as the previously stated checkerboard assay methods.

## 2.4 Results and discussion

### 2.4.1 Characterization of *S. aureus* wild-type NCTC 8325-4

The goal of this experiment was to characterize a wild-type strain of *S. aureus* to use to test for synergy activity in the checkerboard assay. By characterizing the behavior of *S. aureus*, optimal treatment of the bacteria could be implemented to acquire accurate results. Through a growth curve, the log and lag phases and the relationship between absorbance and colony forming units (CFUs) was determined, providing consistent methodology for synergy testing for bioactivity assays.

A growth curve was constructed by plotting the OD600 (primary y-axis) and CFU/mL (secondary y-axis) versus time as shown in **Figure 3**. The growth curve was collected each time a new bacteria stock was prepared and cryopreserved. This allowed the specific CFU/mL to be calculated. Thus, further assays were standardized to a concentration of  $5 \times 10^5$  CFU/mL. A growth curve for each strain of bacteria was constructed every six months using the same methodology to confirm the exponential growth phase and the relationship between CFU and absorbance.

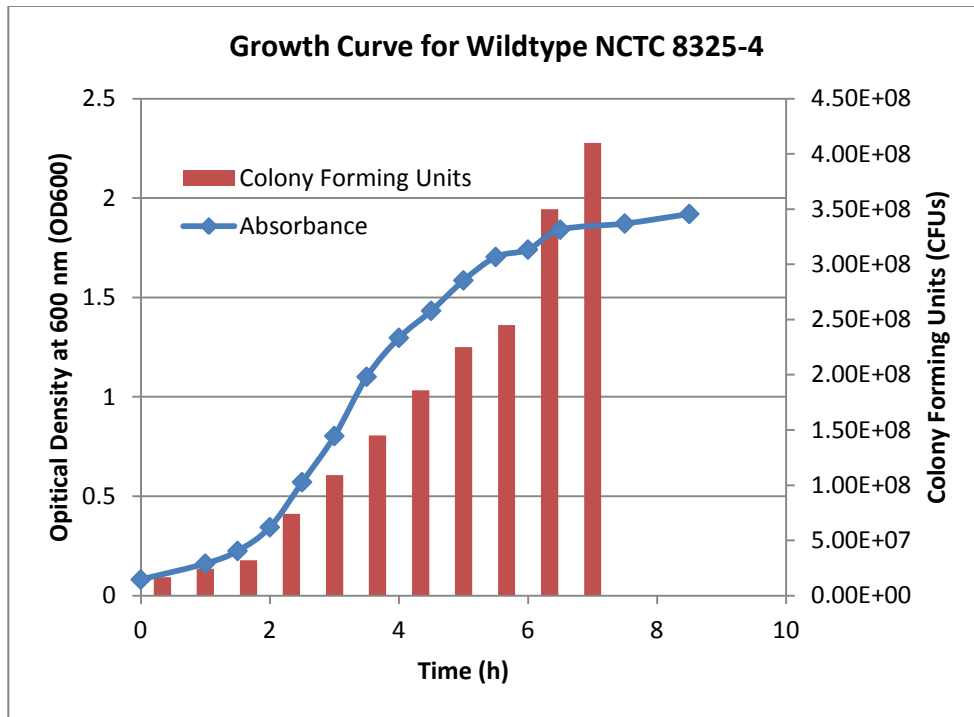


**Figure 3. Growth curve for the wildtype *S. aureus* (NCTC 8325-4).** Log phase was determined to be 2.5 hrs to 5.5 hrs. Colony Forming Units (CFUs) were plotted as a function of time and correlated to absorbance.

The relationship between OD600 and CFU/mL was established by the data collected for the growth curve (**Figure 3**) and a calculation to determine the desired OD600 to correspond with  $5.0 \times 10^5$  CFU/mL using the best fit line for the plot of OD600 vs. CFU/mL (**Figure 4**). This final diluted stock solution at  $5.0 \times 10^5$  CFU/mL was then dispensed at 50  $\mu$ L per well in the synergy assay to give  $1.0 \times 10^5$  CFU/mL at final well volume, consistent with CLSI guidelines.<sup>11</sup>



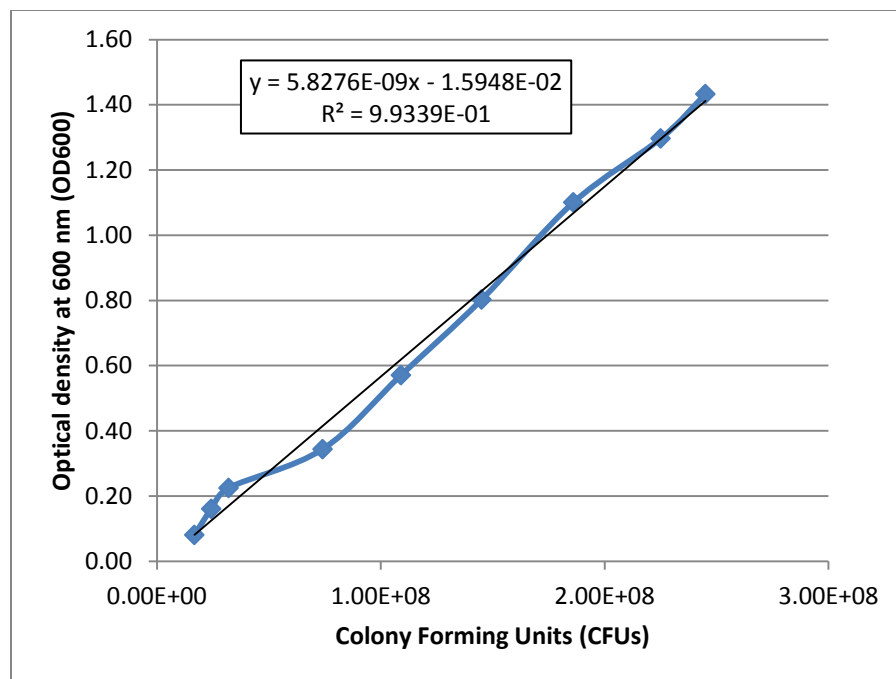


**Figure 4. Calibration curve determining the colony forming unit per milliliter of solution (CFU/mL) at an OD600**

#### **2.4.2 Detection and quantification of berberine in extracts of *Hydrastis canadensis***

The goal of this experiment was to determine and distinguish the antimicrobial compound berberine within the aerial and root portions of the plant, and to determine which portion contained more synergists identified via the checkerboard assay. Before testing extracts for antimicrobial synergy against the wild-type *S. aureus*, the quantity of berberine within the extract was determined. It was hypothesized that quantifying the level of berberine and standardizing it in the bioassay would allow for characterization of each extract as a synergist using the traditional checkerboard assay. Furthermore, the relative abundance of possible synergists to the antimicrobial compound berberine

could be evaluated. This could help further optimize preparation of *Hydrastis canadensis* extracts for commercial applications.

The quantification of berberine within various extracts allowed testing for synergy in *Hydrastis canadensis*. A crude ethanol extract of both the root portions and aerial portions of the plant were prepared using standard commercial methodology. Each extract was then standardized to berberine. The alkaloid berberine (**Figure 2**) was identified in all extracts based on the mass to charge ratio (m/z), CID fragmentation patterns and retention times matching with the standard compound (**Figure 5**).

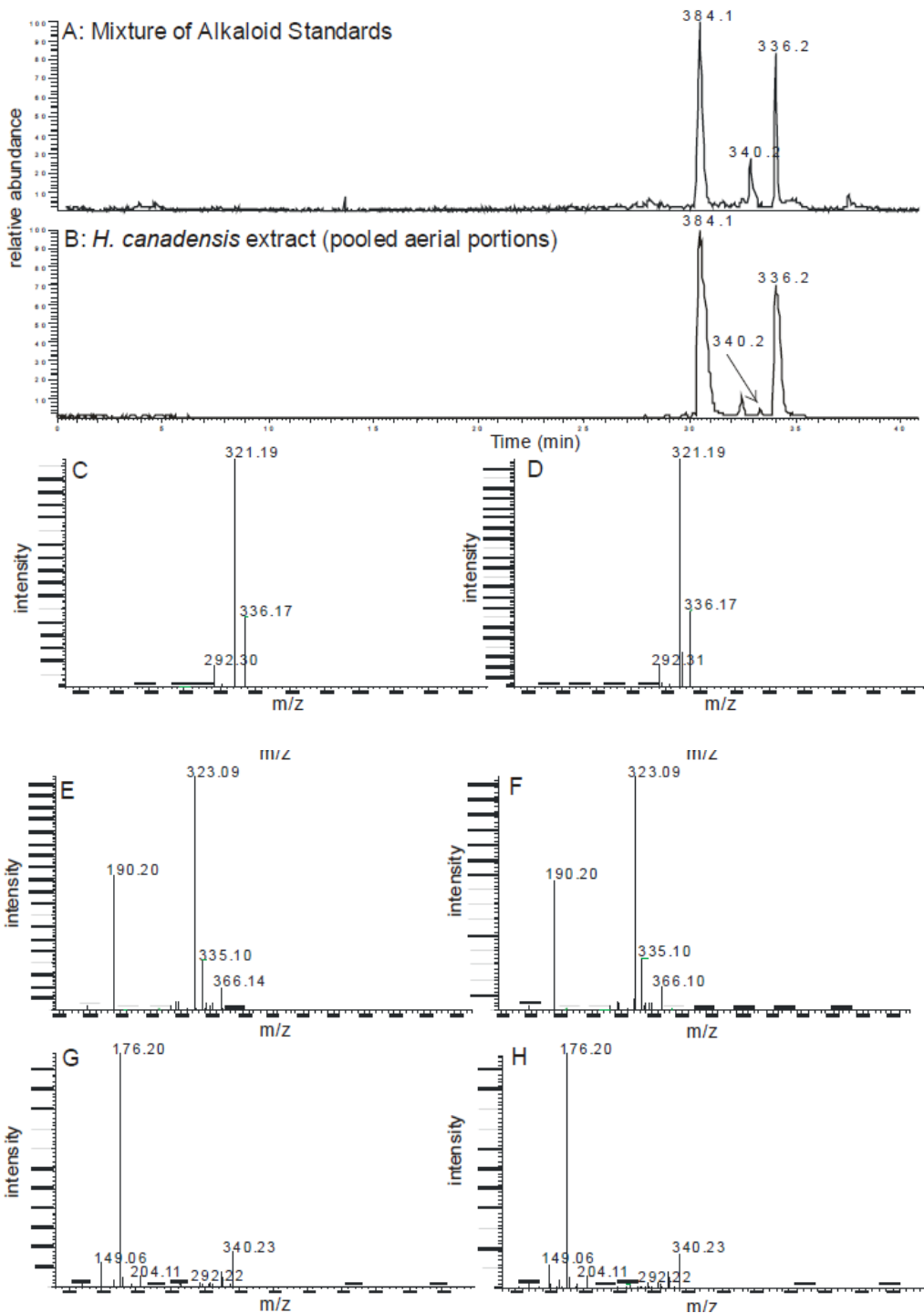


**Figure 5. Comparison of base peak LC-MS chromatograms for the berberine, hydrastine and canadine in equimolar concentrations at 1  $\mu$ M (A) and a 100-fold dilution of the ethanolic extract from the pooled aerial portions of *H. canadensis*.**

Berberine and two other alkaloids found in *Hydrastis canadensis*, canadine and hydrastine, were identified from the aerial portion of *Hydrastis canadensis* by matching m/z, retention time, and fragmentation patterns with that of standards (**Figure 5**). The numbers above the peaks indicate the m/z value of the ion detected, which was consistent with M<sup>+</sup> for berberine (monoisotopic mass of 336.12 g/mole), and MH<sup>+</sup> for hydrastine and canadine (monoisotopic masses of 384.14 and 340.15 g/mole, respectively). CID fragments of the M<sup>+</sup> ion for berberine (**Figure 5C**), the MH<sup>+</sup> ion for hydrastine (**Figure 5E**), and the MH<sup>+</sup> ion for canadine (**Figure 5G**), corresponded to ions in the extract (**Figure D, F, and H**). In all other extracts and fractions, alkaloids were identified in the same manner.

Calculations of the concentration of berberine using the calibration curve of the standard showed that the roots contained a higher concentration than the leaves (**Table 1**). The pooled ethanol root/rhizome extract had an average of 2 times more berberine (16.6 ± 0.3 mM) than the aerial ethanol extract (8.0 ± 0.1mM) (**Table 1**).

**Table 1. Quantity of alkaloids in extracts from the pooled root and rhizome ethanol extract, pooled aerial ethanol extract, or crude chloroform aerial extract.**

Concentrations were calculated from calibration curves for standards of each alkaloid analyzed with LC-MS in the positive mode.

	<b>berberine (mM) ± SE</b>	<b>hydrastine (mM) ± SE</b>	<b>canadine (mM) ± SE</b>
<b>Pooled aerial ethanolic extract</b>	8.0 ± 0.1	2.61 ± 0.05	0.054 ± 0.008
<b>Pooled root/rhizome ethanolic extract</b>	16.6 ± 0.3	3.79 ± 0.07	0.069 ± 0.011
<b>Crude Chloroform Extract</b>	7.78 ± 0.60	1.12 ± 0.12	0.45 ± 0.0040

### **2.4.3 Synergy assessment of both root and aerial of commercially prepared extracts**

The goal of this experiment was to determine which portion of the plant (aerial or root) acted more synergistically with berberine to help prepare future commercial application of *H. canadensis* as an herbal supplement. By characterizing the bacteria with the growth curve and quantifying the alkaloid berberine within the different samples testing for synergy between the different extracts was able to be performed. Extracts with known concentrations of berberine were tested in a checkerboard assay in combination with berberine to see if there was an additive or synergistic interaction.

As indicated by the FIC value of 0.375 (**Table 2**) and by the convex shape of the isobologram (**Figure 6**) the ethanol aerial extract of *H. canadensis* synergistically enhanced the antimicrobial activity of berberine. Interaction between the roots and

berberine was observed to be additive when used in combination in the checkerboard assay with an FIC value of 0.50 (**Table 2**). For validation purposes, berberine was tested in combination with itself (**Figure 6**), and the effect was additive (FIC of 1.00, linear isobologram). The ratio of synergism to the level of berberine was determined to be much higher in the aerial ethanolic extract.

**Table 2. MIC and FIC Values (Indicative of Synergy) for *Hydrastis canadensis* extracts and fractions against Wild-Type *S. aureus* (NCTC8325-4).**

	MIC ( $\mu\text{g}/\text{mL}$ )	FIC Index
<b>Berberine</b>	150	1.00
<b>Ethanol Root</b>	150	0.75
<b>Ethanol Aerial</b>	75	0.375

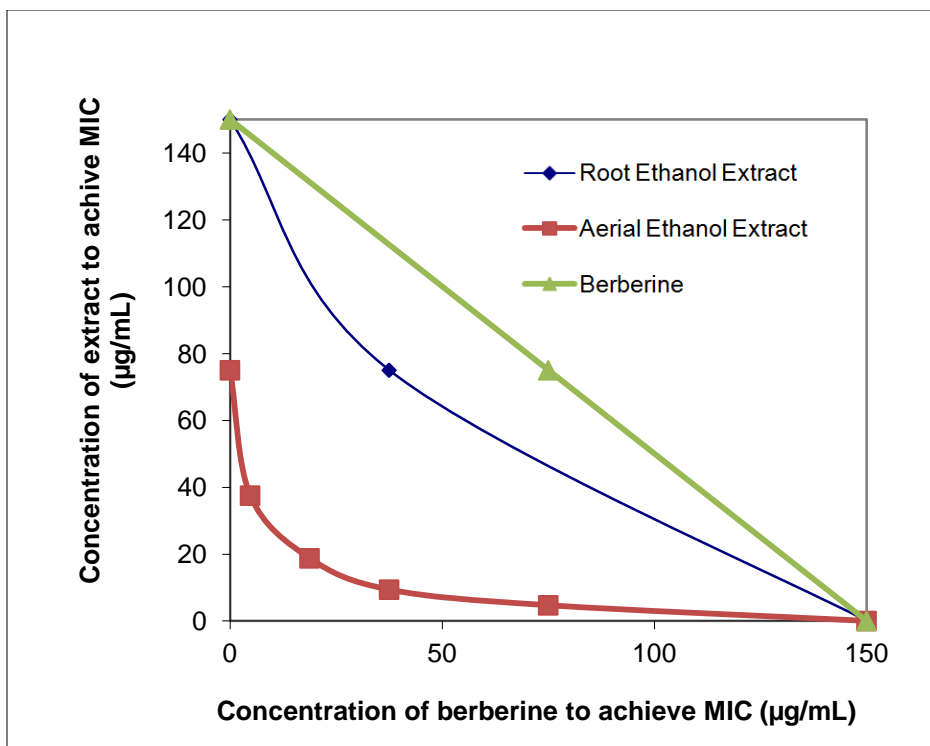


**Figure 6. Isobologram indicating inhibition of bacterial growth by *H. canadensis* extracts and added berberine.** Berberine alone was also included in the assay for validation and to serve as a positive control for an additive effect. Extracts were dissolved in 2% DMSO in Müller Hinton broth. Assays were performed in triplicate in a 96-well plate with  $5 \times 10^5$  CFU/mL *S. aureus*.

The results of this experiment as well as the one performed in section 2.4.2 provided insight to how commercial preparation of *H. canadensis* could be improved to enhance the antimicrobial of extracts. The data shows higher berberine content in the root portion of the plant with a higher synergistic activity in the aerial portion. Therefore, a combination of the two could potentially make effective treatment.

#### **2.4.4 Synergism within extracts and fractions of *Hydrastis canadensis* in synergy-guided fractionation approach**

The goal of this experiment was to use synergistic activity with berberine as the method for fractionation to isolate possible synergist from a large scale chloroform extract. By standardizing the concentration of berberine within each of these extract preparations, synergistic activity with berberine could be analyzed between the different fractions. Furthermore, individual fractions tested in combination help to direct the fractionation process. This methodology has the potential to be applied to a variety of complex extracts to identify possible synergists for a desired bioactivity.

Below is the synergy-guided fractionation schematic for the crude chloroform extract of *H. canadensis* (**Figure 7**). The fractionation process and identification of synergists were performed by Dr. Hiyas Junio. During each stages of fractionation a modified checkerboard assay was implemented in order to determine synergistic activity of each fraction with berberine. The most synergistically active fractions were selected for further fractionation until pure compounds were obtained.



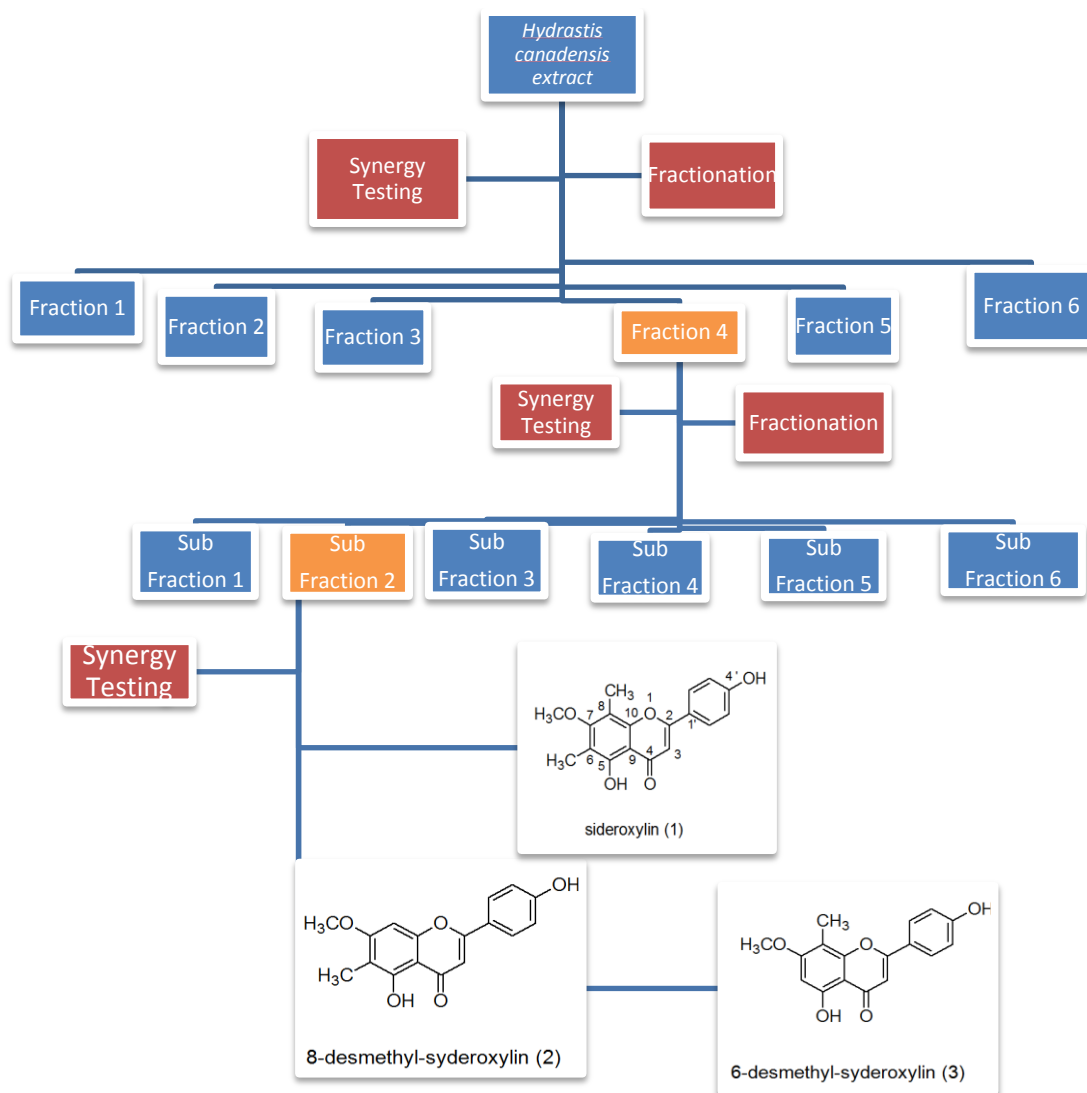


**Figure 7. Fractionation and synergy testing for the chloroform extract from *Hydrastis canadensis*.** Synergy testing is used to identify extracts and fractions likely to contain combinations of compounds that work together. Dr. Hiyas Junio was able to isolate 3 flavonoids (sideroxylin (1), 8-desmethyl-syderoxylin (2), and 6-desmethyl-syderoxylin (3)).<sup>112</sup>

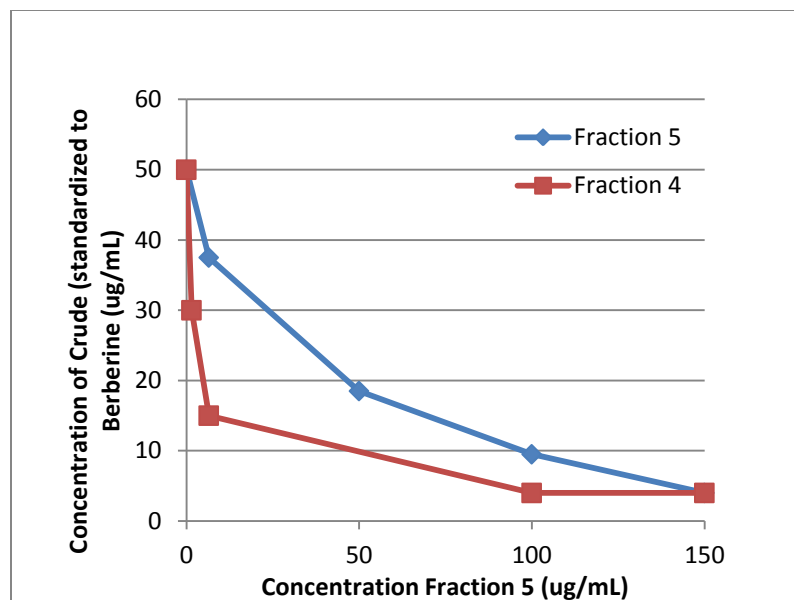


**Figure 8. Isobologram indicating inhibition of bacterial growth by fractions 4 and 5 from the chloroform extract in combination of the crude chloroform extract.** Extracts were dissolved in 2% DMSO in Müller Hinton broth. Assays were performed in triplicate in 96-well plate with  $5 \times 10^5$  CFU/mL *S. aureus*.

From the isobologram FIC Index values were calculated. With a FIC Index value of 0.32 for fraction 4 and 0.82 for fraction 5 (**Table 3**) and the concave shape of the isobologram (**Figure 8**) fraction 4 was characterized as a synergist when combined with the chloroform extract and fraction 5 was characterized as being additive in combination. In this case there was no standardization to berberine, yet a synergistic interaction could be observed. Although not as significant of an effect as shown when fraction 4 was combined with berberine (**Figure 9**), it is important to note the possible applications to other natural products where no active constituents have been identified. Also, continuation of this application during the fractionation process would

help isolate the bioactive compound (additive effect) and the synergistic compounds (synergistic effect). Based on this data it was hypothesized that Fraction 4 would most likely contain compounds responsible for the observed synergistic activity. However, this approach was not implemented due to berberine being well characterized as the primary antimicrobial agent found within *H. canadensis*.

**Table 3. MIC and FIC Values (Indicative of Synergy) for *Hydrastis canadensis* Extracts and fractions against Wild-Type *S. aureus* (NCTC8325-4).**

	MIC ( $\mu\text{g/mL}$ )	FIC Index
<b>Fraction 4</b>	>150	0.32
<b>Fraction 5</b>	>150	0.82

Fraction 4 was further fractionated into six subsequent fractions by Dr. Hiyas Junio (**Figure 7**) based on its apparent synergistic activity in combination with the crude extract (**Figure 8**) and berberine (**Figure 9**). Each of the subsequent fractions were assessed for synergistic activity using the checkerboard assay, and subfraction 2 exhibited the greatest synergistic activity with an FIC value of 0.03 (**Table 4**).

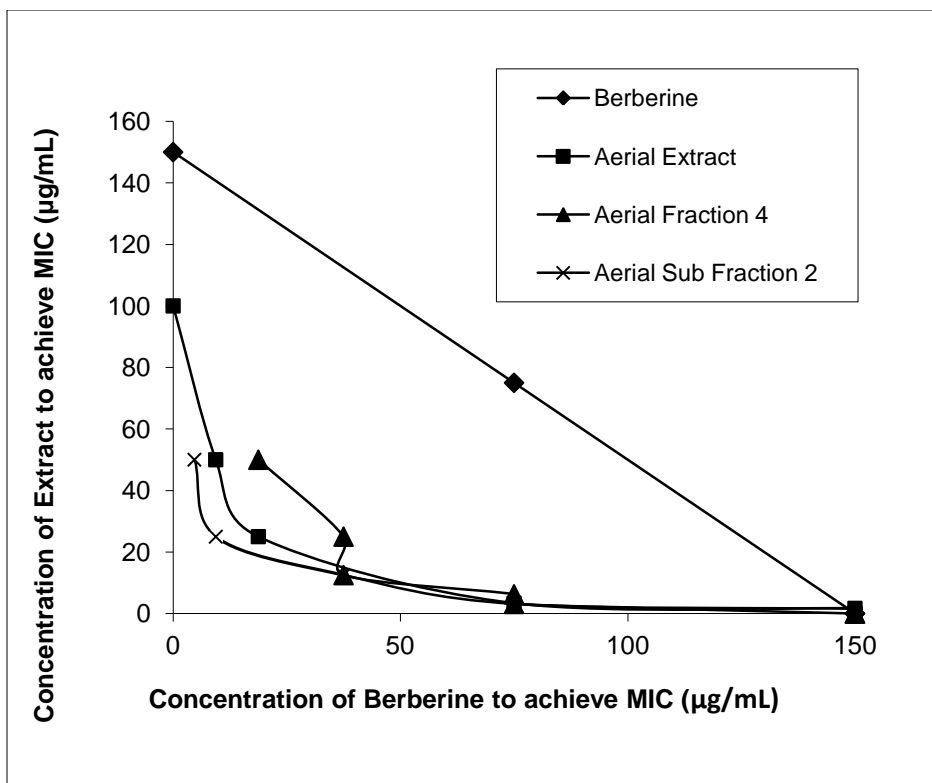


**Figure 9. Isobologram for berberine, the chloroform aerial extract of *Hydrastis canadensis*, the most active fraction from the first stage of separation (aerial fraction 4), and the most active fraction from the second stage of separation (aerial subfraction 2).** All were tested in combination with berberine. The crude chloroform extract and its two fraction synergistically enhanced the antimicrobial activity of berberine, as demonstrated by the convex shape of the isobolograms, and the FIC values reported.

**Table 4. MIC and FIC Values (Indicative of Synergy) for *Hydrastis canadensis* extracts and fractions against Wild-Type *S. aureus* (NCTC8325-4).**

	MIC ( $\mu\text{g/mL}$ )	FIC Index
<b>Berberine</b>	150	1.00
<b>Stage 1 Crude Aerial</b>	100	0.19
<b>Stage 2 Fraction 4</b>	>50	0.13
<b>Stage 3 Sub-Fraction 2</b>	>50	0.03

When following the synergy-guided fractionation process from crude extract to isolated synergist, the level of synergistic activity increased (**Table 4**). Fraction 4 (**Figure 9**) was the most active of the fractions collected from the first stage of separation from this extract. At its maximal solubility the concentration of was 50  $\mu\text{g/mL}$ , Fraction 4 (**Figure 9**) was characterized as a potentiator by having no antimicrobial activity observed at this concentration while enhancing the effect of berberine by lowering its MIC to 4.7  $\mu\text{g/mL}$ . Subfraction 2 (**Figure 9**) was the most active of the fractions collected from the second-stage separation and exhibited a maximal solubility concentration of 50  $\mu\text{g/mL}$  and was characterized as a potentiator by having no antimicrobial activity observed at this concentration while enhancing the antimicrobial activity of berberine. After further characterization by Dr. Junio of subfraction 2, 3 flavonoids (**Figure 6**) were identified as synergists, 6-desmethyl sideroxylin, sideroxylin, and 8-demethysidroxyln.<sup>112</sup>

## 2.5 Conclusion

With the increasing resistance to therapeutic strategies and overall healthcare cost *S. aureus* has acquired as mentioned in the first chapter, it has become more important to implement new strategies to address this growing problem. One suggested avenue is a multidrug therapy approach using a strategy in which activity of antimicrobial compounds is enhanced by other compounds in a synergistic manner. Thus, this methodology in identifying synergists in the complexity of a plant extract provided a useful tool in discovering compounds that may increase the efficacy of presently used treatments.

From an economic aspect, roots from *Hydrastis canadensis* are more commonly employed medicinally because of their high alkaloid content compared to the leaves. The results do concur the root extract is higher in alkaloid content; however when the aerial portions are standardized to berberine the level of synergy in the aerial portion of the plant is significantly higher. This indicates that some constituent(s) other than berberine in the extract from *Hydrastis canadensis* aerial portions synergistically enhance the antimicrobial effect of berberine. These constituents were determined to be flavonoids acting as potentiators with no observable antimicrobial effect..

Commercially, a combination of root and aerial extracts of *Hydrastis canadensis* could be more beneficial than current preparations seeing as though the findings show the aerial portion of the plant have higher levels of synergists while the roots have

higher level of alkaloids . Although, further studies are needed to determine the safety and efficacy of such a combination, the data here provides useful information to the future cultivation strategies in commercial development. Through the implementation of the aerial portions of the plant, a large portion of the *Hydrastis canadensis* population can be preserved by conserving the plant during harvest.

Although the checkerboard assay has been traditionally used to characterize two individual components (Drug A and Drug B) as synergists, antagonists, or additive in nature, this study demonstrates that synergy in complex extracts can be identified by standardizing a constituent within that extract with a specific biological activity and testing it against itself at varying concentrations. In the case of *Hydrastis canadensis*, the aerial ethanolic extract of the plant contains a higher ratio of synergism to berberine ratio compared to that of the roots. Furthermore, by testing for synergism as a guide for the fractionation process using the modified checkerboard assay, synergism within the plant could be attributed to specific isolated compounds.

A suggested synergism can also be observed without standardizing a constituent found within the extract as seen with Fraction 4 and 5 in combination with the crude chloroform extract. Although berberine was not standardized within this checkerboard assay, a comparison of interaction between fractions and the crude extract can be useful to identify fractions with a greater synergistic activity. In addition, this methodology is useful in determining the relative abundance of synergists in different

portions of the plant, which can aid in the commercial application and preparation of *Hydrastis canadensis*. Furthermore, future synergy-guided fractionation processes of complex natural products may not have known bioactive compounds, and this approach could help facilitate the fractionation process. Fractions with bioactive compounds should behave in a more additive manner with the crude extract whereas synergists should have a more synergistic effect with the crude extract.

In general this study has shown that a synergy-guided fractionation approach can be implemented to determine possible antimicrobial agents, in this case berberine, within a complex extract and distinguish the antimicrobial agent from synergists (flavonoids). As opposed to bioactivity-guided fractionation, synergy-guided fractionation with the crude extract allowed for the identification of an extract containing a synergist before the fractionation process was conducted. Furthermore by testing subsequent fractions with the original crude extract, we were able to determine which fractions were the most likely candidates to contain synergist. The process serves as a useful tool to identify synergist along with antimicrobial compounds from a complex plant extract.



## CHAPTER III

### MECHANISM OF ACTION OF SYNERGISTS FROM *HYDRASTIS CANADENSIS*

#### 3.1 Abstract

**Rational:** The goals of this study were to characterize the mode of action by which complex aerial and root extracts of *Hydrastis canadensis* act to enhance the antimicrobial effect of berberine against various strains of *S. aureus*, and to determine whether synergists isolated from *Hydrastis canadensis* act as multi-drug resistance (MDR) pump inhibitors.

**Methods:** *S. aureus* strains NCTC-8325-4 (wildtype), K1902 (NorA knockout), K2703 (NorA complemented) were used to determine efflux pump inhibition for chloroform aerial extracts of *Hydrastis canadensis* through confocal microscopy. K1902 and K2703 were characterized via a growth curve and implemented in a fluorescence-based ethidium bromide efflux assay along with NCTC-8325-4 to evaluate the efflux pump inhibitory activity of complex extracts and isolated synergists from *Hydrastis canadensis*.

**Results and Discussion:** The aerial extracts of *Hydrastis canadensis* had more pronounced efflux pump inhibitory activity against wildtype *S. aureus* than did root

extracts based both on confocal microscopy measurements and the ethidium-bromide efflux assay. The flavonoids 8-desmethyl-sideroxylin, 6-desmethyl-sideroxylin and sideroxylin isolated from sub-fraction 2 in **Figure 20** also inhibited the efflux of ethidium bromide by wildtype *S. aureus*, suggesting efflux pump inhibitory activity for these compounds. Consistent with this conclusion, no significant difference between treated and control cells was observed for efflux pump (NorA) knockout *S. aureus*. Of the flavonoids tested, 6-desmethyلسideroxylin had the most pronounced efflux pump inhibitory activity.

**Conclusions:** Extracts from *Hydrastis canadensis* contain flavonoids which inhibit efflux pumps in *S. aureus*. The aerial portions of the plant appear to have highest efflux pump inhibitory activity, likely due to the presence of higher concentration of flavonoids.

## **3.2. Introduction**

### **3.2.1 Multi-Drug-Resistant pumps in *S. aureus***

The number of antibiotics to which *S. aureus* has developed a resistance to over the past ten years has risen considerably. As a result, many antimicrobial compounds have been rendered ineffective. A major mechanism by which bacteria become resistant to antibiotics is an up-regulation in the number of multi-drug resistant efflux pumps (also referred to as MDR pumps).<sup>93</sup> Efflux pumps work through actively exporting an antimicrobial agent from the cell via efflux before the antimicrobial agent reaches

high concentrations.<sup>94</sup> The multidrug efflux system in *S. aureus* consists of transporter proteins which export a broad range of structurally unrelated compounds.<sup>95</sup>

The gene sequence of *S. aureus* N315, which is comparable to the NCTC 8325-4 strain, consists of a 2.81 Mb genome with a total of 212 transporters.<sup>96</sup> There have been 20 of these 212 transporters identified as multidrug efflux pumps with high levels of genomic conservation in the N-terminal ends relative to the C-terminal. Thus, it is hypothesized that the N-terminal end is involved in activation while the C-terminal is important for substrate specificity<sup>19</sup>.

The NorA transporter, a MDR pump, is found in clinical isolates of *S. aureus* able to efflux a range of structurally different compounds.<sup>97</sup> It is considered the major chromosomal MDR pump in this species of bacteria.<sup>98</sup> In *S. aureus*, NorA enhances resistance to azoles, acriflavin, fluoroquinolones, puromycin, chloramphenicol, ethidium bromide, and other quaternary amine compounds including the alkaloid berberine. The NorA pump itself clusters, forming a total of 12 transmembrane proteins, which rely on the proton motive of force in order to efflux antimicrobial agents outside the cell. By taking in protons into the bacterial cell using a proton gradient, the efflux pumps are able to export antimicrobial substrates outside the cell before they reach high enough concentrations to kill the cells.<sup>21</sup>

One of the major pioneers in evaluating efflux pump inhibition as a mechanism of increasing the efficacy of antimicrobial agents was Frank R. Stermitz. In 2001, his lab

was able to isolate two efflux pump inhibitors that were active against *S. aureus.*, 5'methoxyhydnocarpin D from leaves of *Berberis trifoliolata* and phenphorbide *a* from *Berberis fendleri*. These efflux pump inhibitors enhance the antimicrobial effect of berberine, an antimicrobial agent found within the plants.<sup>105</sup> It was these research findings that lead to the investigation of *H. canadensis* and its purified flavonoids a possible source of efflux pump inhibition.

### **3.2.2 *Hydrastis canadensis* as a possible efflux pump inhibitor**

Methanol extracts of aerial portions of *Hydrastis canadensis* have been shown to achieve MIC (minimum inhibitory concentrations) of 40 and 160 µg/mL against *C. glabrata* and *C. albicans*. Furthermore, the methanol extract of this plant was shown to be effective against azole-sensitive clinical isolates of *C. glabrata* (BPY112 and BPY126) which over expresses multidrug efflux pumps Cg,CDR1, CgCDR2, and CgSNQ2. Two strains of azole-resistant *C. albicans*, over expressing CDR1 and CDR2 were also inhibited by the extract of *Hydrastis canadensis*.<sup>99</sup> The data from this paper suggest that secondary metabolites in the aerial portion of *Hydrastis canadensis* may be synergistic by acting as MDR pump inhibitors.<sup>100</sup>

### **3.2.3 *Hydrastis canadensis* an inhibitor of MDR pumps in the liver**

Berberine has been shown to be an effective compound to have an effect at lowering cholesterol in blood plasma. High cholesterol is a primary cause of heart disease and can significantly increase blood pressure. Typically, these chronic illnesses

are treated with a class of compounds called statins (atorvastatin (Lipitor®) and lovostatin (Mevacor®, Altacor®, Altoprev®). Where presently used statins work by inhibiting HMG-CoA reductase which is involved in the biosynthesis of cholesterol; berberine has been shown to act in a different manner. Berberine up-regulates the mRNA encoding hepatic low-density lipoprotein receptor (LDLR), which regulates the uptake of plasma low-density lipoproteins (LDL) control into the liver where it is oxidized into bile acids.<sup>101</sup>

The high content of berberine found in *Hydrastis canadensis* extracts lead to the testing of root extracts standardized to berberine for LDL levels in the blood and comparing the results to berberine alone at the same concentrations. It was shown the root extract of *H. canadensis* was more effective at up-regulating LDLR in HepG2 when compared to pure berberine at the same concentration.<sup>102</sup> This led the Abidi group to explore the mechanism of action to obtain this observed activity.

When treated with *Hydrastis canadensis* extracts obtained from four different lots, the level of LDLR mRNA expression was elevated when compared to berberine alone at the same levels of concentrations standardized to berberine. Verification of activity was confirmed by a Northern blot analyses and quantification using real time PCR of the RNA harvested from the treated HepG2. It was hypothesized the elevation of the LDLR mRNA resulted from mRNA stabilization because the LDLR promoter activity was unaffected by treatment. In a time course study, the level of LDLR mRNA increased at a faster rate when treated with the plant extract compared to purified berberine. Furthermore, at the same concentrations of berberine in pure berberine alone and in the extract, the treatment with

extract caused a ~13 fold increase in accumulation of berberine within the HepG2 cells. It was also noted berberine is actively effluxed from bacterial cells by multidrug resistance pumps and therefore the group postulated the multi-drug transporter 1 (MDR1) pgp-170 in HepG2 cells plays a role in the accumulation of berberine within the cell.<sup>103</sup>

To test for the MDR1 inhibitory effects of *Hydrastis canadensis* a known substrate for MDR 1 that fluoresces, DiOC<sub>2</sub>, was monitored with verapamil serving as the positive control. The results showed an increase in the uptake of DiOC<sub>2</sub> when treated with the plant extract compared to the vehicle control and the treatment was comparable with the positive control verapamil. The group hypothesized minor constituents in the extract act as natural antagonists for the MDR1 transporter leading to the increased uptake of berberine in HepG2 causing an overall increase in LDLR mRNA expression.<sup>104</sup>

It has also been well established *S. aureus* and other bacteria have MDR pumps directly responsible for the efflux of the alkaloid berberine outside the cell.<sup>105</sup> Paired with the enhancement of the antimicrobial effect of berberine shown in chapter II and the results from the Albidi group with the increase uptake of berberine in HepG2 cells it was hypothesized the unknown minor constituents in *Hydrastis canadensis* that were postulated to be MDR 1 inhibitors could be the flavonoids isolated and identified as synergists in the previous chapter. Furthermore, we hypothesized the aerial portion of the plant would have a greater efflux inhibitory activity based on the higher concentrations of flavonoids determined by Dr. Junio in the Cech lab.<sup>106</sup> The goal of the experiment described in this

chapter was to test these hypotheses by measuring the efflux pump inhibitory activity of *H. canadensis* extracts and their purified flavonoids.

### **3.2.4 Ethidium bromide based assay for efflux pump inhibition**

A different approach for identifying possible efflux pump inhibitors than measuring MIC values with or without treatment (EPIs) has been to use ethidium bromide, a fluorescent dye, which is a substrate for most MDR efflux pumps in *S. aureus*. By measuring intracellular fluorescence readings of the dye both with and without the potential efflux pump inhibitor one can determine the net effect of the candidate compound. Efflux of ethidium bromide via the NorA pump has been observed in *S. aureus* using confocal microscopy.<sup>107</sup> Ethidium bromide fluoresces a bright red when intercalating to the DNA in *S. aureus*. By loading bacterial cells with ethidium bromide, a decrease in fluorescence can be observed over time. This inhibition activity can be quantified by measuring the fluorescence directly using a spectrophotometer.

## **3.3 Experimental**

### **3.3.1 Confocal microscopy to measure efflux pump inhibition**

The growth curve and CFU/mL of SA-K1758 (*norA* deleted) and SA-K2708 (*norA* complemented) were measured using the same protocol described in Section **2.2.1**. The confocal microscopy method was used to visualize efflux of ethidium bromide outside the cell using a NorA knockout strain of *S. aureus* (SA-K1758) and a NorA complemented strain (SA-K2378). The bacteria were grown to an OD600 of 0.84 in Müller-Hinton

broth. Ethidium bromide (25  $\mu\text{M}$ ) and the known efflux pump inhibitor carbonyl cyanide *m*-chlorophenylhydrazone<sup>108</sup> (CCCP, 100  $\mu\text{M}$  final concentration) were added, and the bacteria were incubated at 20°C with agitation (200 RPM) for 20 minutes. This solution was diluted to OD<sub>600</sub> = 0.36 with broth containing ethidium bromide and CCCP at 25  $\mu\text{M}$  and 100  $\mu\text{M}$ . Aliquots (1 mL) were centrifuged at 20°C for 5 minutes at 13,000 x g in a Spectrafuge 24D centrifuge (Labnet). The pellets were stored on ice for <1 hr. Prior to measurement, the pellets were thawed for 5 minutes and resuspended in 1 mL of fresh broth containing 10% DMSO and treatment of plant extract at 1 mg/mL or CCCP 100  $\mu\text{M}$ . The solution was placed on a slide with a cover slip. Each sample was observed at t = 1 minute and t = 5 minutes using a confocal microscope (Olympus 1X81/Confocal Laser Scanning Microscope with Olympus Fluoview500 software, a HeNe-Green (543 nm) excitation laser and an, Olympus PlanApo 60x11.40 oil objective). Measurements were carried out using three strains of *S. aureus* (NCTC SA-8325-4, K1758, SA-K2702).

### **3.3.2 Quantization of relative fluorescence**

The efflux pump inhibition assay was conducted using a previously published method.<sup>109</sup> Wild-type *S. aureus* (NCTC 8325-4) and an isogenic NorA deletion mutant (K1758 NorA deleted) were grown to OD<sub>600</sub> = 0.74 in Müller-Hinton broth. Ethidium bromide (25  $\mu\text{M}$ ) and carbonyl cyanide *m*-chlorophenylhydrazone (CCCP, 100  $\mu\text{M}$ ) were added, and the bacteria were incubated at 20 °C with agitation (300 RPM) for 20 min.



This solution was diluted to  $OD_{600} = 0.40$  with broth containing ethidium bromide and CCCP at  $25 \mu\text{M}$  and  $100 \mu\text{M}$ , respectively. Aliquots (1 mL) of this solution were centrifuged at  $20 \text{ }^\circ\text{C}$  for 5 min at  $13,000 \times g$  in a Spectrafuge 24D centrifuge (Labnet). The pellets were stored on ice for  $<1$  hr. Prior to measurement, the pellets were thawed for 5 min and 1 mL of fresh broth containing DMSO (10% final assay concentration) and treatments (CCCP, extract or pure compound) were added to achieve a final concentration of  $50 \mu\text{g/mL}$ . Fluorescence of these solutions was measured every second for 300 s with  $\lambda_{\text{ex}} = 530 \text{ nm}$ ,  $\lambda_{\text{emiss}} = 600 \text{ nm}$ , and slit widths of 5 mm.

### **3.4 Results and discussion**

#### **3.4.1 NorA knockout (SA-K1758) and NorA complemented (SA-K2708) growth curve**

The goal was to characterize the mutant strains of *S. aureus* SA-K1758 and SA-K2708 to optimize growing conditions and implementation in following experiments. By determining the log and lag phase of the different strains the growth time for each bacteria was determined for the subsequent efflux assays.

A growth curve was constructed by plotting the  $OD_{600}$  (primary y-axis) and CFU/mL (secondary y-axis) versus time as shown in **Figure 10**. The growth curve was collected each time a new bacteria stock was prepared and cryopreserved. This allowed the specific CFU/mL to be calculated. Thus, further assays were standardized to a concentration of  $5 \times 10^5$  CFU/mL. A growth curve for each strain of bacteria was

constructed every six months using the same methodology to confirm the log growth phase and the relationship between CFU/mL and absorbance.

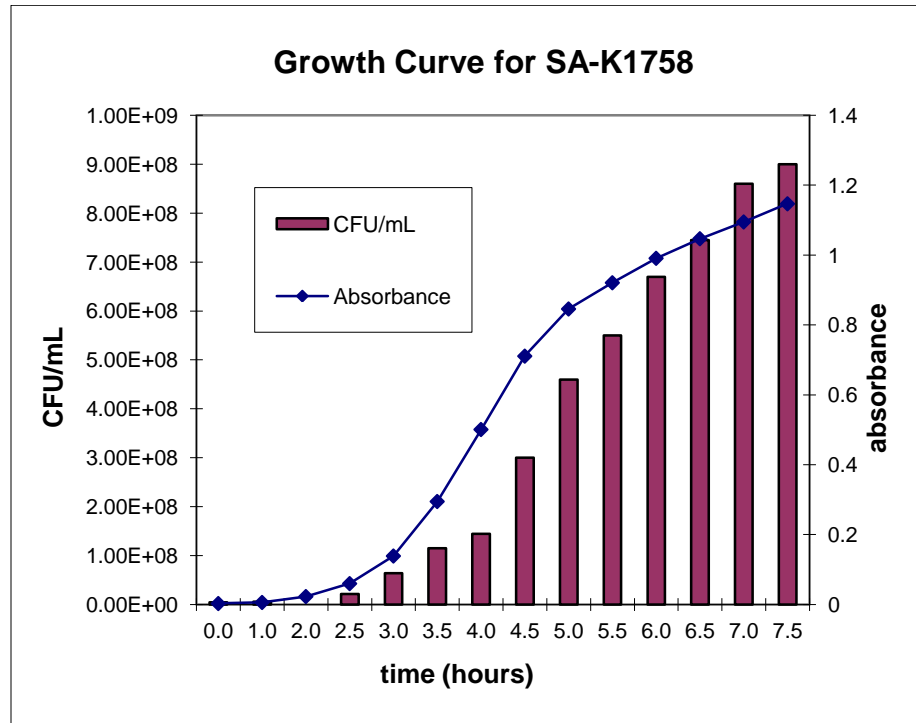


**Figure 10. Growth curve for the NorA knockout *S. aureus* (SA-K1758).** Log phase was determined to be 3.5 hrs to 6.5 hrs. Colony Forming Units (CFUs) were plotted as a function of time and correlated to absorbance.

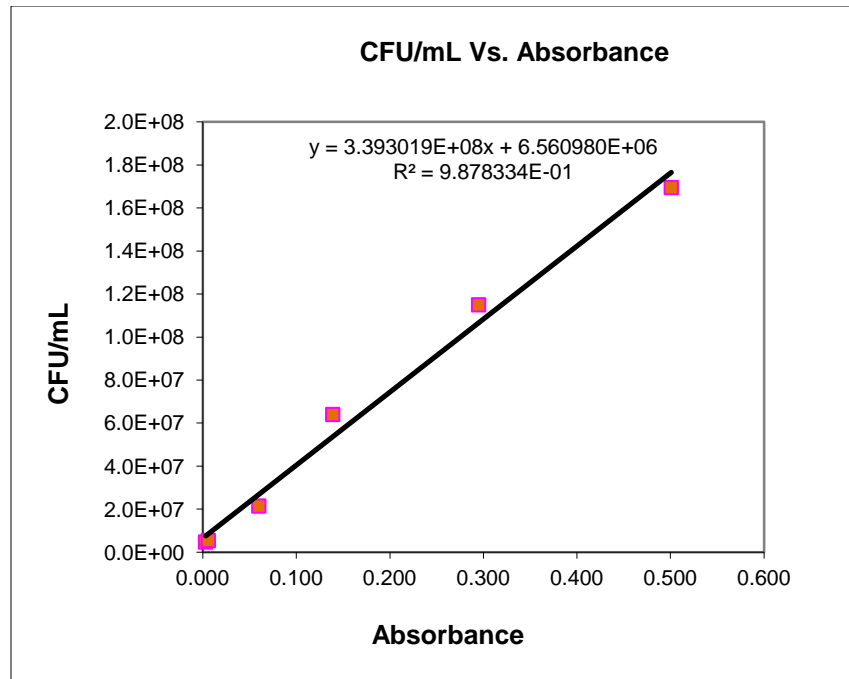


**Figure 11. Calibration curve determining the colony forming unit per milliliter of solution (CFU/mL) at an OD600 for SA-K1758**

The same methodology was performed for the complemented strain in order to optimize growing conditions for the fluorescence assays.

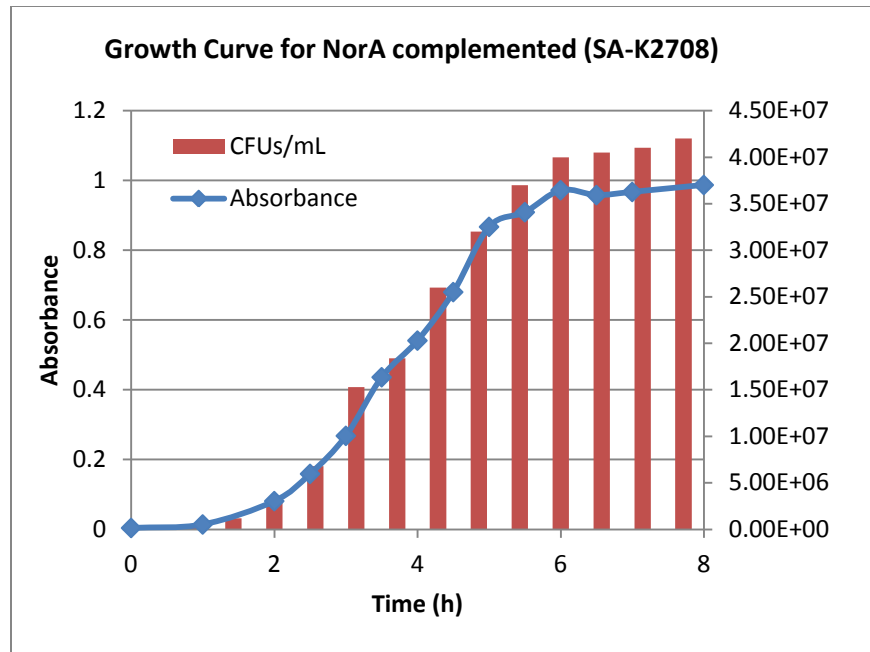


**Figure 12. Growth curve for the NorA complemented *S. aureus* (SA-K2708).** Log phase was determined to be 2.5 hrs to 5.5 hrs. Colony Forming Units (CFUs) were plotted as a function of time and correlated to absorbance.

The log phase of the SA-K2708, the complemented strain producing an abundance of NorA MDR pumps, was determined to be 2.5 hrs to 5.5 hrs which is significantly different than the knockout strain (SA-1758) with a range of 3.5-6.5, but consistent with the wild-type which had a log phase with the range of 2.5-5.5 hrs in the same growing conditions (**Figure 12**)

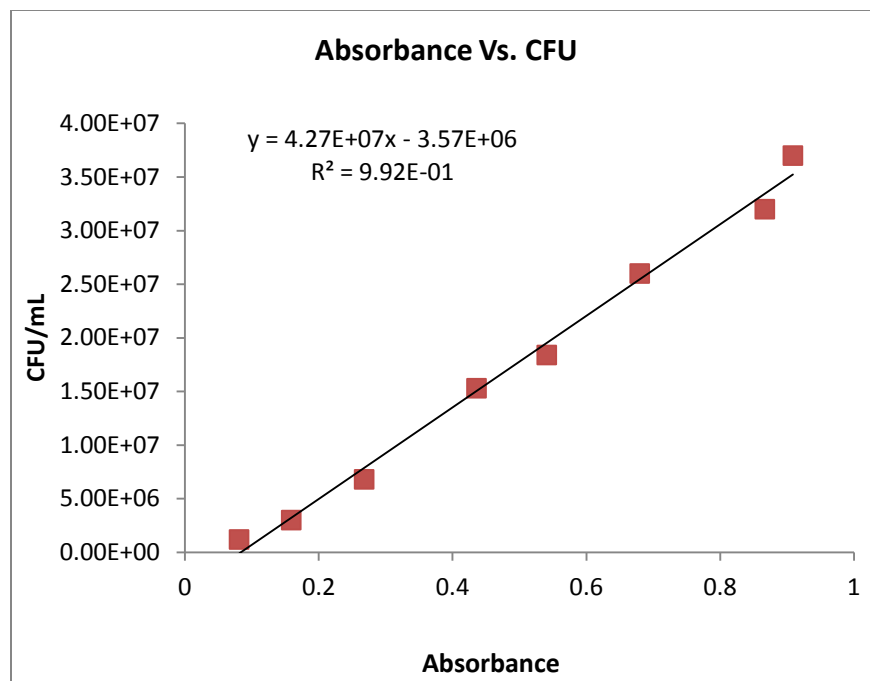


**Figure 13. Calibration curve determining the colony forming unit per milliliter of solution (CFU/mL) at an OD600 for SA-K1758**

The relationship between OD600 and CFU/mL was established by the data collected for the growth curve (**Figure 12**) and a calculation to determine the desired OD600 to correspond with  $5.0 \times 10^5$  CFU/mL was performed using the best fit line for the plot of OD600 vs. CFU/mL (**Figure 13**). This final diluted stock solution was added to 20 mL of broth and grown to an OD600 of 0.8-1.1 in the confocal microscopy and efflux inhibition assays.

### **3.4.2 Confocal microscopy with mutant strains of *Staphylococcus aureus***

The goal of this experiment was to determine if various extracts from *Hydrastis canadensis* inhibited the efflux of ethidium bromide within different strains of

*Staphylococcus aureus*. By loading bacteria with ethidium bromide and suspending them with or without treatment, efflux could be observed directly using a confocal microscope. The NorA knockout strain (SA-K1758) served as our reference control and mimicked NorA inhibition by having the gene encoded for NorA deleted. From one minute after suspension to five minutes after suspension the observed fluorescence was expected not to change. The rationale behind starting the observation of fluorescence after one minute was that this was the time necessary to prepare a slide for analysis on the confocal microscope.

The NorA complemented strain (SA-K2708) was assessed to determine if a NorA inhibitor was present upon treatment. By observing the fluorescence over time, inhibition was observed through comparison with the positive control CCCP. The level of fluorescence observed corresponded to the amount of ethidium bromide within the cell intercalating with the bacterial DNA. Because ethidium bromide diffuses into the cells and is actively transported out by the NorA efflux pump, if there was a high relative fluorescence over time, then it was concluded there was little efflux of ethidium bromide outside the cell via the NorA pumps. If there was a low to no observable relative fluorescence over time it was concluded the bacteria effluxed the majority of ethidium bromide outside the cells via the NorA pumps. If fluorescence was retained in the NorA complemented strain in response to treatment with the extract, then it was concluded there was a NorA pump inhibitor (or other related efflux pump inhibitor) present.

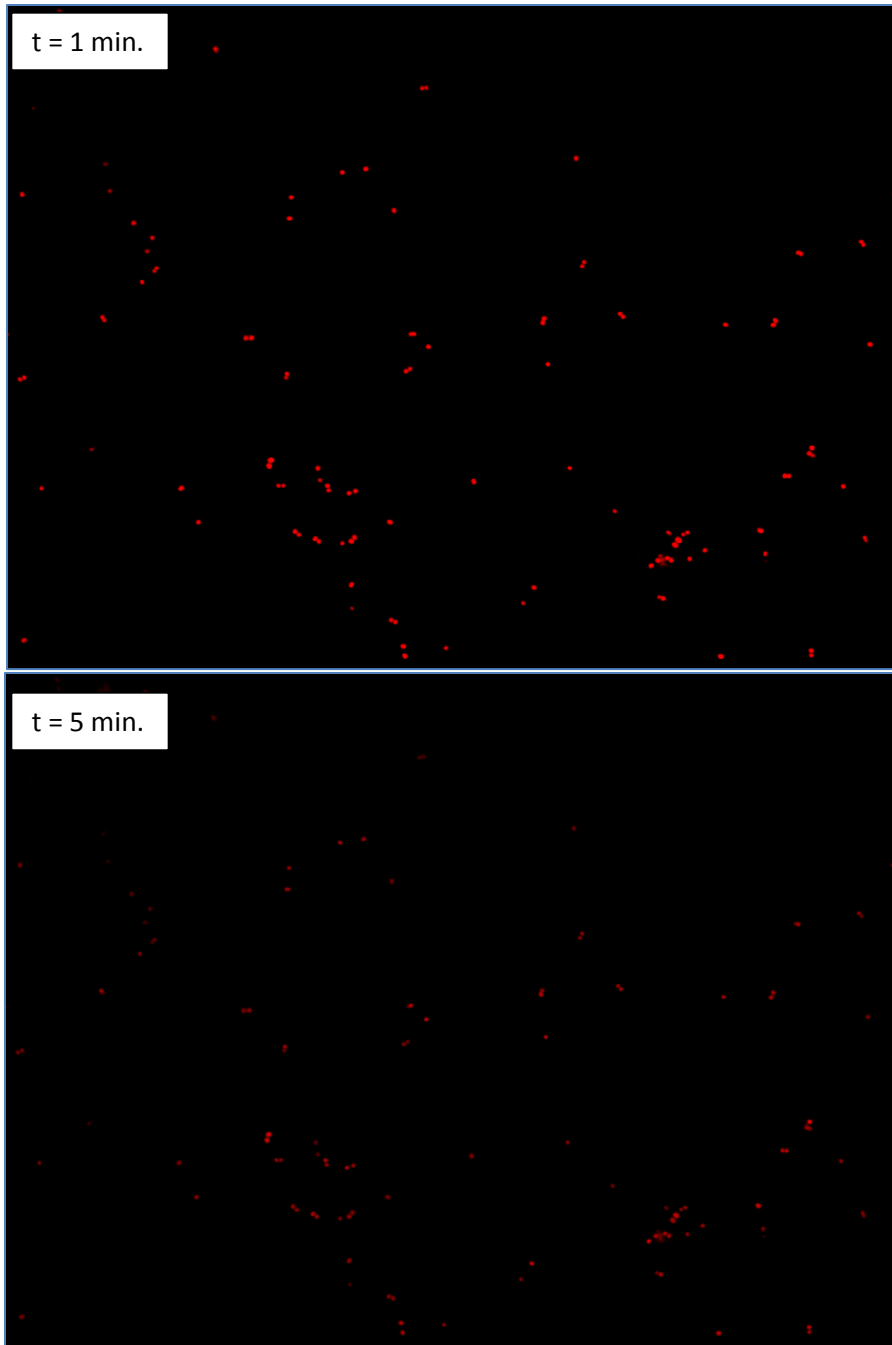
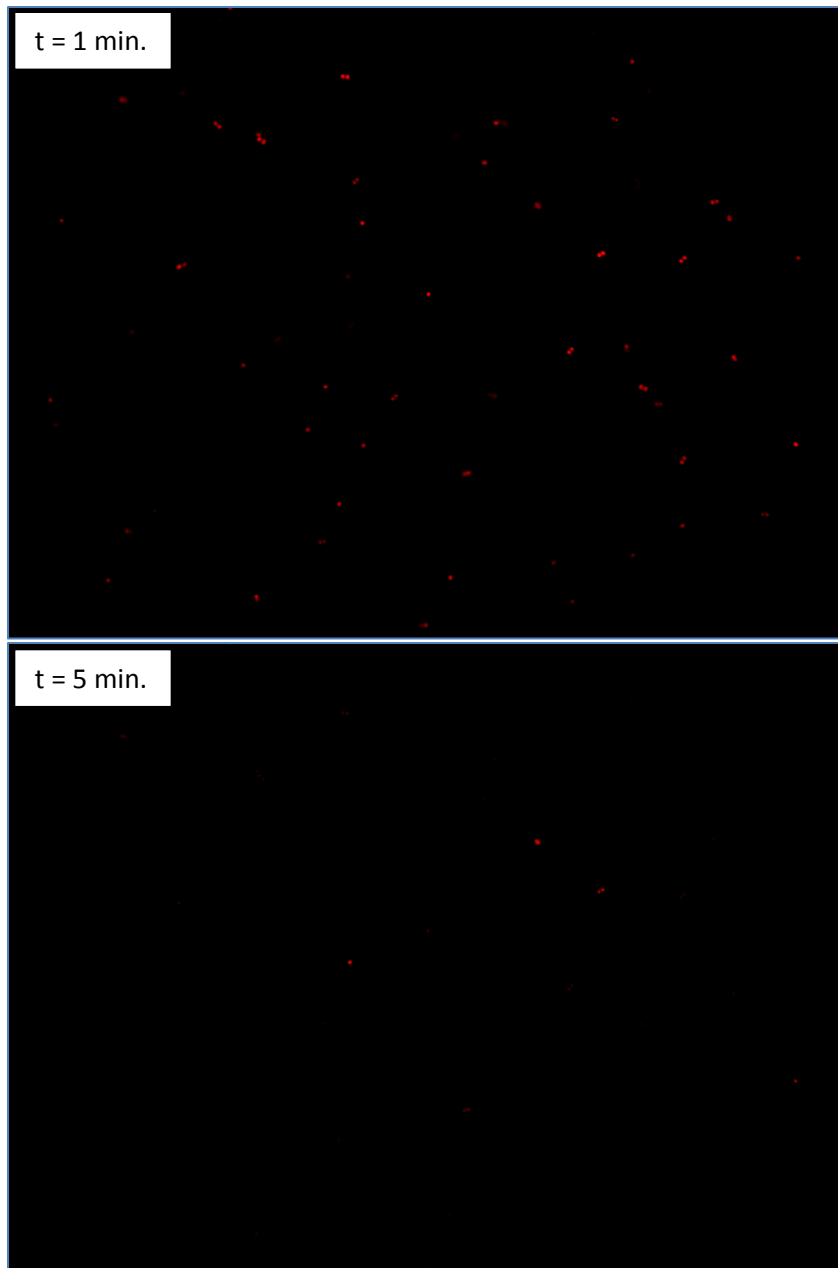


Figure 14. Confocal microscopy image of NorA knockout *S. aureus* (SA-K1758) after one minute and 5 minutes suspended in MH broth.

The two images of the NorA knockout strain show that the level of red fluorescence observed in the bacterial cells changes very little from one to five minutes. The slight change could be attributed to passive diffusion of ethidium bromide outside the cell or other MDR pumps besides the NorA pump that may exist in the knockout strain. Nevertheless, using SA-K1758 (NorA knockout) as a standard to compare to, if treatment of *Staphylococcus strains* with the NorA pump expressed mimic the relative fluorescence as shown in **Figures 14** it was hypothesized the NorA efflux pumps are unable to efflux ethidium bromide outside the cell as a result of inhibition.

The knockout strain (SA-1758) was tested with carbonyl cyanide *m*-chloro-phenylhydrazone, CCCP (positive control), to determine any effects of fluorescence it may have over the four minute time period (**Figures 15**).





**Figure 15. NorA knockout strain (SA-K1758) after one minute and five minutes suspended in broth containing 100  $\mu$ M carbonyl cyanide m-chloro-phenylhydrazone, the control efflux pump inhibitor.**

When the knockout strain was treated with the positive control CCCP at a concentration of 100  $\mu$ M the level of fluorescence was not significantly different between 1-5 minutes. However, it was noted a slight increased in fluorescent signal after the five minute period. Observing less fluorescent cells in **Figure 15** after one minute compared to the five minute time period under treatment of the positive control suggested other MDR (NorB, NorC, SepA) pumps produced by *S. aureus* could have been inhibited through the disruption of the proton motive force. Another possible explanation is the bacteria's tendency to migrate out of the camera lens during the course of the 4 minute interval. This could be a possibility seeing as though the intensity of the fluorescence appears not to decrease.

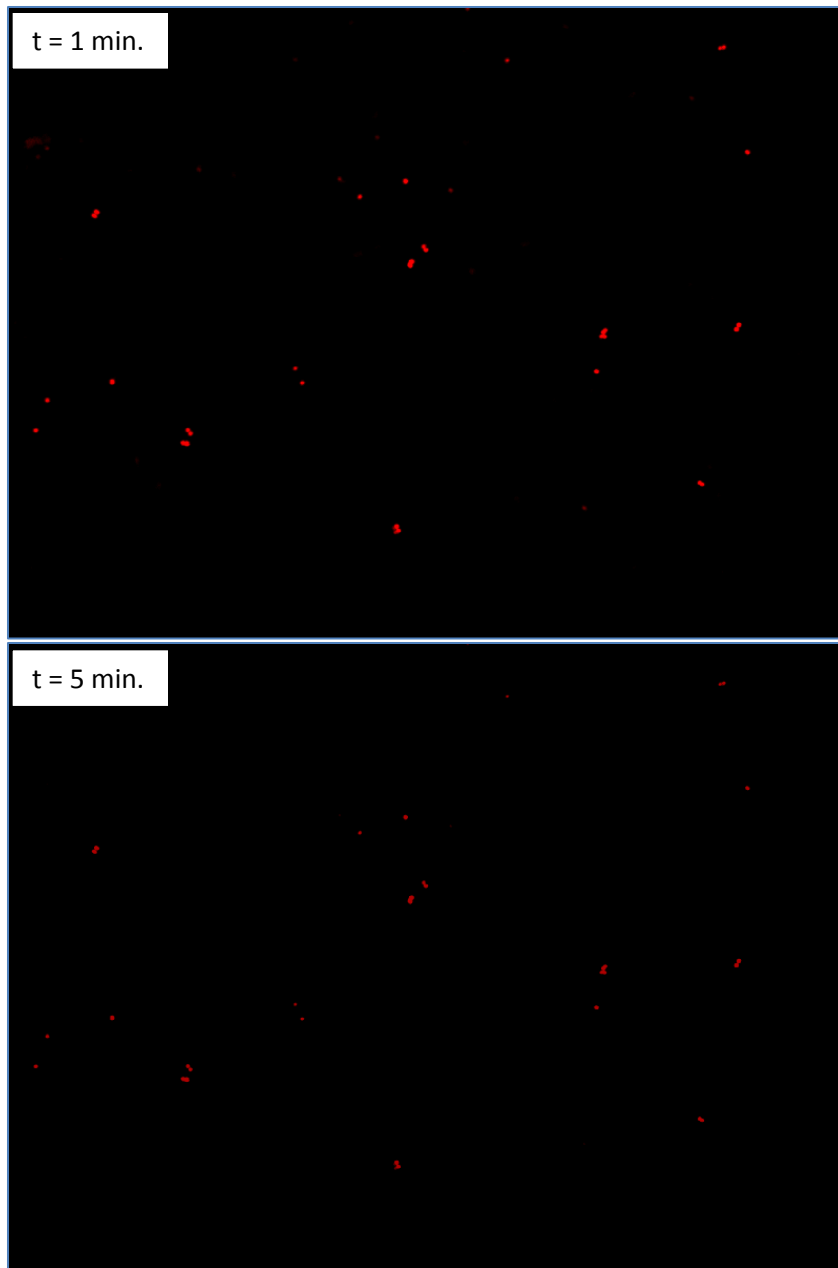
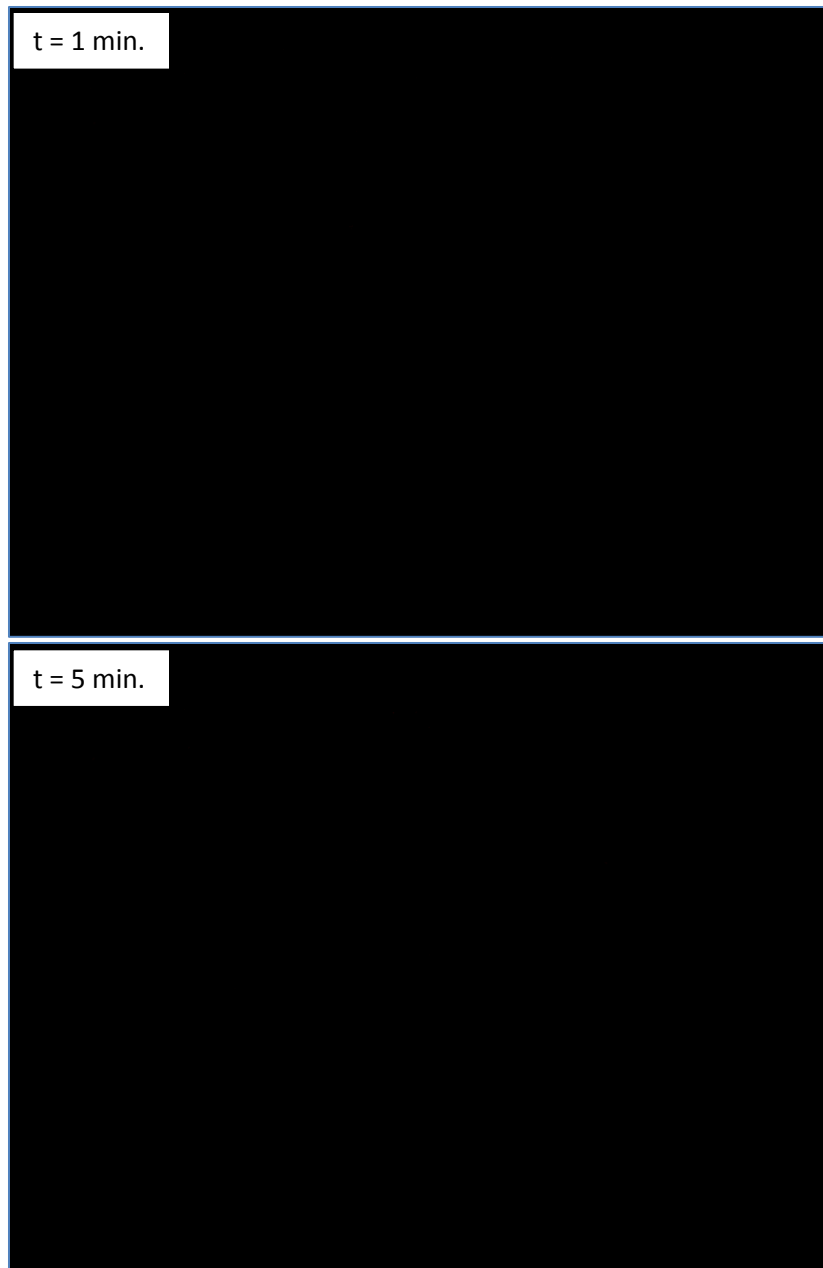


Figure 16. NorA knockout strain (SA-K1758) after one minute and 5 minutes suspended in broth and 1mg/mL aerial ethanolic extract of *Hydrastis canadensis*.

When the knockout strain was treated with the aerial ethanolic extract of *Hydrastis canadensis* there was no observable change in fluorescence between one and five minutes of being resuspended (**Figure 16**). This confirmed the extract itself had no effect on the fluorescent properties of the ethidium bromide being exported from the cells without the NorA pump. Thus, any retention of fluorescence using the complemented NorA strain (SA-K2708) would not have resulted in the inherent fluorescent properties of the extract, but would have resulted from the inhibition of the NorA pump.



**Figure 17. NorA complemented strain (SA-K2708) after one minute and five minutes suspended in MH broth.**

The confocal images of the NorA complemented strain after suspension using broth (vehicle control) showed no observable fluorescence of ethidium bromide at  $t = 1$  minute or  $t = 5$  minutes (**Figure 17**). Seeing no fluorescence suggested the no (or very little) ethidium bromide was retained in the cells. It was concluded the increased production of the NorA pump, for which ethidium bromide is a substrate, effluxed the ethidium bromide outside the cell within the first minute of suspension with broth. Upon repetition, including increased concentration of bacteria, no change in results were observed.

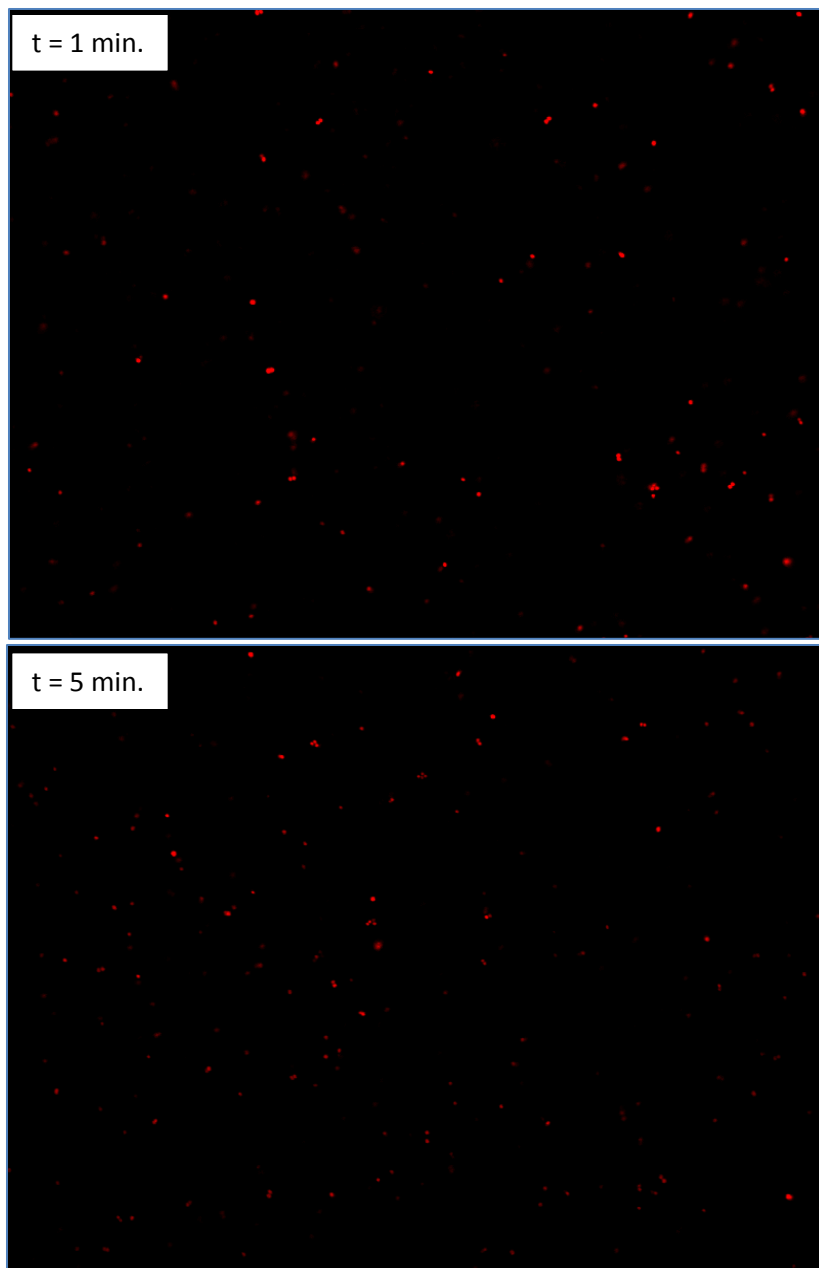


**Figure 18. NorA complemented strain (SA-K2708) after one minute and five minutes suspended in broth containing 100  $\mu$ M carbonyl cyanide m-chloro-phenylhydrazone (CCCP).**

When the NorA complemented (SA-K2708) was treated with the positive control CCCP, the level of fluorescence was retained after one minute (**Figure 18**) fluorescence of the ethidium bromide within the cell was observed using the confocal microscope. Although the fluorescence appeared to decrease slightly after five minutes, enough ethidium bromide was retained inside the bacteria cells to observe fluorescence. This suggested that CCCP inhibited the efflux of ethidium bromide outside the cells by preventing the function of the NorA efflux pumps, which is consistent with the published activity of CCCP as a compound that disrupts the proton motive force.<sup>110</sup>



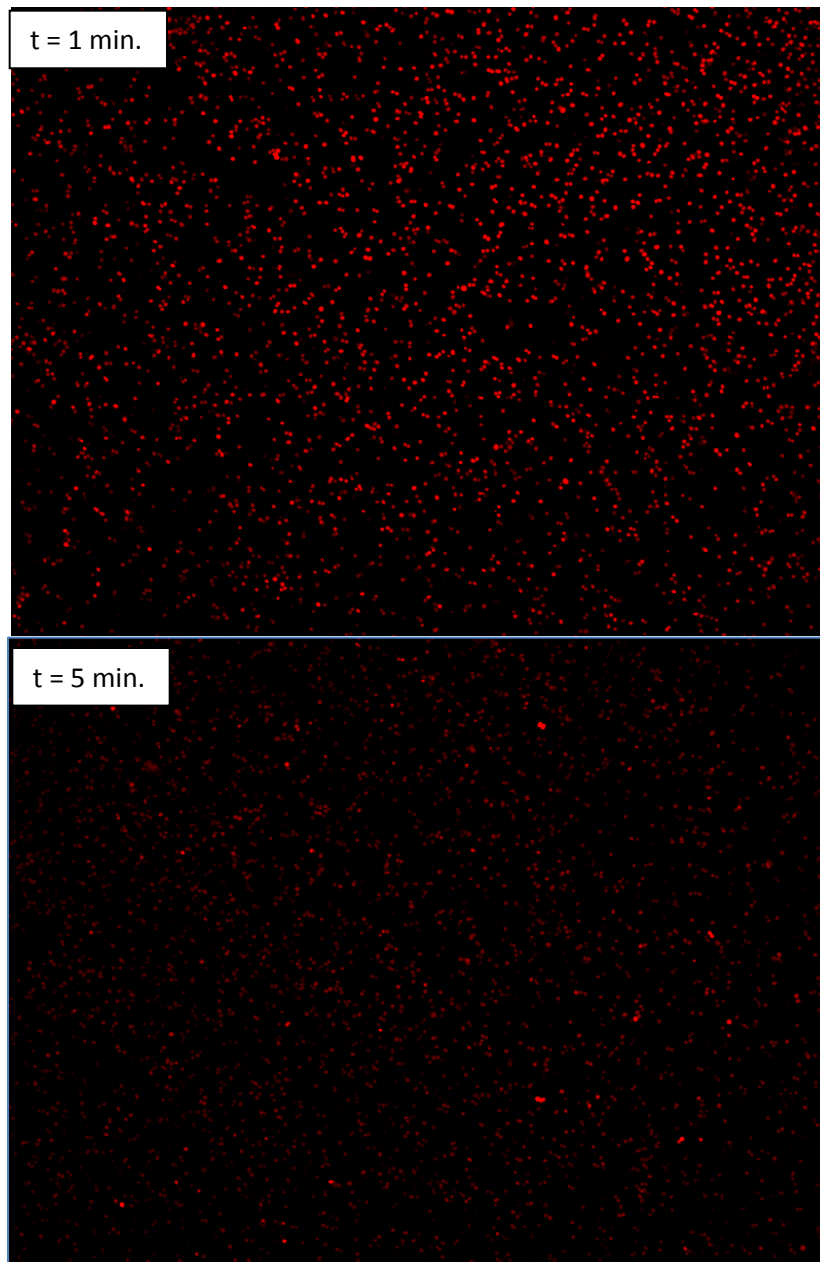


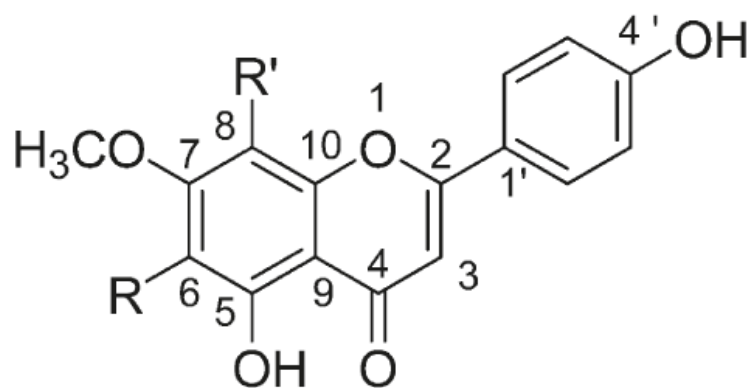
Figure 19. NorA complemented strain (SA-K2708) after one minute resuspended in broth in broth and 1 mg/mL aerial ethanolic extract of *Hydrastis canadensis*. Image was taken using confocal microscope.

When the NorA complemented (SA-K2708) was treated with the aerial ethanol extract of *Hydrastis canadensis*, the level of fluorescence measured after one minute was significant enough to be observed (**Figure 19**). Although the fluorescence appeared to decrease slightly after five minutes, enough ethidium bromide was retained inside the bacteria cells to observe fluorescence. It was concluded the plant extract inhibited the efflux of ethidium bromide outside the cell because the retention of fluorescence compared to the vehicle control was significantly higher.

Through comparing the images of the knockout strain and the complemented strain, inhibition of ethidium bromide efflux was confirmed. In the study with SA-1758 (NorA knockout) there was no change in fluorescence upon treatment with the plant extract when compared to the vehicle and positive controls; however, the NorA complemented strain (SA-2708) showed a significant retention in fluorescence over the total time of 5 minutes when treated with the plant extract and CCCP compared to vehicle control, which showed no fluorescence.

### 3.4.3 Quantification of efflux inhibition

The goal of this experiment was to quantify the inhibition of NorA efflux pumps by *H. canadensis* extracts and flavonoids by measuring the fluorescence over time with cells loaded with ethidium bromide. Using this technique, we sought to determine whether root or aerial *H. canadensis* extracts were more effective at inhibiting efflux, and to also determine the mode of action for synergists isolated from *H. canadensis*. We tested the hypothesis, based on previous literature<sup>111</sup>, that *H. canadensis* flavonoids (**Figure 20**) inhibit the function of the NorA MDR pump. Efflux pump inhibitory activity would explain the observed synergism with the antimicrobial alkaloid berberine, reported in Chapter II and elsewhere.<sup>112 113</sup>



- 1: R = CH<sub>3</sub>, R' = CH<sub>3</sub>  
 2: R = CH<sub>3</sub>, R' = H  
 3: R = H, R' = CH<sub>3</sub>

Figure 20. Synergists isolated from *H. canadensis* following the synergy-guided fractionation process (Figure 6) were determined to be the flavonoids sideroxylin (1), 8-desmethyl-sideroxylin (2), and 6-desmethyl-sideroxylin (3).<sup>114</sup>

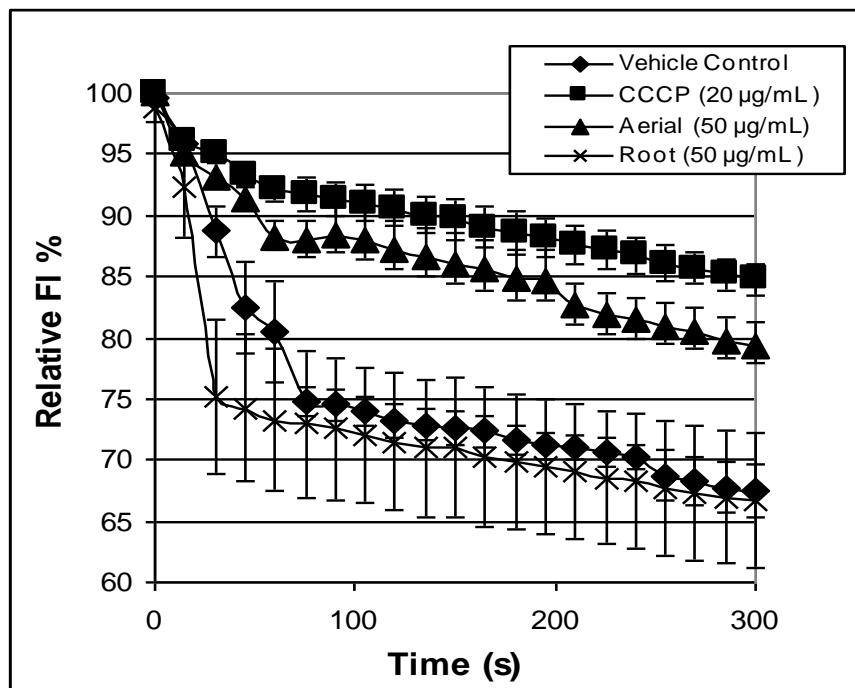


**Figure 21. Percent fluorescence over time for *S. aureus* (NCTC 8325-4) loaded with ethidium bromide and treated with various extracts and controls.** Treatments included the known efflux pump inhibitor CCCP (positive control), and extracts from the roots and aerial portions of *H. canadensis*. All extracts and CCCP were dissolved in Müller Hinton broth containing 2% DMSO. Data points represent the average of three separate experiments (using 3 different pellets of *S. aureus*). Error bars are  $\pm$  standard error.<sup>113</sup>

An ethanol extract prepared from aerial portions *H. canadensis* (as described in Section 2.3.2) was shown to inhibit efflux of ethidium bromide from wild-type *S. aureus* (Figure 21), but not for the knockout strain (Figure 22). For wild-type *S. aureus*, the percent of ethidium bromide fluorescence after 5 minutes compared to the initial reading for bacteria in broth alone was  $66.7\% \pm 5.5\%$  for the root extract ( $50\ \mu\text{g}/\text{mL}$ ),  $79.2\% \pm 1.2\%$  for the aerial extract ( $50\ \mu\text{g}/\text{mL}$ ), and  $84.73\% \pm 1.29\%$  for the positive control (CCCP at  $20\ \mu\text{g}/\text{mL}$ ). The results for the CCCP and the aerial extract were significantly different from that of the negative control (ethidium bromide loaded

bacteria in Müller Hinton broth with 2% DMSO), with p values of 0.002 and 0.02, respectively. There was no significant difference in % fluorescence between the root extract and the negative control after 3 minutes. For the *norA* deleted *S. aureus*, no significant inhibition of ethidium bromide efflux was observed for any of the treatments (*H. canadensis* aerial extract, *H. canadensis* root extract, or CCCP) after 5 min (**Figure 22**). This suggested the NorA MDR inhibitors were present in the aerial portions of the plant but not the roots. These findings are consistent with the greater synergistic activity observed for the aerial extract, as described in Chapter II.

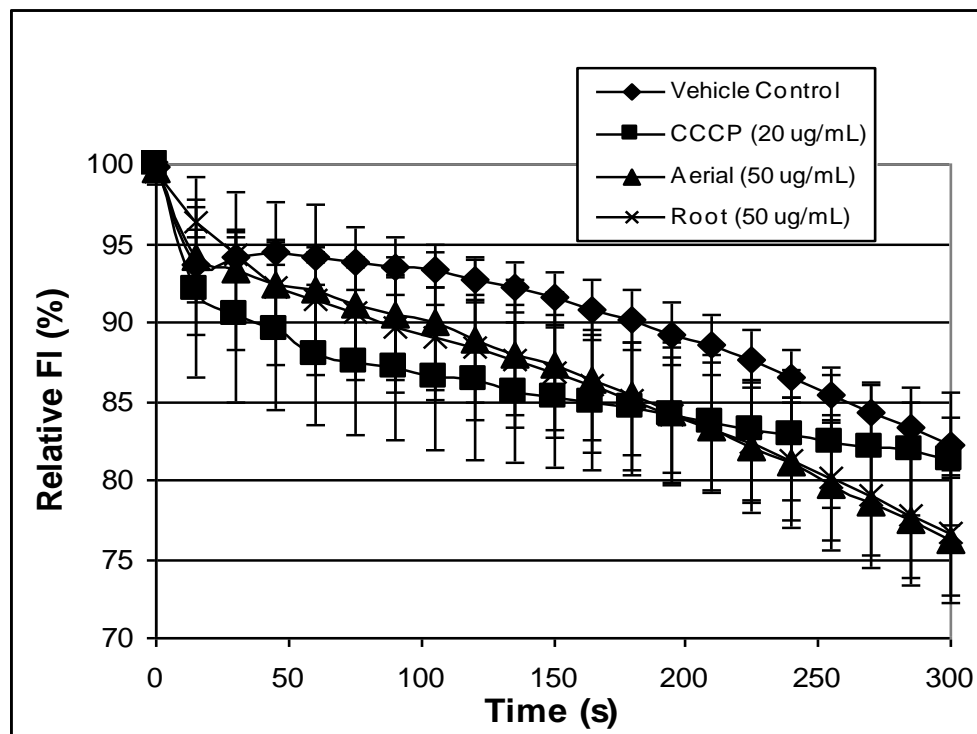


**Figure 22. Percent fluorescence over time for the *norA*-deleted (SA-K1758).** Conditions were the same as described for Figure 21.

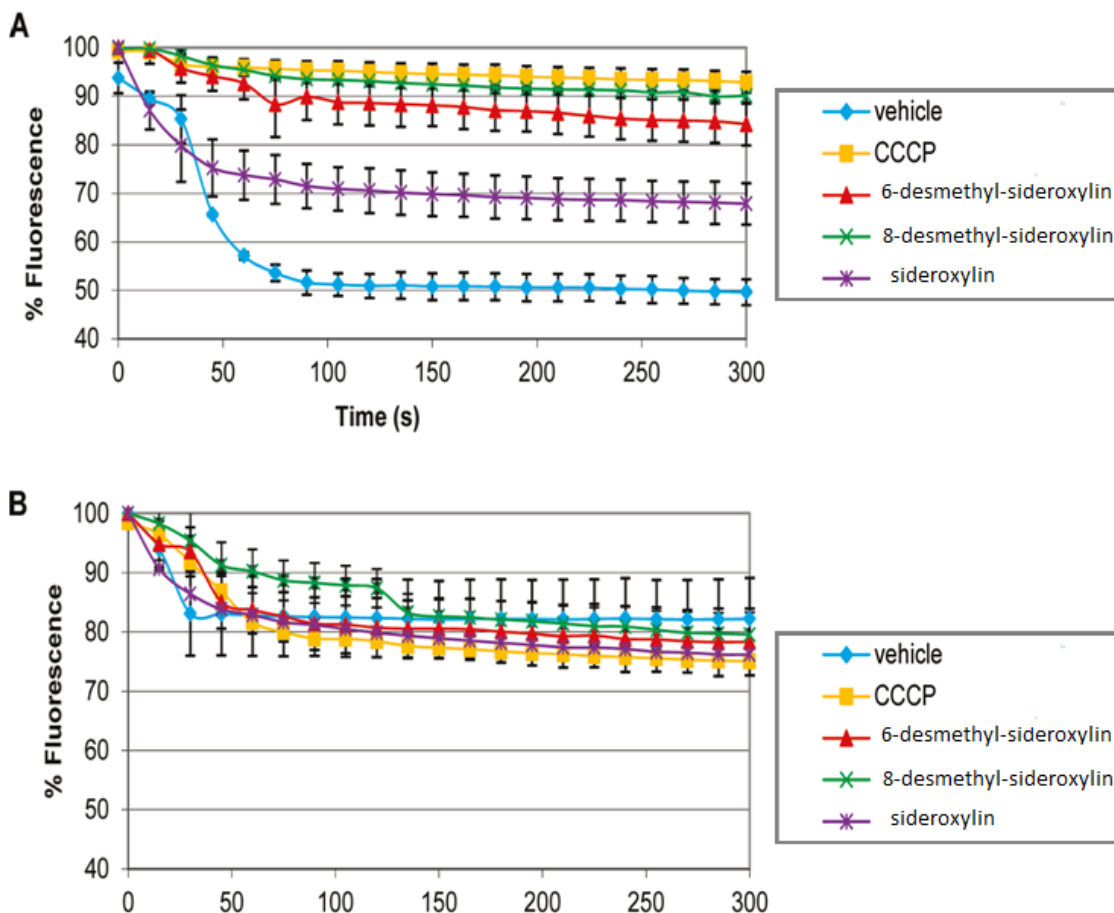


**Figure 23. Percent fluorescence over time for the three flavonoids from *Hydrastis canadensis* inhibit the NorA efflux pump of *S. aureus* (NCTC-8325-4) (A) and the NorA deleted (SA-1758) (B) . Treatments included the known efflux pump inhibitor CCCP (positive control). The flavonoids were dissolved in Müller Hinton broth containing 2% DMSO. Data points represent the average of three separate experiments (using 3 different pellets of *S. aureus*). Error bars are +/- standard error.<sup>112</sup>**

The results from the ethidium bromide efflux assay with the flavonoids illustrated in **Figure 23** with wild-type *S. aureus* (NCTC-8325-4) showed the positive control carbonyl cyanide m-chlorophenylhydrazone (CCCP) and the three flavonoids retained higher levels of fluorescence in relation to the vehicle control after 5 minutes.



The vehicle control only retained 50% relative fluorescence where as the positive control (CCCP) retained 92% relative fluorescence. Although all three flavonoids significantly inhibited efflux of ethidium bromide (**Figure 23**), they had differing potencies. Of the flavonoids, 8-desmethyl-sideroxylin retained the highest relative fluorescence after 5 minutes with a value of 90% followed by its isomer 6-desmethyl-sideroxylin (88%), and sideroxylin showed partial NorA inhibition (70%) (**Figure 23**). Overall, these findings suggest that the flavonoids isolated from the synergy-guided fractionation process are NorA efflux pump inhibitors. This hypothesis was verified with the knockout (SA-K1758) efflux assay (**Figure 23B**), where neither the flavonoids nor the positive control showed any statistically significant influence on ethidium bromide efflux after 5 min.

### **3.5 Conclusion**

Through implementing various mutant strains of *S. aureus*, a possible mechanism of action in which extracts prepared from *Hydrastis canadensis* enhance the antimicrobial effect of berberine was determined. By characterizing each strain of bacteria to maintain consistent growth conditions, a direct comparison of the results amongst the efflux pump inhibition assays could be preformed. Using a fluorescent substrate for the NorA efflux pump a qualitative observation of the efflux of both the knockout (SA-1758) and complemented (SA-2708) strains was observed under different

treatments. By directly comparing these two strains, activity specifically related to the NorA efflux pump can be determined.

By complementing the synergy-guided fractionation process with NorA efflux pump inhibition with the wildtype *S. aureus* (NCTC-8325-4) we were able to determine the synergistic flavonoids isolated from the aerial portion of *Hydrastis canadensis* acted as NorA efflux pump inhibitors. Through measuring the relative fluorescence of ethidium bromide over time a quantification of activity for both crude extracts and specific compounds can be determined. By comparing the relative fluorescence to that of the knockout strain (SA-1758) verification of the flavonoids' bioactivity could be confirmed as a NorA efflux pump inhibitor.

A broader application of the results is the observation the aerial extracts of *Hydrastis canadensis* appear to be more effective at inhibiting the NorA pump compared to the root extract at the same concentrations. Although there is a higher alkaloid antimicrobial content in the roots (Chapter II) the increased efflux inhibition in the aerial portion of the plant the implementation of sustainable aerial extracts could be of more use in the treatment of infection. This could facilitate commercial application of extracts prepared from *H canadensis* and the optimization of a combination of aerial and root extracts for total antimicrobial activity of an commercially available therapeutic agent prepared from *Hydrastis canadensis* may be worth pursuing.

## CHAPTER IV

### A NEW METHOD TO IDENTIFY NATURAL PRODUCT QUORUM QUENCHERS: MASS SPECTROMETRY-BASED MEASUREMENTS OF AUTOINDUCING PEPTIDE PRODUCTION

#### 4.1 Abstract

**Rationale:** The objectives for these experiments were to directly quantify and optimize the production of autoinducing peptide-I (AIP I) from a clinical strain of MRSA (AH1293), develop a methodology to observe the inhibition of AIP I (quorum quenching) in a 96-well plate assay, and to utilize a bioactivity-guided fractionation approach to identify AIP I inhibitors (quorum quenchers) from natural products.

**Methods:** Methicillin-resistant *S. aureus* (MRSA, AH1263) was grown over a 48 hour period and AIP I production was assessed using LC-MS. Complex extracts of *Hydrastis canadensis* and a *Penicillium* fungus were fractionated using HPLC into 96-well plates and putative quorum quenchers identified. A large scale extraction of *Hydrastis canadensis* was fractionated based on its bioactivity as a quorum quencher to identify possible AIP inhibitors from the plant.

**Results and Discussion:** It was determined that AIP could be identified in the supernatant of filtered bacterial cells using high resolution mass spectrometry (HRMS). In a time course study, it was also determined 20 hours is the optimal growing period under aeration for this MRSA strain, producing concentration of  $27.6 \pm 0.25 \mu\text{M}$  AIP I. Quorum quenching could be observed in a HPLC separation of complex extracts into a 96-well plate for a *Penicillium* fungus. The wells where inhibition was observed corresponded to those containing anthraquinones known to be inhibitors of the Agr pathway. *Hydrastis canadensis* was also shown to be a quorum quencher and the constituents responsible were narrowed down to specific fractions using bioactivity-guided fractionation.

**Conclusion:** Autoinducing peptides can be identified in the supernatant of filtered MRSA (AH1263) cells using UPLC-high resolution mass spectrometry. The Agr system is sensitive enough to use a 96-well plate assay to observe the inhibition of AIP I and probable constituents as quorum quenchers from complex natural products. Detection of AIP via mass spectrometry provides a more direct method for in the identification of possible quorum quenchers compared to fluorescent methods that have previously been used.

## 4.2 Introduction

Presently, *S. aureus* is one of the leading causes of hospital acquired infections, with the fraction of these caused by MRSA increasing each year. In fact, *S. aureus* is the primary source of hospital-acquired infections in sites in which surgery was performed and respiratory tract infections, and second leading cause for nosocomial pneumonia, and cardiovascular infections.<sup>115</sup> In 2005 alone, MRSA related infections numbered over 100,000 and were responsible for over 18,000 deaths.<sup>116</sup> Recently, more virulent strains of MRSA have even spread to the community, called community acquired (CA) MRSA.<sup>117</sup>

A major reason for the hypervirulence of the *S. aureus* strains that cause community acquired MRSA is that they have a highly active quorum sensing system.<sup>118</sup> The quorum-sensing system in *S. aureus*, also called the accessory gene regulator or “Agr” system, is a cell density dependent regulatory system that controls the production of many host-damaging agents or “virulence factors”. The Agr quorum sensing system consists of four genes, AgrD is the precursor for the Agr system activator autoinducing peptide (AIP), AgrA, AgrB, and AgrC are transmembrane proteins responsible for the detection, transportation, and activation of the autoinducing peptide **Figure 24**.<sup>119</sup> This system has a positive reinforcement aspect meaning as the concentration of AIP increases, the pathway is up-regulated in an exponential manner. This system becomes activated when the autoinducing peptide (AIP I) binds to the transmembrane AgrC protein, which further increases AIP production, and eventually stimulates the production of toxin production as well as virulence factors leading to pathogenesis. A

principal concern of MRSA infections is the toxin production causing the negative side effects of inflammation, fever, tissue necrosis, and fatigue. Toxin production itself is a direct result of the activation of the P2 and P3 promoters that lead to RNAlII production in the Agr quorum-sensing pathway.

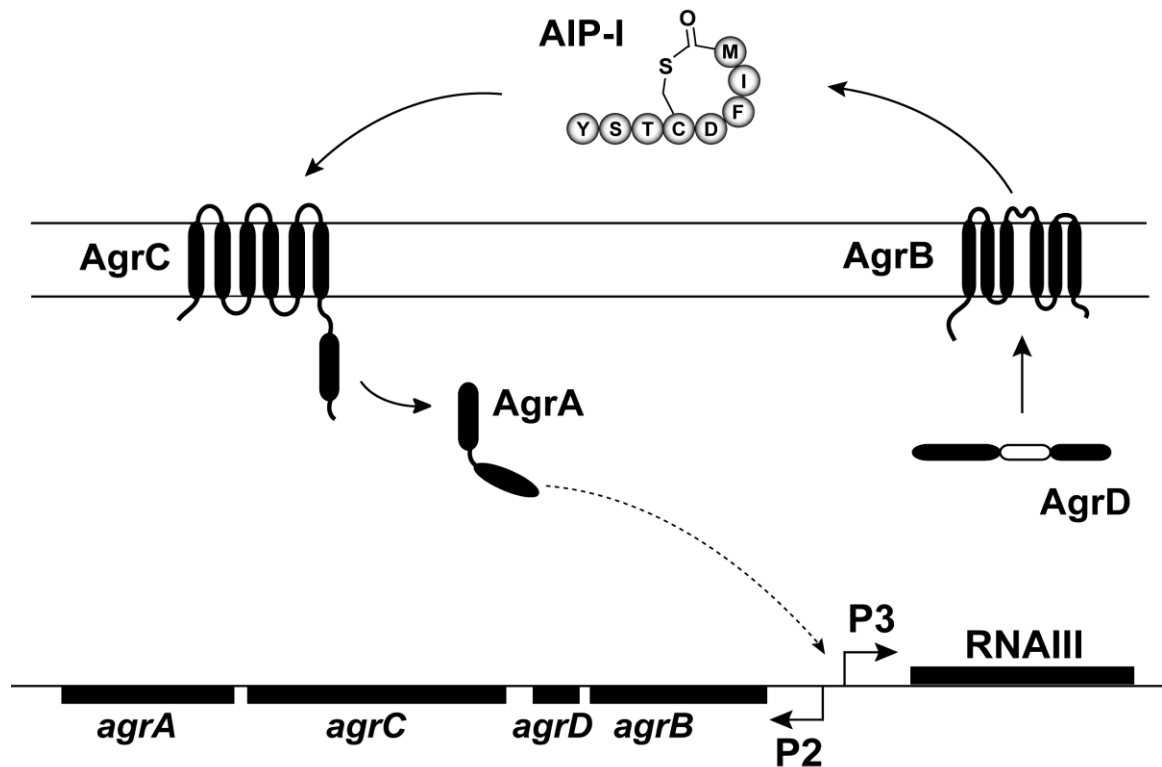


**Figure 24. The Agr system consists of four genes, *agr ABCD*.** The AgrD is the precursor to AIP I, and upon binding to the AgrB it forms a macrocyclic thiolactone (AIP I) and is transferred through the cytoplasmic membrane. AIP I then binds to the AgrC protein, causing the phosphorylation of the AgrA, resulting in the activation of both the P2 or P3 promoter. The P2 promoter activates the Agr system by turning on the AgrABCD genes, while the P3 promoter activates various responses in the bacteria, including the production of virulence factors.<sup>120</sup>

Detection and elucidation of autoinducing peptides has primarily been accomplished through bioluminescence assays using the *lux* reporter gene.<sup>121</sup> In these bioluminescence is a result of the activation of the P3 promoter and production of RNAIII. The RNAII is tagged with a Lux reporter to indicate its production. Any disruption to the Agr quorum pathway as a response to treatment would lead to a

decrease in RNA III production and thus bioluminescence. Therefore, quorum quenching is determined by a decrease in relative bioluminescence compared to a vehicle control.<sup>122</sup> This approach inherently does not enable absolute quantification and does not directly measure AIP I production, rather it measures a downstream effect of the Agr system. Furthermore, there are cases where fluorescence based assays yield false results due to fluorescence quenching, particularly in complex extracts such as those under investigation in this study. For these reasons, a primary objective of this experiment is to develop a new assay that directly measures AIP I, a direct product of the Agr system, and to modify it to be compatible with a 96-well plate assay to test fractionated extracts as shown in the schematic of **Figure 25**.



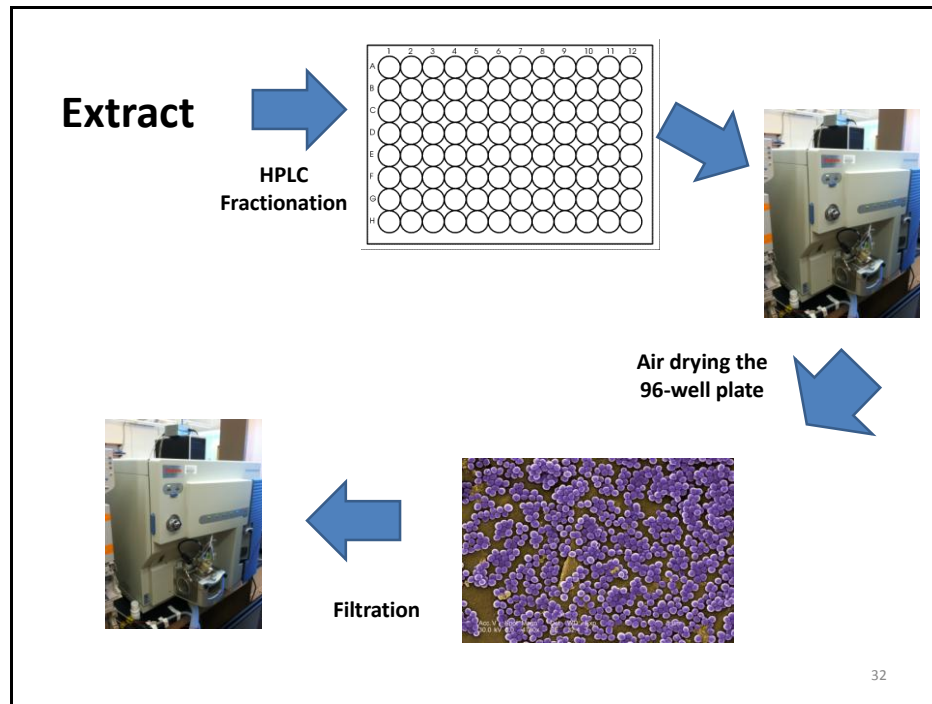


**Figure 25. Schematic showing the detection of AIP I in 96 well plate format.**

The extract is fractionated and analyzed on the mass spectrometer. The plate is dried and resuspended with MRSA (AH1263), grown under aeration (20 hrs), filtered and the culture supernatant analyzed using mass spectrometry to determine the AIP I production.

### 4.3. Methods

#### 4.3.1 Detection and quantification of AIP I in MRSA (AH1263) in a time-course study

For the time course study, a 24 hr culture of MRSA (USA 300 strain AH1263) was diluted 1:100 in tryptic soy broth and grown with shaking for 48 hrs. An aliquot was removed every hour, the  $OD_{600}$  was recorded, and the culture was filtered through a 0.2  $\mu$ M membrane and analyzed using LCMS.

Samples were analyzed utilizing an LTQ Orbitrap XL mass spectrometer with electrospray ionization source (Thermo, San Jose, CA) coupled to an Acquity UHPLC HSS T3 (Waters, Milford, MA). A C18 column (Acquity BEH, 2.1 mm × 50 mm, packing) was used. Flow rate was 0.25 mL/min, and injection volume was 3 µL. Samples were eluted at 0.25 mL/min using a two-step gradient from 80:20 to 40:60 water:acetonitrile (both containing 0.1% formic acid) from 0 to 5 min, then from 40:60 to 80:20 from 5 to 5.5 min. The Orbitrap was operated over a scan range of m/z 300 to 2000, with resolving power of 30,000. MS–MS was conducted in data dependent scanning mode, using a collision induced dissociation (CID) activation energy of 35%. Instrument parameters were as follows, tube lens voltage, 100 V, source voltage, 4.50 kV, source current, 100.00 µA, and heated capillary voltage, 20 V. The AIP I concentration was calculated based on a calibration curve generated as area of the relevant selected ion peak versus concentration. A mass of  $961.3794 \pm 0.0048$  (calcd accurate mass for the  $[M+H]^+$  ion of AIP-I,  $\pm 5$  ppm) was set for the selected ion chromatogram, and AIP I concentrations were calculated using the slope of the best-fit line of this calibration curve, as determined with linear regression analysis. This 5 ppm window was chosen to reduce interference from isobaric matrix components.

#### **4.3.2 AIP inhibition assay in 96-well plate from fractionated natural products**

An aerial ethanol extract of *Hydrastis canadensis* and a crude chloroform extract from a *Penicillium* fungus were separated on an analytical HPLC into a 96-well plate. A

20  $\mu$ L sample at 10 mg/mL in methanol was injected onto a Gemini-NX C18 column (250 x 4.6 mm). Samples were separated at a 1 mL/min flow rate with fractionation every 15 seconds. The gradient was MeOH:Water from 10:90 to 100:0 over 24 min, yielding a total of 60 fractions into the 96-well plate. The positive control for all inhibition assays was an autoinducing cyclic peptide (AIP II) from another strain of *S. aureus* known to disrupt the Agr quorum sensing pathway in *S. aureus*.

Mass profiles were generated for each well in each plate. Each well was analyzed utilizing an LTQ Orbitrap XL mass spectrometer in the same methodology described earlier. The wells were dried down under air and resuspended in broth inoculated with *S. aureus* USA 300 strain AH1263 after 2 hours of aeration at 300 rpm. The plate was incubated under aeration (300 rpm) for 20 hours with OD<sub>600</sub> readings made every 4 hours to observe growth inhibition. The plate was filtered, and the supernatant was analyzed using UPLC-Mass spectrometry in the same manner described for the time-course study.

#### **4.3.3 Large scale extraction separation**

Pre-weighed air-dried leaves of goldenseal were homogenized using a commercial grinder. The ground leaves were percolated with methanol for 24 hr., at which time the solvent was removed and replaced with an equivalent volume of methanol. The residue-free methanol extract was collected and concentrated in vacuo using a rotary evaporator (Heidolph Laborota 4000 Efficient). The methanol extract was

re-suspended in 9:1 methanol:water and then partitioned with hexane in a separatory funnel. The aqueous methanol layer dried in vacuo and saved while the aqueous layer partitioned with 4:1 ratio of chloroform to methanol in water in a separatory funnel. The hexane layer was collected, dried in vacuo and was set aside for testing.

First stage separation was carried out using a normal phase (silica) gravitational column and fractions collected based on volume. The extract was mixed with celite, ground into a fine powder and separated using a hexane:chloroform:methanol gradient. The initial gradient was 40:60 hexane/chloroform and increased to 0:100 after 3 liters were collected. Collection was then isocratic at 0:100 hexane:chloroform for another liter after which a solvent gradient of 75:25 chloroform:MeOH was initiated and collected for an additional 5 liters. Each liter was assigned a fraction number. An aliquot from each fraction was dried and resuspended at 200 µg/mL with Muller Hinton broth and USA 300 AH1263 and tested for AIP inhibition in the same manner described above.

Second stage chromatography was performed with a Combi *Rf* flash chromatograph (Teledyne-Isco; Lincoln, NE, USA) using a 120 g silica gel column. The gradient for this separation was run based on column volume (CV). The second stage separation utilized increasing concentration of ethyl acetate (EtOAc) in hexane followed by increasing methanol in ethyl acetate up to 100% methanol. The flow rate was at 85 mL per minute with total run length of 22.3

CV (50.3 min). The initial solvent composition of 100:0 hexane/EtOAc was maintained for 0.9 CV (2.03 min) and was then followed by a steep gradient change to 0:100 Hexane/EtOAc over 12 CV (27.1 min). The solvent composition was held isocratic for 3.10 CV (7.00 min) after which the solvent system was switched to MeOH/EtOAc at 3:97 for 1.8 CV (4.06 min) followed by 10:90 over 1.3 CV (2.93 min), 20:80 over 1.0 CV (2.56 min), and the final gradient at 100:0 MeOH/EtOAc over 1.0 CV (2.56min), then held isocratic at the same condition for 1.2 CV (2.71 min) to wash the column.

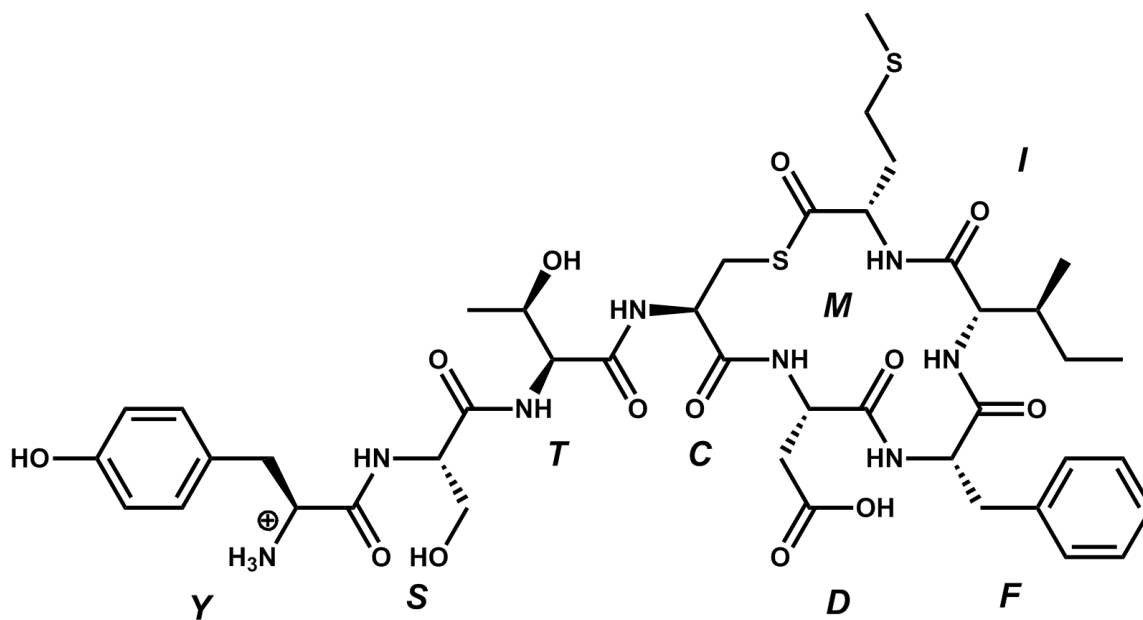
#### **4.4 Results and discussion**

##### **4.4.1 Time-course production of AIP I by MRSA- AH1263**

The goal of this study was to directly measure, quantify, and optimize the production of the autoinducing cyclic peptide (AIP I) from MRSA (strain AH1263) using ultrahigh performance liquid chromatography (UHPLC) coupled to high resolving power mass spectrometry in a time course study. By developing an analytical method to detect AIP I directly from *S. aureus* media, the levels of AIP I production could be quantified. Direct quantification provides insight to the amount of AIP I needed to reach pathogenesis.

The virulent factor AIP I consists of an eight amino acid sequence with a thiolactone ring linking the sulfhydryl group of the cystine to the  $\alpha$ -carboxyl group of the C-terminal methionine as shown in **Figure 26**. This compound has an exact mass of 960.37140 **Figure 26**, and was hypothesized to be detected in the supernatant of

filtered MRSA. AIP I was detectable in both a standard AIP I at 30  $\mu\text{M}$  in Müller-Hinton broth and a filtered spent media after 20 hours of growth (**Figure 27**). Retention time and the fragmentation pattern of the standard AIP I matched the filtered supernatant of the spent media (**Figure 28**).<sup>121</sup>



**Exact Mass: 961.37940**

**Figure 26. Structure of the cyclic octapeptide AIP 1 in its positively charged form.**

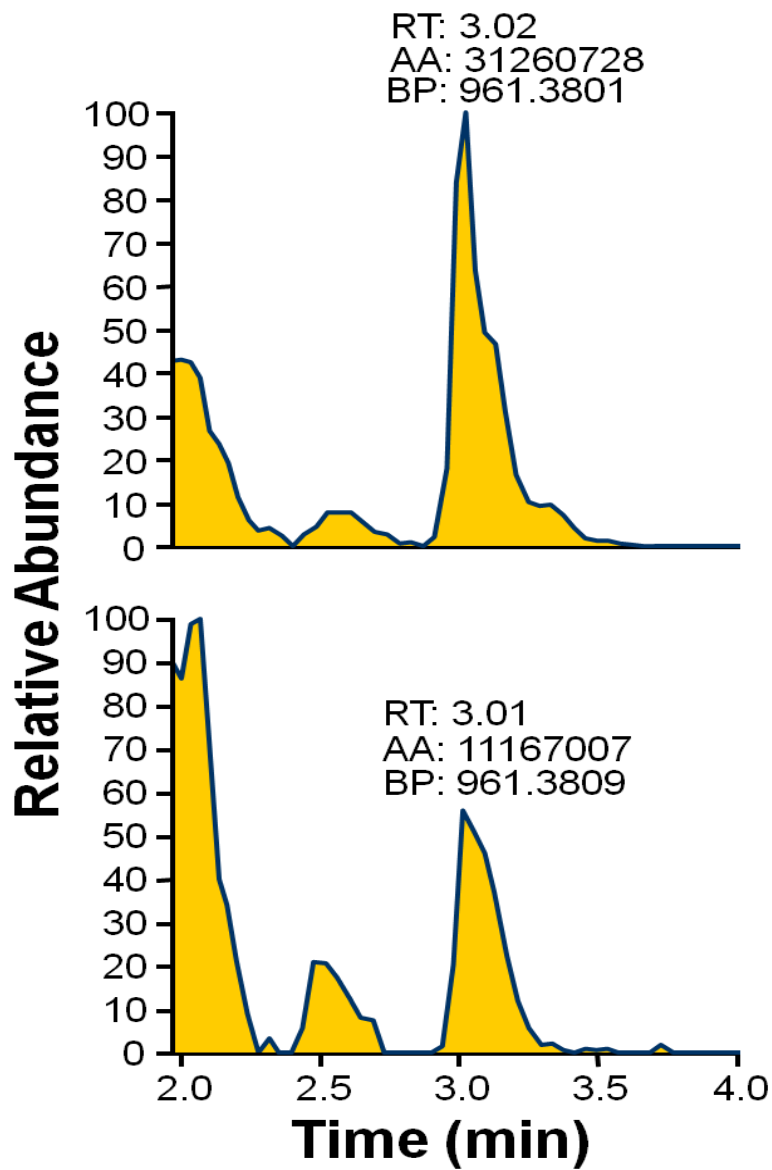
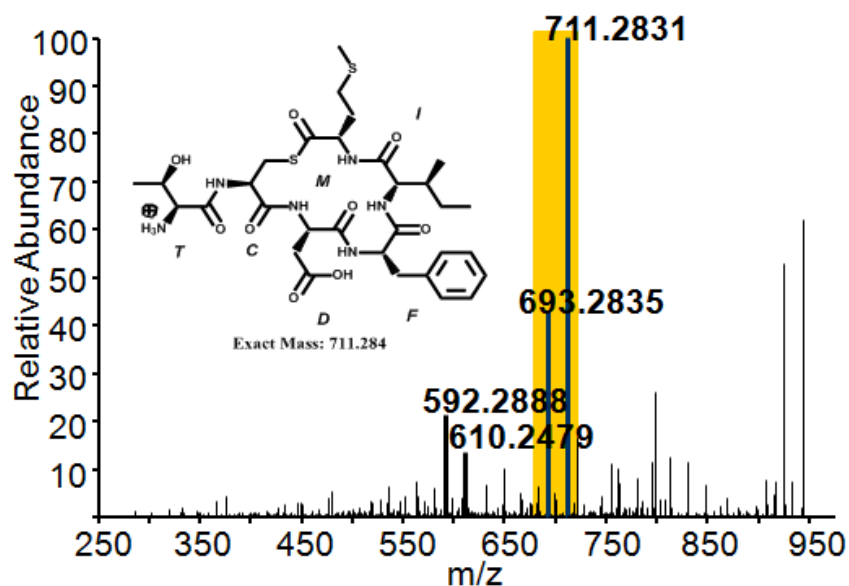


Figure 27A. UHPLC-MS chromatograms of AIP I standard at a concentration of 31  $\mu$ M in tryptic soy broth (*Top*) and a filtered supernatant sample from MRSA-AH1263 after 20 hours incubation in tryptic soy broth.



**Figure 27B.** The MS/MS sepctrum for AIP I, showing the signature fragmentation pattern of the peptide along with its structure. The thiolactone ring remains intact with a mass of 711.2831 confirming the detection of the thiolactone ring of AIP I in **Figure 27A**.<sup>121</sup>

Once it was shown that AIP I could be detected in the spent media, a time-course study was conducted to determine the optimal growing conditions for production of this peptide. Also, by applying a calibration curve of AIP I to the data obtained from the time-course study, the concentration of AIP I could be determined as well (**Figure 28**). Hypothetically, quantification of AIP I would allow other instruments to be utilized for the detection of AIP I as long as they were tuned to detect the peptide at the described  $\mu\text{M}$  concentrations (20  $\mu\text{M}$ ). By establishing the quantification of AIP I production over the course of time, future research may be aided in understanding the Agr pathway and the threshold concentration needed to promote virulence in further



detail. The results from this experiment were essential to establish the best conditions under which to test for the inhibition of the production of AIP I in 96-well plate assay format.

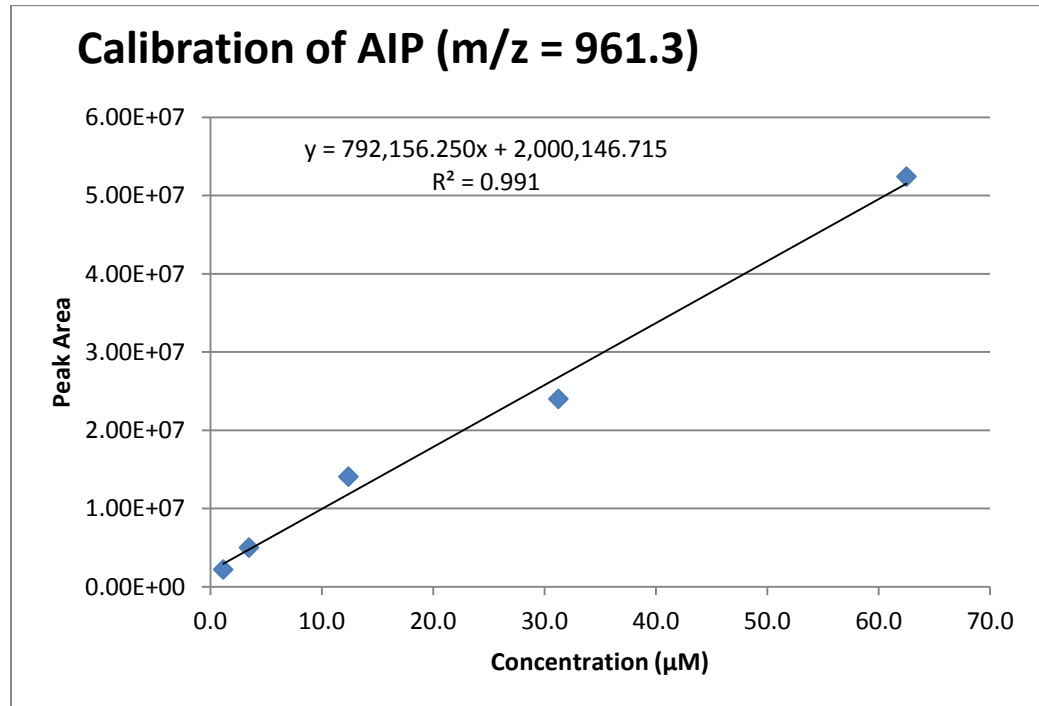


**Figure 28. Cabration curve of AIP I in tryptic soy broth.**

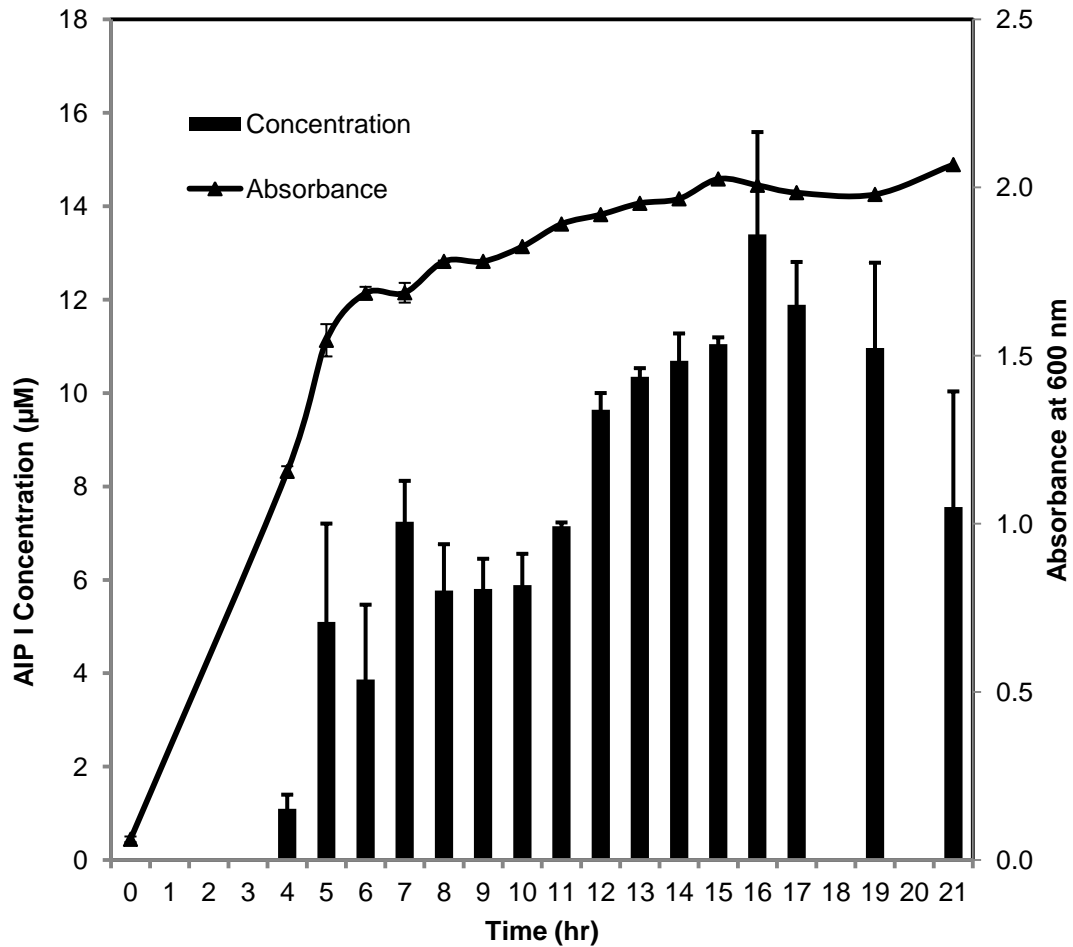


**Figure 29. The concentration of AIP I produced by Methicillin-resistant *S. aureus* was measured over a 48 hour time course study.** This plot shows the concentration of AIP I and absorbance vs. time.

The time-course study (**Figure 29**) shows that the production of AIP I begins to levels after 20 hr, indicating the optimal growth period for MRSA AH1263. Although the bacteria entered lag phase (the point where absorbance does not increase significantly over time) at around 8 hours, AIP I production continued to rise steadily until the 20 hour time point. This suggested significant increase in AIP I production occurs after the

bacteria reach a stationary phase. This data helped to determine optimization of the 96-well plate assay described later.

#### **4.4.2 Method development AIP I inhibition assay in 96-well plate using a *Penicillium* fungus**

The goal of this study is to determine if fractionating a crude concentrated extract could indicate compounds responsible for disrupting the Agr quorum sensing pathway through inhibiting the production of AIP I. The purpose is to develop a methodology to identify active biological extracts, and to correlate the activity to likely constituents within the extract.

Dr. Nicholas Oberlies' lab at the University of North Carolina at Greensboro, through the isolation and testing of unique compounds from a *Penicillium* fungus, identified a series of anthraquinones that inhibit AIP I production by MRSA strain AH1263 in the  $\mu\text{M}$  concentration range (**Figure 30**). We employed a crude extract of the same *Penicillium* fungus as a test case for our methodology of identifying quorum quenchers. The goal was to determine if this crude extract could be fractionated into a 96 well plate and the active molecules identified based on their ability to suppress the production of AIP I.

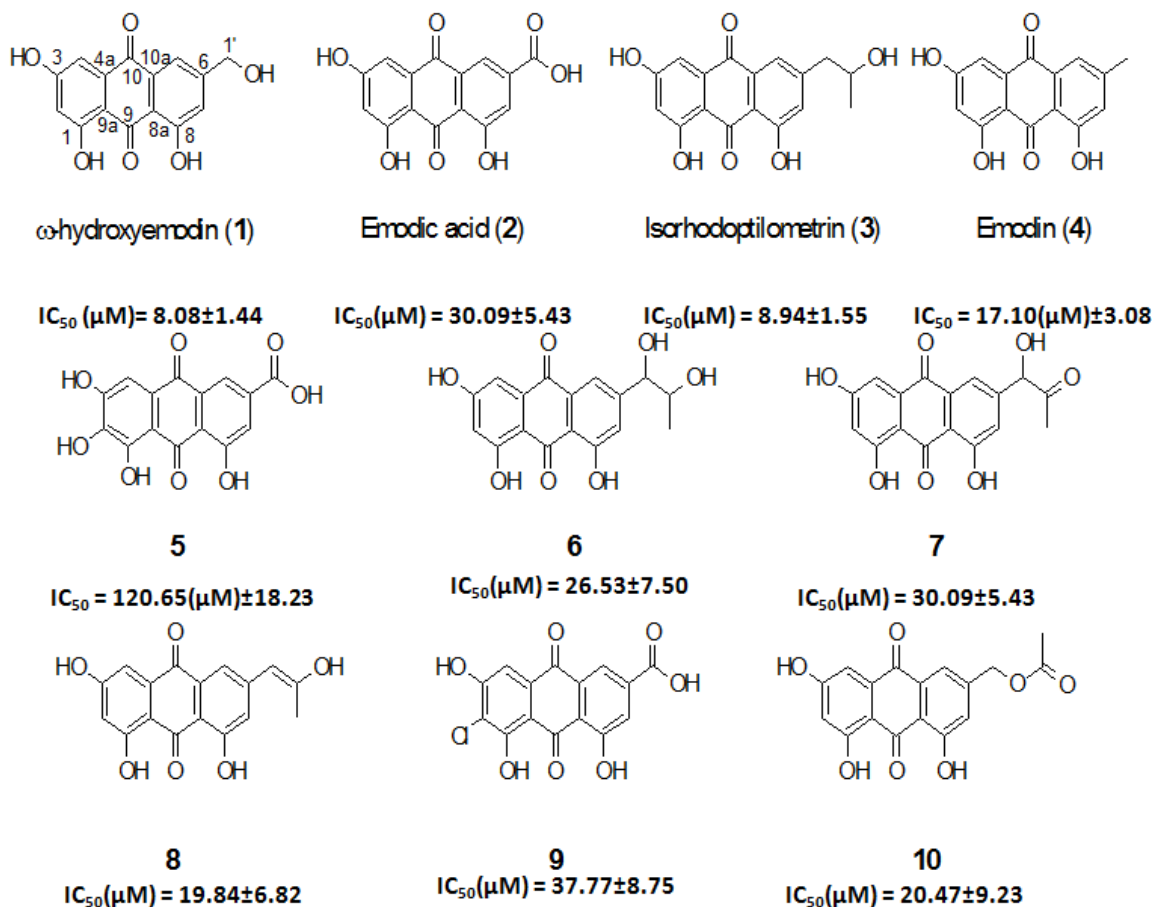


**Figure 30. Bioactive anthraquinones isolated and identified from a *Penicillium* fungus in the laboratory of Dr. Nicholas Oberlies.** The  $IC_{50}$  values indicate the molar concentration needed to observe a 50 % decrease bioluminescence in the *lux* reporter compared to the vehicle control in a gene reporter assay (measured in the laboratory of Dr. Alexander Horswill). The amounts isolated from a large scale extract are also indicated. It is important to note that the compounds without labels have previously never been identified.<sup>123</sup>

After the crude *Penicillium* extract was fractionated using the analytical HPLC, each individual well in the 96-well plate was analyzed using high resolution mass spectrometry to develop unique mass profiles. Four of the bioactive anthraquinones isolated by the Oberlies group were identified in high relative abundance in wells 66-74 (Figure 31). It is likely that the remaining anthraquinones were present in this range of wells, but were undetectable after the single-stage separation process.

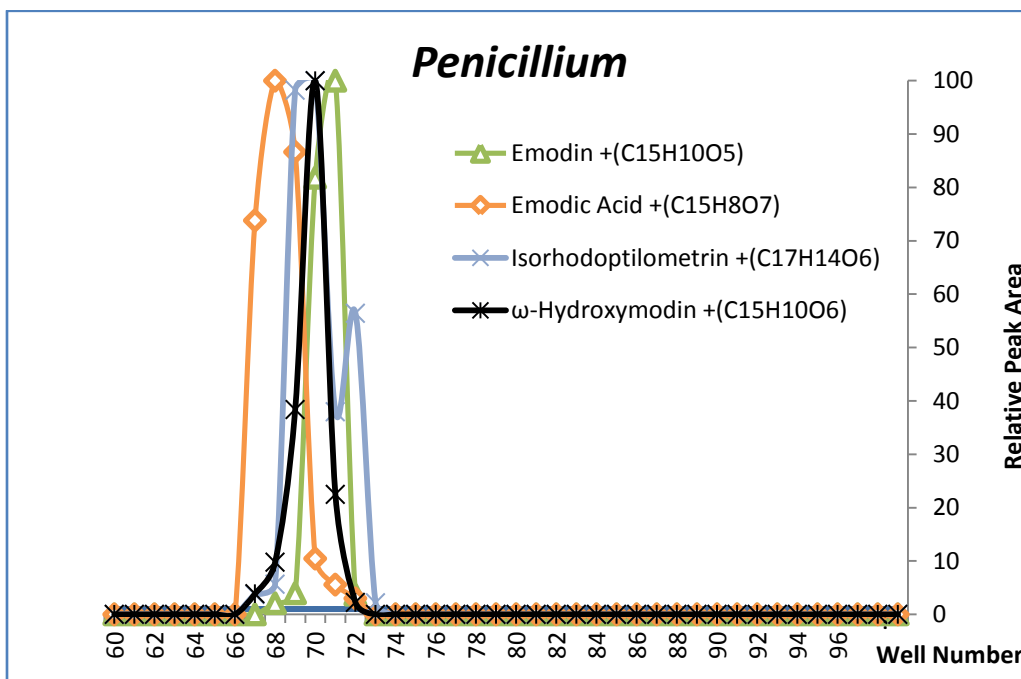


**Figure 31. Detection of the anthraquinones from analysis of a *Penicillium* extract fractionated on an analytical HPLC.** Plotted is the relative peak area (for each individual anthraquinone separately) vs. well number.

The plate containing the *Penicillium* fractions was dried down and resuspended in tryptic soy broth containing MRSA (AH1263) and incubated under aeration with the optimal AIP I producing conditions established above. This plate was then filtered to remove bacteria and relative AIP I levels were measured using mass spectrometry. There were some wells (68-71) in which the amount of AIP I was much lower than others, suggesting inhibition (**Figure 32**). The OD<sub>600</sub> for all wells were not significantly different suggesting no inhibition in the total growth of the bacteria was observed. Absorbance was also monitored throughout the growing process in a duplicate plate every 4 hours to ensure no growth inhibition was observed even a “time lag” effect. This is important because growth inhibition would lower the production of AIP I and lead to a false positive. Again, AIP II served as the control inhibitor and is represented at the end of the well number to indicate a positive control for the inhibition of AIP I production.

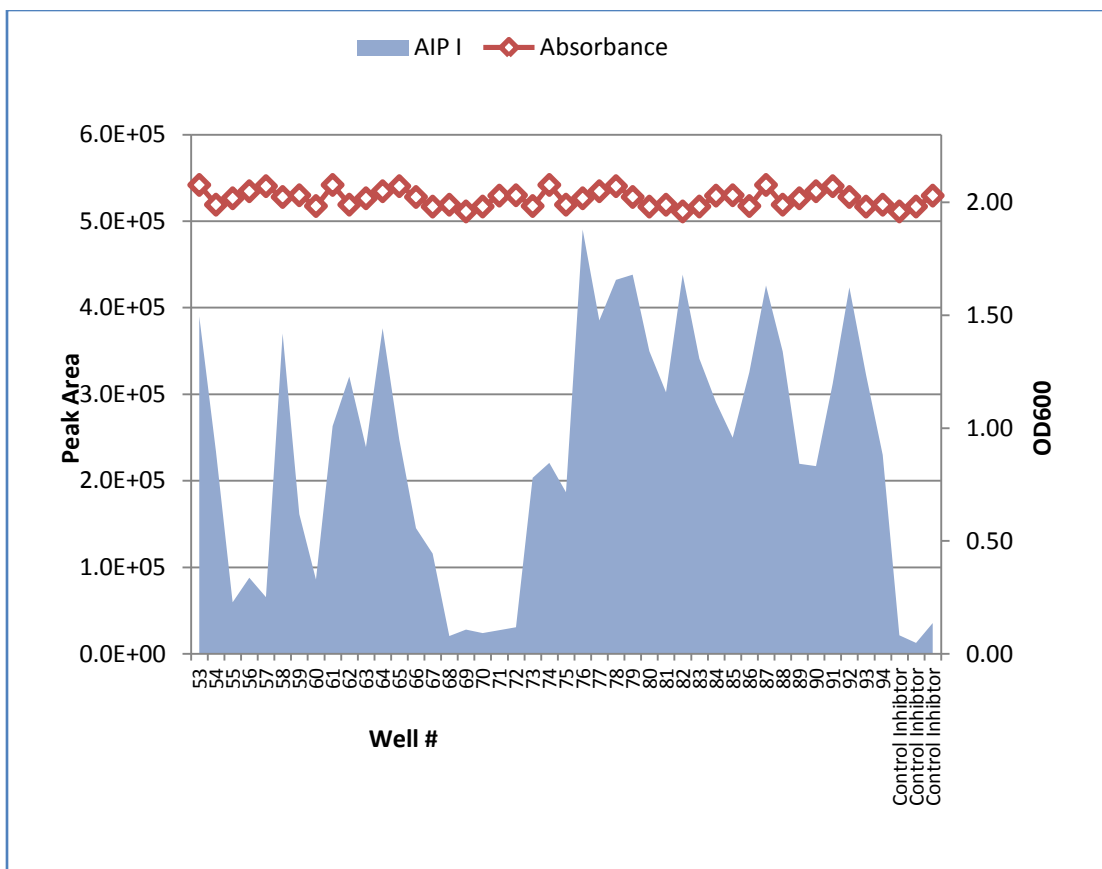


**Figure 32. AIP I detection in *Penicillium* fractions incubated with MRSA using UPLC-MS.** Wells with low levels of AIP I are presumed to contain quorum quenching compounds. A clear suppression of AIP I production was identified from well 68-71.

When the data for anthraquinone detection (**Figure 31**) was overlaid with the data for the AIP I detection (**Figure 32**), it was apparent that the same wells that were very active in suppressing the production of AIP I by MRSA also contained the anthraquinones that had previously been identified as quorum quenchers (**Figure 33**). Although other constituents from the extract undetectable in the mass spectrometer could be responsible for this observed bioactivity, it is hypothesized the anthraquinones were the primary inhibitors of the Agr pathway based on their previous characterized

activities. More importantly, this correlation of mass profiles to activity verified the methodology in detecting possible quorum quenching activity from a complex extract separated in a 96-well plate.

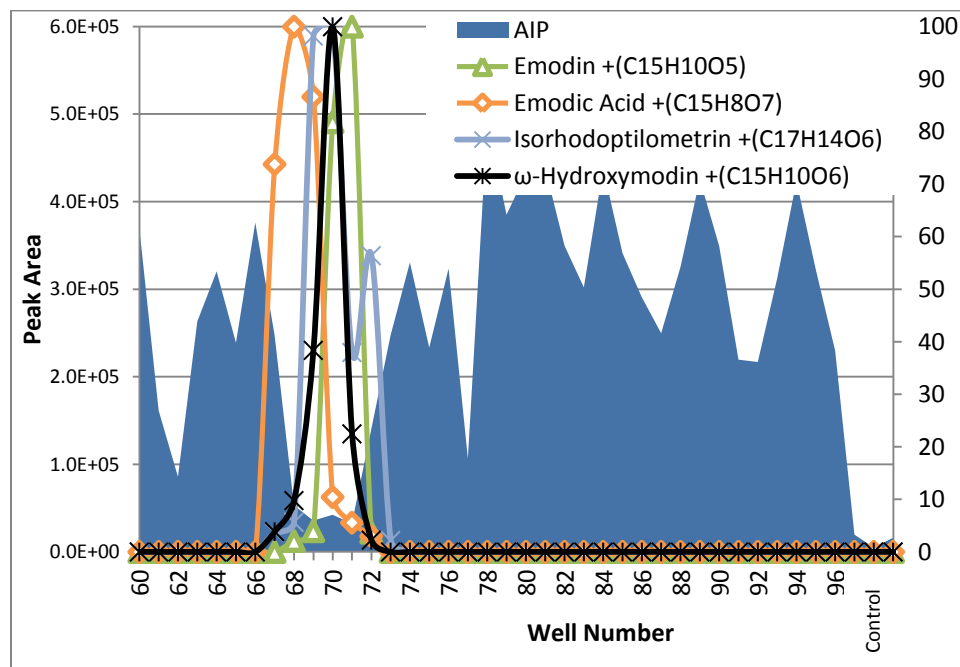


**Figure 33. Overlay of the relative peak areas of the anthraquinones identified using the UPLC-MS with the detection of AIP I.** Bioactivity (AIP I suppression) correlates with the relative abundance of the anthraquinones, confirming the new methodology used to determine AIP I suppression from complex extracts.



#### 4.4.3 AIP I Inhibition assay with *Hydrastis canadensis* after 96-well plate separation

The purpose of this study was to test the methodology employed with the *Penicillium* fungus to see if we could identify disruption of the Agr quorum sensing pathway using a natural product with a known AIP I inhibition effect, but unknown constituents responsible for this effect to correlate inhibition to likely bioactive constituents. The proposed benefits of implementing this method are as follows: a more rapid approach to identifying potential AIP I inhibitors from a complex extract, the potential to separate antimicrobial compounds from possible AIP I inhibitors to eliminate false positives when testing a crude extract, and the ability to determine if activity corresponds to a known constituent of the extract or a previously unidentified compound (dereplication).

It was previously established that a crude methanol extract of the aerial portion of *Hydrastis canadensis* partially inhibited quorum sensing in MRSA sub-growth inhibitory concentrations determined by directly measuring AIP I production.<sup>124</sup> Our ultimate goal is to identify the quorum quenching compound(s) responsible for the activity of this crude extract. By implementing the same methodology as in the previous experiment with the *Penicillium* fungus, we showed there were significant decreases in AIP I production by MRSA-AH1263 after the crude extract was separated using the analytical HPLC into a 96-well plate (**Figure 34**). Also, since the separated extract of *Hydrastis canadensis* was analyzed using the high resolution mass spectrometer before

being tested in the inhibition assay, mass profiles for each well were measured and could be compared with AIP I inhibition results.

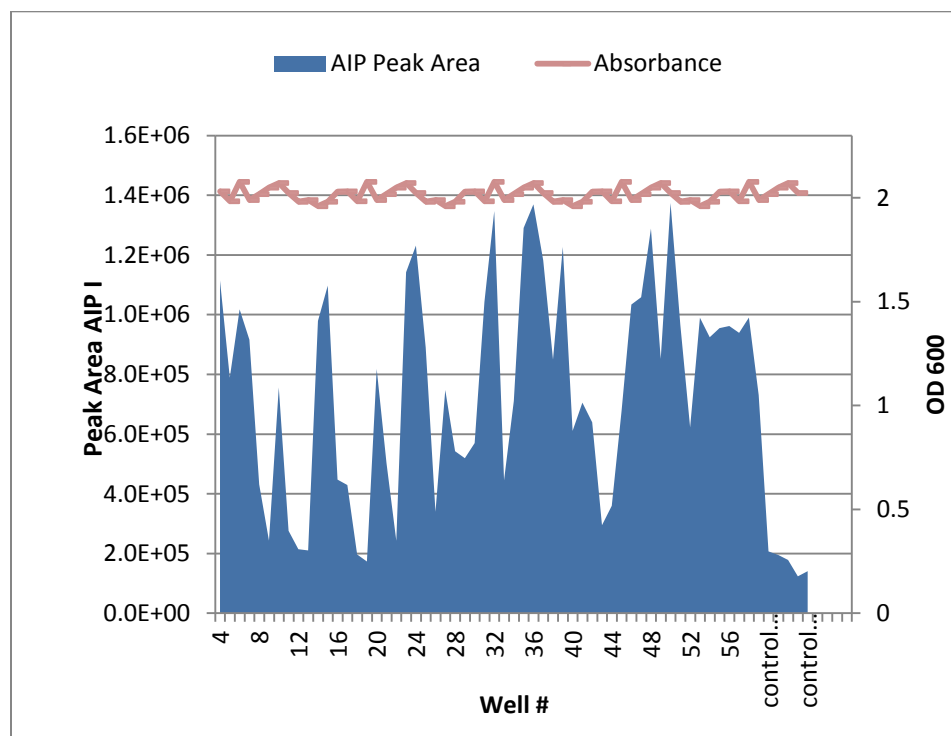


**Figure 34. 96-well plate separation of *Hydrastis canadensis* using analytic HPLC AIP I detection using UPLC-MS.** The lower the level of AIP I Peak area detected the more disruptive those wells were to the Agr quorum sensing pathway. A clear large suppression of AIP I production was identified towards the beginning of separation wells between wells 9 to 22. The figure also shows OD600. It was determined there was no growth inhibition of the bacteria based on the no significant decrease in absorbance amongst wells during the growth of the bacteria.

After observing the suppression of AIP I production, possible masses unique to the wells with activity were correlated with activity (**Figure 35**). Furthermore, by using a high resolution mass spectrometer (Orbi-trap) molecular formula could be determined for the masses corresponding to activity. The known antimicrobial alkaloid berberine

was also plotted to show AIP I suppression did not correspond its antimicrobial properties. This however was not the case when the OD<sub>600</sub> was monitored during the 20 hour incubation period every 4 hours. The wells containing the berberine (wells 4-7) showed a time lag in growth reaching the lag phase around 12 hours as opposed to 8 hours for the rest of the wells.

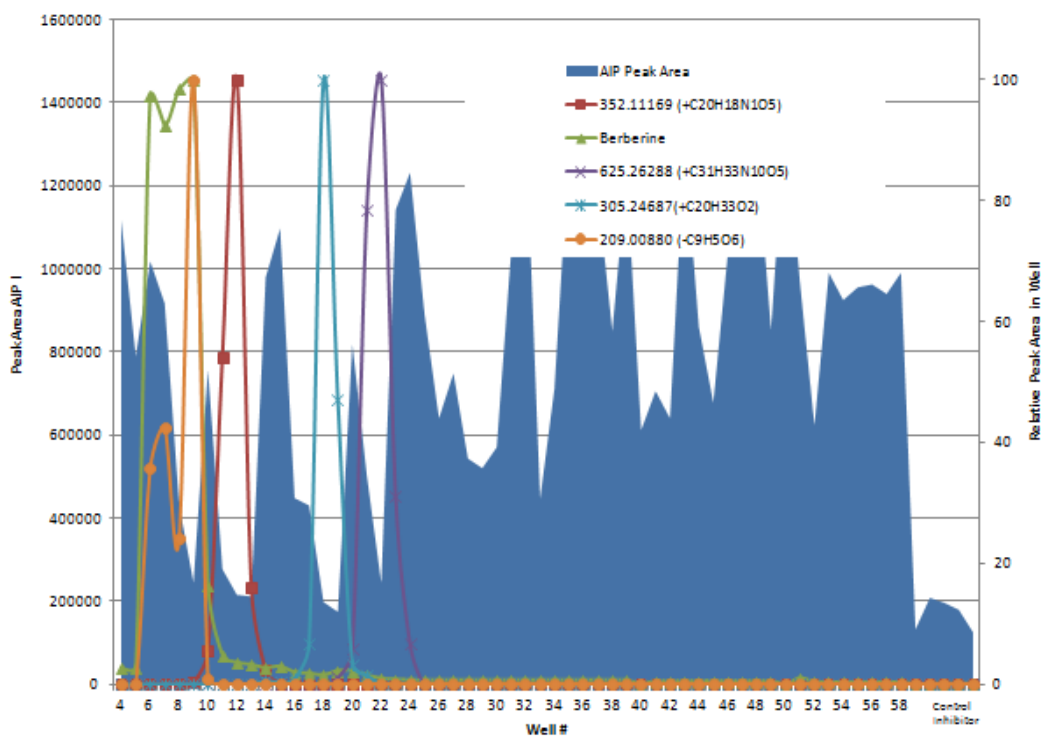


**Figure 35. Plotted are the unique masses in relative abundance corresponding to AIP I suppression.** Molecular formulas were determined using accurate mass data from the Orbi-trap mass spectrometer. The abundance of berberine a known antimicrobial alkaloid is also shown. The control inhibitor is shown on the later part of the graph in the final wells.

Through this experiment, we detected likely inhibitors of the Agr quorum sensing pathway that would be interesting to isolate from a large scale extraction. In wells 8-10 a compound with the mass of 209.00880 ([M-H]<sup>-</sup>) corresponded with bioactivity by increasing in peak while the relative peak area of AIP I decreased. The chemical formula was determined to be C<sub>9</sub>H<sub>5</sub>O<sub>6</sub><sup>-</sup> with a +0.2 ppm error, and the formula in the neutral form had seven hits when searched against the Dictionary of Natural Products. For wells 10-14 a significant activity was observed corresponding to a mass of 352.11169 ([M-H]<sup>-</sup>). Its chemical formula was determined to be C<sub>20</sub>H<sub>18</sub>N<sub>1</sub>O<sub>5</sub><sup>-</sup> (+ 3.2 ppm error) and returned zero hits when search against the Dictionary of Natural Products in its neutral form. The activity for wells 17-20 correlated with an observed mass of 305.24687 ([M+H]<sup>+</sup>). Its formula was calculated to be C<sub>20</sub>H<sub>33</sub>O<sub>2</sub><sup>+</sup> (- 2.4 ppm mass accuracy) and when searched returned 743 hits. For wells 22-24, a mass of 625.26288 corresponded with AIP I suppression. The calculated formula determined to be C<sub>32</sub>H<sub>33</sub>N<sub>10</sub>O<sub>5</sub> ([M+H]<sup>+</sup>) (-4.6 ppm mass accuracy) with zero hits when searched. None of the masses searched in the Dictionary of Natural Products corresponded with previously reported constituents of *Hydrastis canadensis*. Thus, it was determined through these experiments that the bioactivity did not correspond to known constituents found in *H. canadensis*, and therefore it was determined a large scale bioactivity-guided isolation process would be worth pursuing.

A limitation of the data shown in **Figure 35** is that it is difficult to discern which wells cause a statistically significant suppression in AIP I production, and which are

simply random fluctuations in AIP I levels. To verify those fractions that showed inhibition of AIP I production in the 96-well plate, samples from the wells that seemed to be active in **Figure 35** were analyzed in triplicate with a separate assay (**Figure 36**). Most wells corresponding to AIP I suppression from the 96-well assay were confirmed as active. Fractions 16 and 24 did not exhibit statistically significant activity (p values = 0.83, and 0.25 respectively) whereas fractions 9, 13 and 19 did as shown in **Figure 36** p-values (0.001, 0.007, 0.015 respectively). Significant difference was determined using a single factor ANOVA test compared to the control with a  $p < 0.05$  considered significant. We used this information in the large scale extraction process to focus on compounds that corresponded to activity in the 96-well plate assay to guide the isolation process.

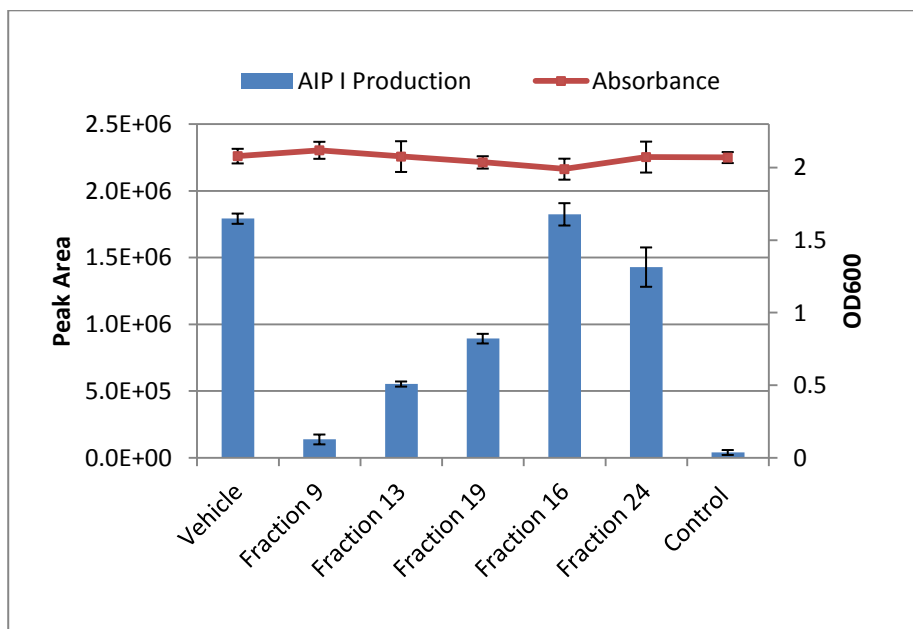


**Figure 36.** Shown in the figure are fractions in the 96-well plate assay that were observed to inhibit AIP I production run in triplicate. Fractions 9, 13, and 19 were determined to disrupt the Agr quorum sensing pathway while fractions 16 and 24 did

To further validate the new assay, several of the same fractions tested for AIP inhibition to the laboratory of Dr. Horswill to test in the *lux* gene reporter assay described previously described (Figures 37-44).<sup>122</sup> In this assay they measured the OD600 and the relative bioluminescence dependent on the concentration of the various fractions. The analysis was run in triplicate and confirmed some of the results obtained in the 96-well plate assay. Both active and inactive fractions determined in the 96-well plate assay were tested to confirm methodology. Also, a vehicle control and the crude plant extract were analyzed for a bioactivity comparison.

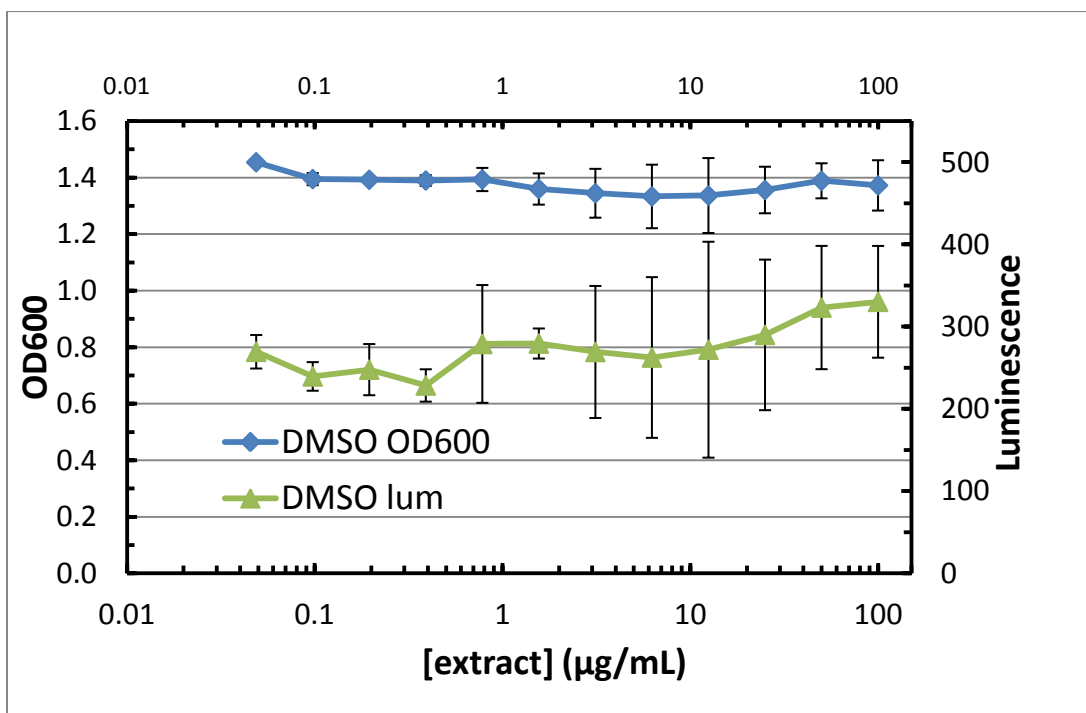


**Figure 37. Vehicle control for the gene reporter bioluminescence assay run in 2% DMSO.** Plotted is absorbance and luminescence run in triplicate.

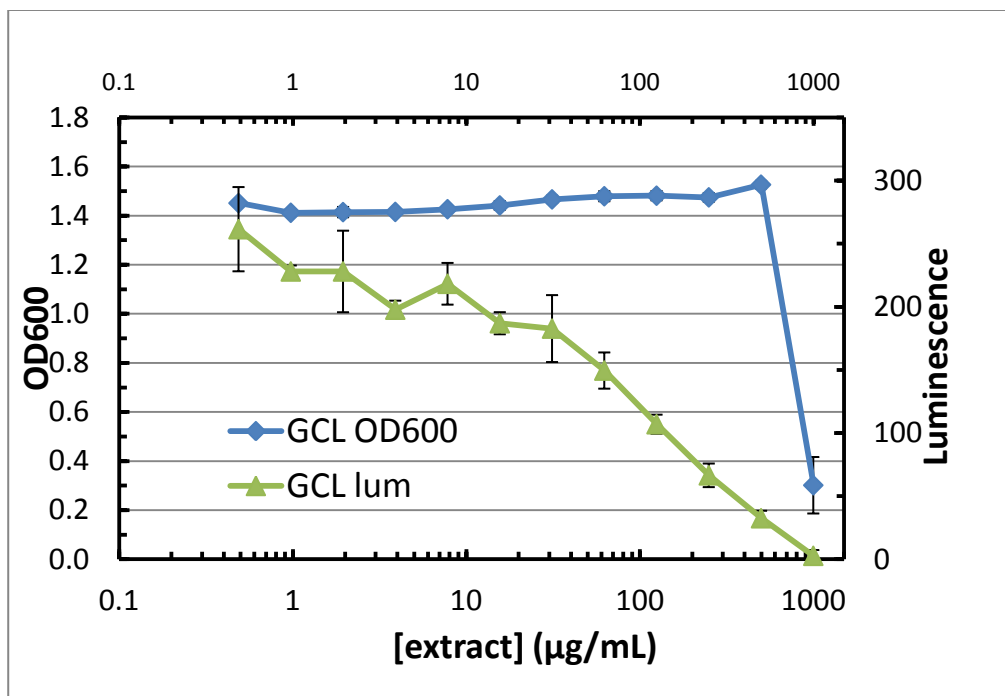


**Figure 38.** Crude *Hydrastis canadensis* extract dissolved in broth and 2% DMSO in the gene reporter assay. Luminescence and OD600 were plotted as a function of concentration.

As the concentration of the plant extract increased the luminescence decreased suggesting there is disruption of the quorum sensing pathway (**Figure 38**). Decrease in luminescence began at a low concentration 5 µg/mL and continued to decrease to 1000 µg/mL. Based on the OD600 readings at 1000 µg/mL the extract inhibited the growth of the bacteria. At this concentration of crude plant extract the antimicrobial concentrations are high enough to inhibit the growth. This growth inhibition confounds the quorum quenching results, but only at high concentrations.

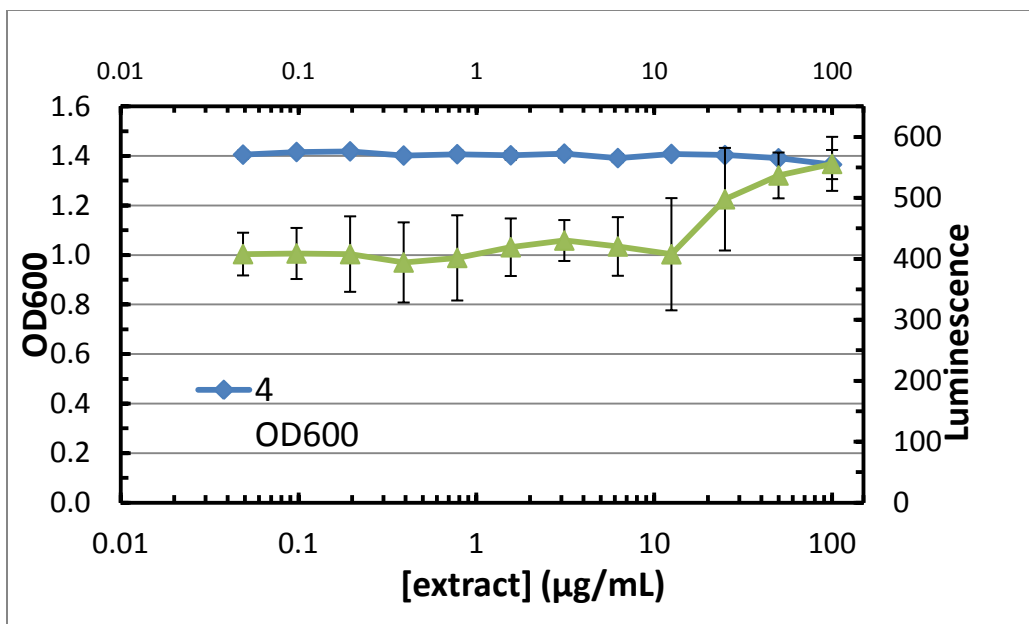


**Figure 39.** Fraction 4 dissolved in broth and 2% DMSO in the gene reporter assay. Luminescence and OD600 were plotted as a function of concentration.



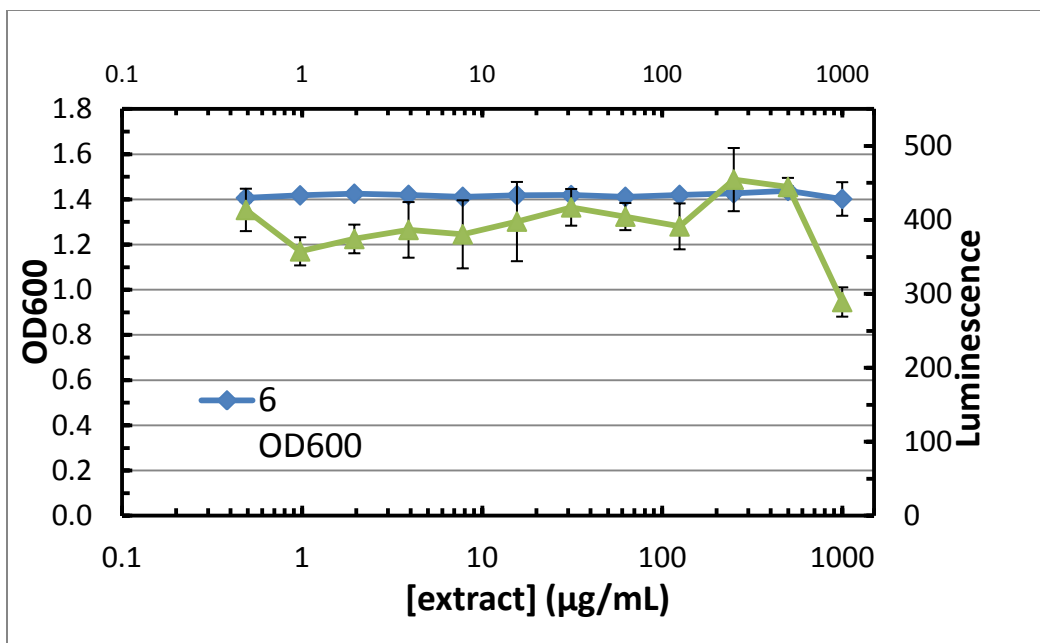


**Figure 40. Fraction 6 dissolved in broth and 2% DMSO in the gene reporter assay. Luminescence and OD600 were plotted as a function of concentration.**

Fractions 4 and 6 had no antimicrobial effect or quorum quenching effect as the concentration increased (**Figures 39-40**). This corresponds to the same result achieved in the 96-well plate assay. Although this fraction contained the known antimicrobial alkaloid berberine, the highest concentration tested (100 µg/mL expressed as dry extract weight per assay volume) was not a high enough concentration to significantly inhibit growth. Based on the results from this assay fraction 4 was not of interest for the identification of quorum quenching or antimicrobial compounds.

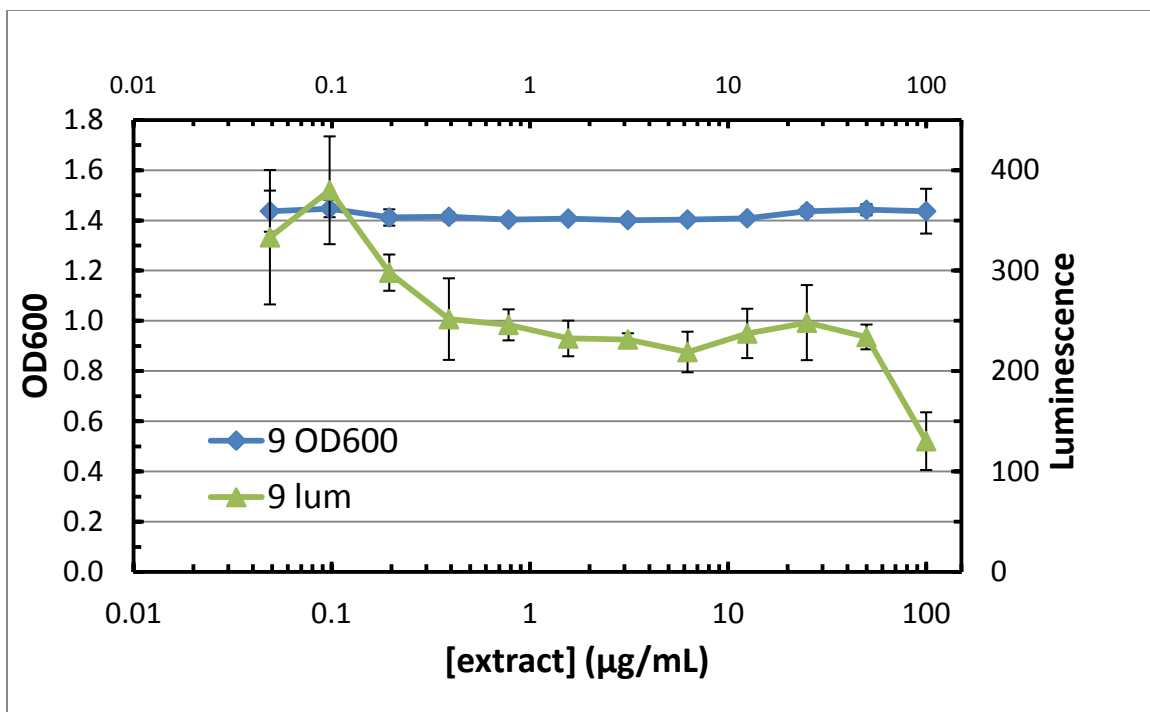


**Figure 41.** Fraction 9 dissolved in broth and 2% DMSO in the gene reporter assay. Luminescence and OD600 were plotted as a function of concentration.

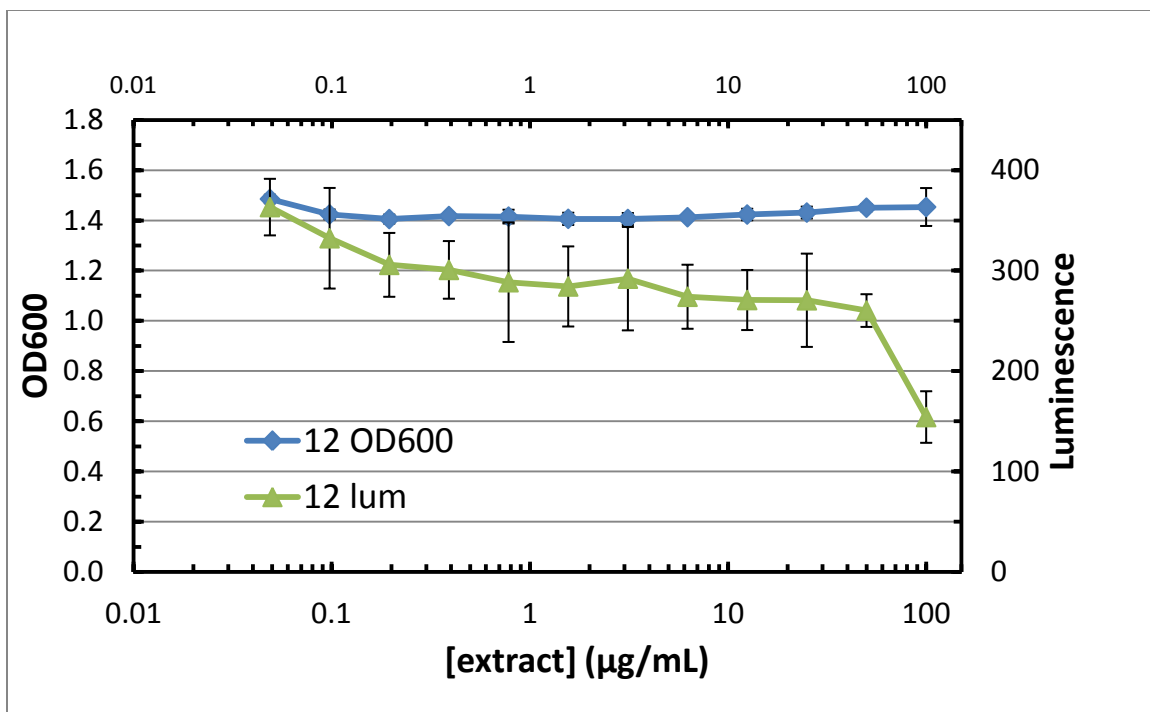


**Figure 42.** Fraction 12 dissolved in broth and 2% DMSO in the gene reporter assay. Luminescence and OD600 were plotted as a function of concentration.

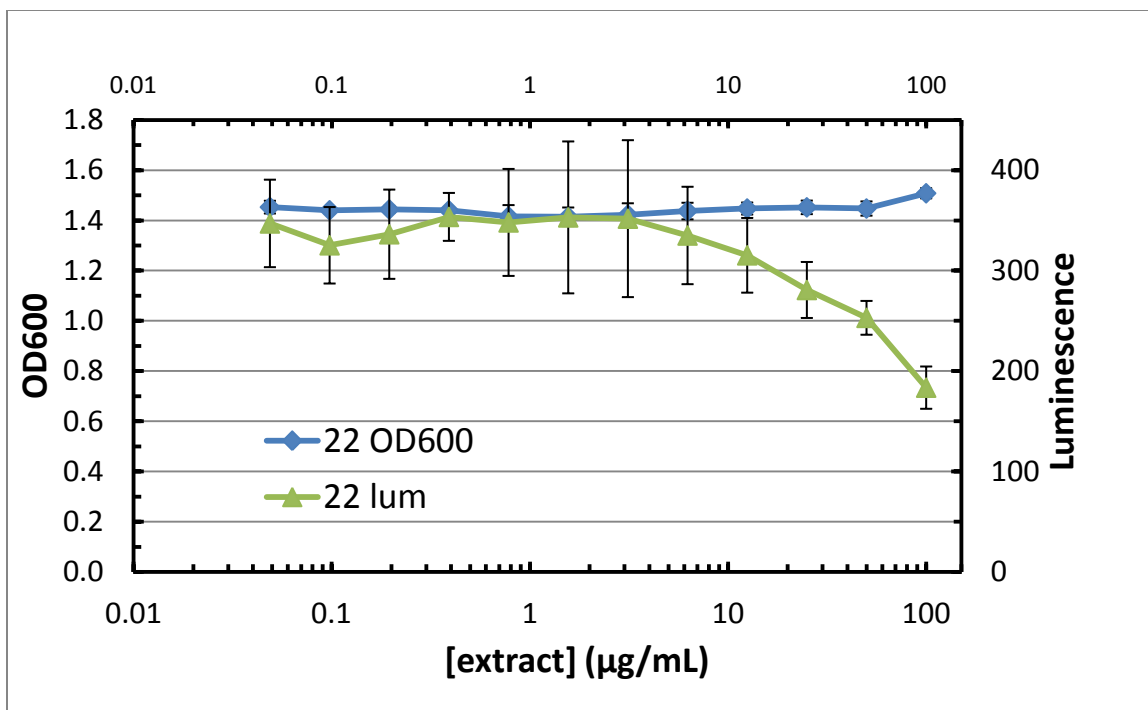


**Figure 43.** Fraction 4 dissolved in broth and 2% DMSO in the gene reporter assay. Luminescence and OD600 were plotted as a function of concentration.

As the concentration of Fractions 9 and 12 and 22 increased, the luminescence decreased while the OD600 did not vary suggesting a quorum quenching effect and not an antimicrobial effect (**Figures 41-43**). In the 96-well plate assay, fraction 9, 12, and 22 also showed quorum quenching activity without lowering the absorbance (**Figure 34**). The verification of these results using the *lux* gene reporter assay confirmed the validity of AIP I inhibition assay as a means to evaluate quorum quenching.

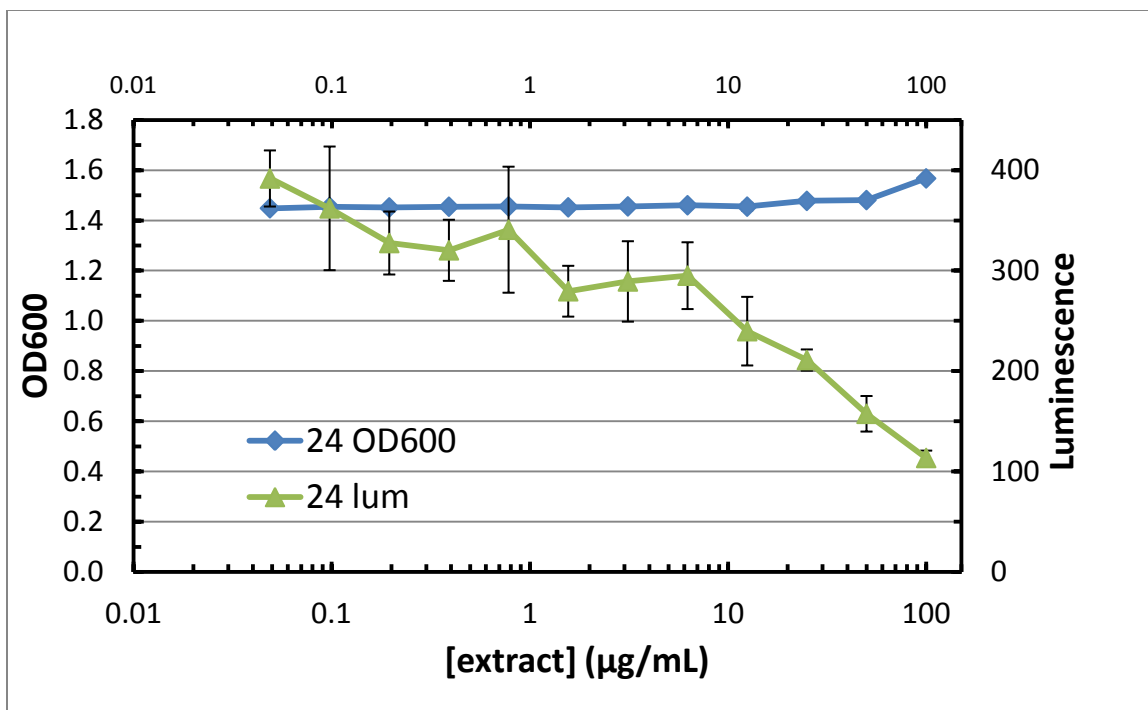


**Figure 44.** Fraction 24 dissolved in broth and 2% DMSO in the gene reporter assay. Luminescence and OD600 were plotted as a function of concentration.

Interestingly, as fraction 24 (Figure 44) increased in concentration, the luminescence decreased while no antimicrobial activity was observed. This did not correspond with the 96-well assay results. The reason for this discrepancy is most likely due to low concentrations of the active constituent in Fraction 24. In the *lux* gene reporter assay, tests were performed at a range of concentrations, whereas the 96-well plate assay, which was based on analytical HPLC separation, the concentration range of each well is between 0.01 – 2.00 µg/mL which is at much lower concentrations. Based on the fluorescence assay fraction 24 is of interest in disrupting the Agr quorum sensing pathway.

#### **4.4.4 Large scale bioactivity guided fractionation of *Hydrastis canadensis***

The goal of this experiment was to isolate the constituents in a large methanol extraction of *Hydrastis canadensis* that were responsible for the AIP I inhibition observed in the previous section. From a flash chromatography separation on the silica gel column, a total of 9 pooled fractions were collected and tested for AIP suppression (**Figure 45**). It was determined fractions 1, 2, 3, and 4 caused significant suppression of AIP based on single factor (p-values, 0.02, 0.01, 0.03, 0.04 respectively). Therefore, fraction 2 was subjected to a second stage of fractionation using a hexane:ethylacetate:methanol gradient as described in Section **4.3.3**.<sup>112</sup>

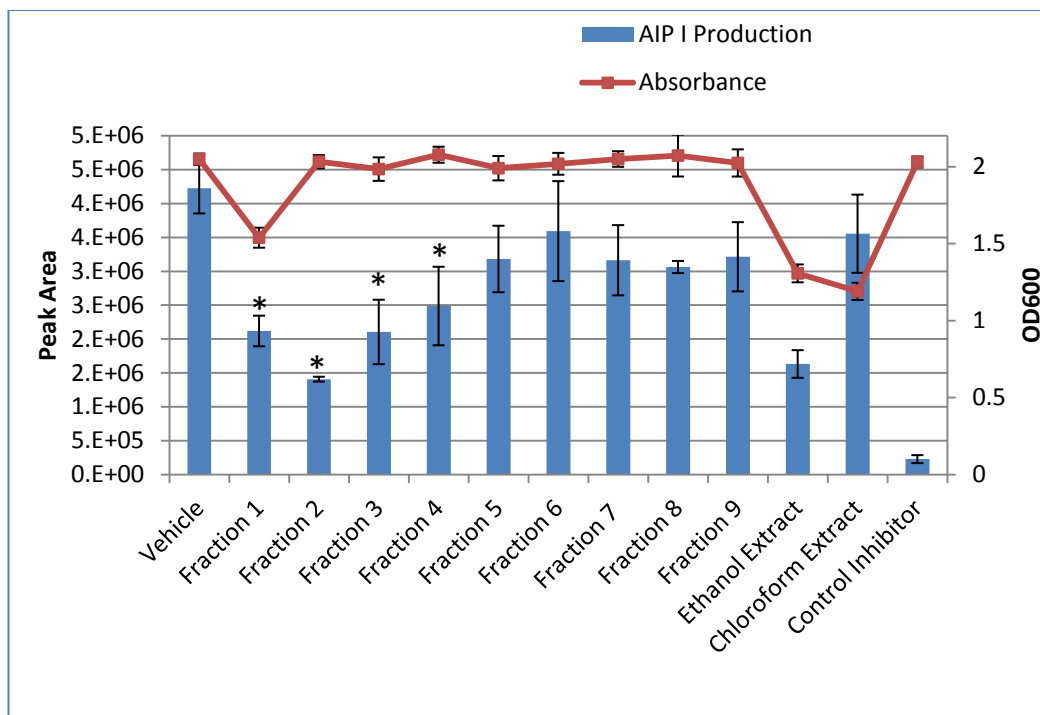


**Figure 45. Suppression of AIP I production by fractions pooled from the flash chromatography separation with hexane:chloroform:methanol with an ethanolic aerial extract.** Fractions 1,2,3, and 4 were determined to be partial AIP I inhibitors. Fraction 2 contained the majority of compounds hypothesized as quorum quenchers from the study described in Section 4.4.3.

The fractionation process using hexane:ethylacetate:methanol of fraction 2 yielded a total of 13 subfraction (Figure 46). The results from this assay showed subfractions 3-9 to be bioactive by being statistically lower than the vehicle control using single factor ANOVA analysis with p value < 0.05 and fractions 11-13 to be inactive in suppressing the production of AIP I. Further stages of separation are necessary to verify the constituents responsible for activity.

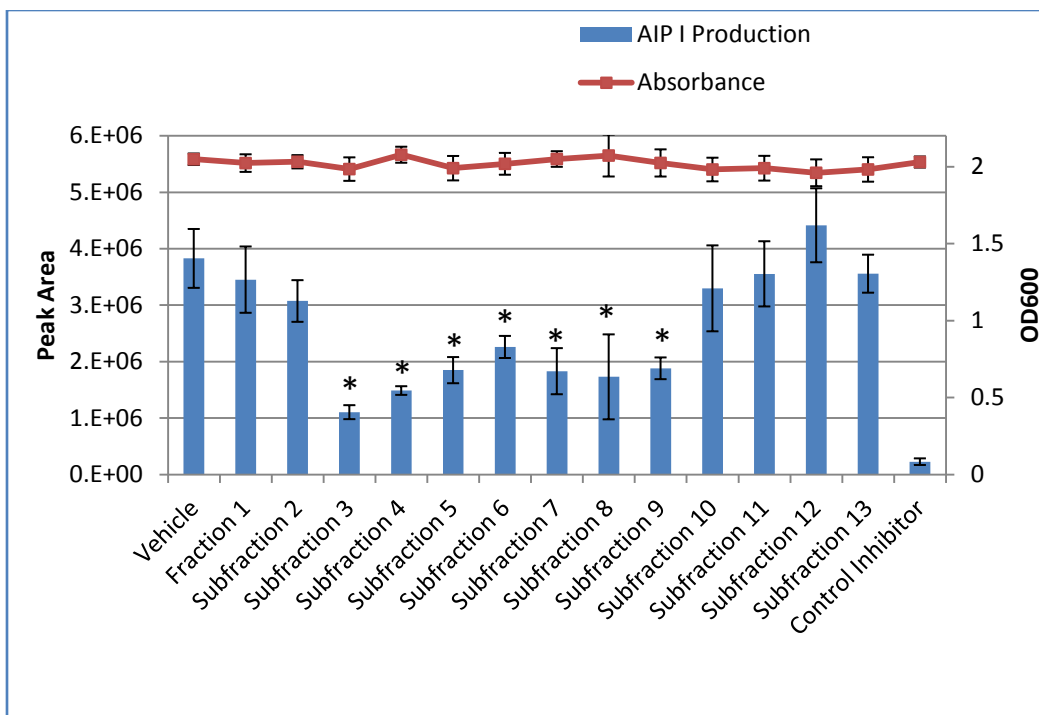


**Figure 46. Suppression of AIP I production in the Agr quorum sensing pathway of MRSA-AH-1263.** Bioactivity was determined based on the lower total peak area for the selected ion chromatogram corresponding to AIP I. Subtractions 3-9 and the positive control (AIP II) caused a statistically significant suppression in AIP I production compared to the vehicle control. Statistical analysis was based on single variable single factor ANOVA analysis with p value < 0.5 considered significant.

#### 4.5 Conclusion

Through the implementation of UPLC-HRMS it was determined that the production of AIP I from MRSA can be directly monitored by analyzing the bacteria culture supernatant. Compared to previous methods, this methodology is an improvement by allowing a product of the Agr quorum sensing pathway to be directly monitored and quantified as opposed to a downstream bioluminescence reporter in the *lux* assay. Also, by establishing a calibration curve to measure the concentrations this



method has the potential to be used to determine bioactive levels of AIP I necessary to elicit toxin production and pathogenesis *in vivo*.

By growing MRSA in a time course study and measuring absorbance and the AIP I levels in the supernatant as a function of time, the conditions that optimized AIP I production were established. This enabled measurements to be made of the suppression of AIP I production when MRSA was combined with extracts from natural products, thereby identifying those extracts with quorum quenching activity. The methodology could be implemented on a variety of natural products and pure compounds to help identify possible therapeutic agents that could be employed to inhibit pathogenesis of MRSA.

Through the separation of crude extracts from natural products into a 96-well plate, key constituents within a complex extract could be identified as quorum quenchers. This assay can prevent the isolation of already known compounds while at the same time identify interesting candidates for bioactivity. Specifically for *Hydrastis canadensis*, the antimicrobial compounds were separated from the quorum quenching fractions preventing the possibility of false positives. In the future this could make the isolation process more efficient by applying a mass-guided separation methodology to isolate compounds of interest as opposed to performing traditional bioactivity-guided separation. It is important to note, however, that a limitation of MS is the inability to confirm structure for truly unknown compounds. Searches against the Dictionary of Natural Products returned many hits for some compounds, and no hits for others.

Neither of these results makes confirmation of structure possible, and large scale isolation for NMR analysis is still necessary for structure elucidation and confirmation of biological activity.

Based on the 96-well screening of the crude natural product extracts we were, however, able to determine whether a large scale isolation process was worthwhile. First, we were able to identify if there was any bioactivity associated with the extract. Second, by taking the OD600 we were able determine whether or not that activity is antimicrobial or quorum quenching. Importantly, quorum quenching compounds could be separated by antimicrobial compounds, which would otherwise have confounded the results of the quorum quenching assay. Third, we could identify likely candidates that correspond to the activity by analyzing the mass profiles of each well, and fourth and finally, we could use accurate mass to determine whether those compounds have already been identified as components of *H. canadensis*.

Future aims in this research include the isolation and structure elucidation of quorum quenchers from *H. canadensis*. Through the established methodology, bioactivity can be measured through the fractionation process until a single compound is isolated. Furthermore, many different natural product extracts are being tested for quorum quenching activity using the 96-well plate assay.

In addition to identifying specific compounds, the mode of action in which *H. canadensis* and other AIP I inhibitors are being investigated. Through using various MRSA strains with deleted AgrC or AgrB receptors, it can be determined if the

exportation of AIP I and/or the reuptake of AIP I is being inhibited. Better understanding of the mode of action in which quorum quenchers inhibit AIP I production could facilitate the development of new therapeutic agents to treat MRSA infections.

## REFERENCES

1. Scott, Douglas R. The direct medical costs of healthcare-associated infections in U.S. hospitals and the benefits of prevention. *Public Health Rep* **2007**: 1-16.
2. Miller LG, Diep BA. Clinical practice: colonization, fomites, and virulence: rethinking the pathogenesis of community-associated methicillin- resistant *S. aureus* infection. *Clin Infect Dis*. **2008**:752–60.
3. Thomas C.G.A. (1988) *Medical Microbiology*. Balliere Tindall, London.
4. Miller LG, Diep BA. Clinical practice: colonization, fomites, and virulence: rethinking the pathogenesis of community-associated methicillin- resistant *S. aureus* infection. *Clin Infect Dis*. **2008**:752–60.
5. Burnet M. & White D.O. (1972) *The Natural History of Infectious Disease*. Cambridge University Press. Cambridge.
6. Mims C.A. (1990) *The Pathogenesis of Infectious Disease*. Academic Press, London.
7. Patel AH, Nowlan P, Weavers ED, Foster T. Virulence of protein A-deficient and alpha-toxin-deficient mutants of *S. aureus* isolated by allele replacement. *Infect. Immun*. **1987** 55: 3103–10.
8. Barber M. Methicillin-resistant staphylococci. *J Clin Pathol*. **1961**: 385–93.
9. Crisostomo MI, et al. The evolution of methicillin resistance in *Staphylococcus aureus*: similarity of genetic backgrounds in historically early methicillin-susceptible and -resistant isolates and contemporary epidemic clones. *Proc Natl Acad Sci U S A*. **2001**: 9865–70.
10. O'Brien FG, et al. Diversity among community isolates of methicillin-resistant *S. aureus* in Australia. *J Clin Microbiol*. **2004**: 3185–90.
11. Selwyn S. (Hospital infection: the first 50 years. *Journal of Hospital Infection* 18 (Suppl. A), **1991**: 5-63.

12. McDermott W. The problem of staphylococcal infection. *British Medical Journal* 2, **1956**: 838-840.
13. Colebrooke L. Infection acquired in hospital. *Lancet* ii, **1955**: 885-891.
14. Shanson D.C. Control of a hospital outbreak of methicillin resistant *S. aureus*: the value of an isolation ward. *Journal of Hospital Infection* , **1985**: 285-292.
15. Cafferkey M.T., Coleman D., McGrath B., Keane CT. & Hotne R. *Staphylococcus aureus* in Dublin. *Lancet* ii, **1985**: 705-708.
16. Lacey R.W. Multi-resistant *S. aureus* — a suitable case for inactivity? *Journal of Hospital Infection* 9,**1987**: 103-109.
17. Casewell M.W. & Phillips I. Hands as a route of transmission for *Klebsiella* species. *British Medical Journal*. **1977**: 12-17.
18. Casewell M.W. & Phillips I. Epidemiological patterns of bacteria colonisation and infection in an intensive care unit. *Lancet* ii, **1978**. 234-245
19. Casewell M.W., Dalton N4.D., Webster M. & Phillips I. Gentamicin -resistant *Klebsiella aerogenes* on a urological ward. *Lancet* ii, **1977**: 444-446.
20. Keane C.T., Coleman D.C. & Cafferkey M. (1991) Methicillin-resistant *S. aureus*: a reappraisal. *Journal of Hospital Infection*, **1991**: 147- 152.
21. Phillips I. Epidemic potential and pathogenicity in outbreaks of infection with EMRSA and EMREC. *Journal of Hospital Infection* 18 (Suppl. A),**1991**: 197-201.
22. Casewell M.W. & Hill R.I.R. The carrier state: methicillin resistant *S. aureus*. *Journal of Antimicrobial Chemotherapy* (Suppl. A),**1986**: 1-21.
23. Richards MJ, Edwards JR, Culver DH, Gaynes RP. Nosocomial infections in medical intensive care units in the United States. *Crit Care Med* **1999**: 887-92.
24. Strausbaugh LJ, Crossley KB, Nurse BA, Thrupp LD Antimicrobial resistance in long-term-care facilities. *Infect Control Hosp Epidemiol* **1997**: 129-40.

25. Crum NF, Lee RU, Thornton SA, Stine OC, Wallace MR, Barrozo C, et al. Fifteen-year study of the changing epidemiology of methicillin-resistant *S. aureus*. *Am J Med* **2006**: 943–51.
26. Lowy FD *S. aureus* infections. *N Engl J Med* **1998**: 520–32.
27. Kuehnert MJ, Hill HA, Kupronis BA, Tokars JI, Solomon SL, Jernigan DB. Methicillin-resistant *S. aureus* hospitalizations, United States. *Emerg Infect Dis* **2005**: 868–72.
28. Centers for Disease Control and Prevention National Nosocomial Infections Surveillance (NNIS) system report, data summary from January 1992 through June 2004, issued October 2004. *Am J Infect Control* **2004**: 470–85.
29. Klein E., Smith D. L. & Laxminarayan R. Hospitalizations and deaths caused by methicillin-resistant *S. aureus*, United States, 1999–2005. *Emerging Infectious Diseases*, **2007**: 1840.
30. Klein EY, Sun L, Smith DL, Laxminarayan R. The changing epidemiology of methicillin-resistant *S. aureus* in the United States: a national observational study. *Am J Epidemiol*. **2013**: 666-74.
31. Carleton HA, Diep BA, Charlebois ED, Sensabaugh GF, Perdreau-Remington F. Community-adapted methicillin-resistant *S. aureus* (MRSA): population dynamics of an expanding community reservoir of MRSA. *J Infect Dis*, **2004**: 1730–8.
32. Martone WJ, Jarvis WR, Edwards JR, Culver D, Haley RW. Incidence and nature of endemic and epidemic nosocomial infections. In: Bennett JV, Brachman PS, editors. *Hospital infections*, 4th ed. Philadelphia: Lippincott Williams and Wilkins; **1998**: 461–76.
33. Cosgrove SE, Carmeli Y. The impact of antimicrobial resistance on health and economic outcomes. *Clin Infect Dis* **2003**: 1433–7.
34. McHugh CG, Riley LW Risk factors and costs associated with methicillin-resistant *S. aureus* bloodstream infections. *Infect Control Hosp Epidemiol* **2004**: 425–30.

35. Tenover FC, Hughes JM. The challenges of emerging infectious diseases: development and spread of multiply resistant bacterial pathogens. *JAMA* **1996**: 300-4.
36. Bridges BA. Hypermutation in bacteria and other cellular systems. *Philos Trans R Soc Lond B Biol Sci* **2001**: 29-39.
37. Podglajen I, Breuil J, Collatz E. Insertion of a novel DNA sequence, 1S1186, upstream of the silent carbapenemase gene *cfiA*, promotes expression of carbapenem resistance in clinical isolates of *Bacteroides fragilis*. *Mol Microbiol*, **1994**: 105-14.
38. Falkow S. Infectious multiple drug resistance. London: Pion Press; **1975**.
39. Medeiros AA. Evolution and dissemination of  $\beta$ -lactamases accelerated by generations of  $\beta$ -lactam antibiotics. *Clin Infect Dis* **1997**: 19-45.
40. Monnet DL, Biddle JW, Edwards JR, et al. Evidence of interhospital transmission of extended-spectrum  $\beta$ -lactam—resistant *Klebsiella pneumoniae* in the United States, 1986 to 1993. The National Nosocomial Infections Surveillance System. *Infect Control Hosp Epidemiol* **1997**: 492-8.
41. Porter RD. Modes of gene transfer in bacteria. In: Kucherlapi R, Smith GR, editors. Genetic recombination. Washington, DC: American Society for Microbiology; **1988**: 1-42.
42. DeFlaun MF, Levy SB. Genes and their varied hosts. In: Levy SB, Miller RV, editors. Gene transfer in the environment. New York: McGraw-Hill; **1991**: 1-32.
43. Forbes BA, Schaberg DR. Transfer of resistance plasmids from *Staphylococcus epidermidis* to *S. aureus*: evidence for conjugative exchange of resistance. *J Bacteriol*, 1983: 627-31.
44. Davies J. Inactivation of antibiotics and the dissemination of resistance genes. *Science*, **1994**: 375-82.
45. Kirst HA, Thompson DG, Nicas TI. Historical yearly usage of vancomycin. *Antimicrob Agents Chem*, **1998**: 1303-4.

46. Archibald L, Phillips L, Monnet D, et al. Antimicrobial resistance in isolates from inpatients and outpatients in the United States: increasing importance of the intensive care unit. *Clin Infect Dis*, **1997**: 211-5.
47. Ploy MC, Grelaud C, Martin C, de Lumley L, Denis F. First clinical isolate of vancomycin-intermediate *S. aureus* in a French hospital. *Lancet*, **1998**: 1212.
48. Davies J, Davies D. Origins and evolution of antibiotic resistance. *Microbiol Mol Biol Rev.***2010**: 417–33.
49. Alekshun MN, Levy SB. Molecular mechanisms of antibacterial multidrug resistance. *Cell.***2007**: 1037–50.
50. Kumar A, Schweizer HP. Bacterial resistance to antibiotics: active efflux and reduced uptake. *Adv Drug Deliv Rev.* **2005**: 1486–513.
51. Kumar A, Schweizer HP. Bacterial resistance to antibiotics: active efflux and reduced uptake. *Adv Drug Deliv Rev.* **2005**: 1486–513.
52. DeMarco CE, Cushing LA, Frempong-Manso E, et al. Efflux-related resistance to norfloxacin, dyes, and biocides in bloodstream isolates of *S. aureus*. *Antimicrob Agents Chem***2007**: 3235-9.
53. Schmitz FJ, Hertel B, Hofmann B, et al. Relationship between mutations in the coding and promoter regions and the *norA* genes in 42 unrelated clinical isolates of *S. aureus* and the MICs of norfloxacin for these strains. *J Antimicrob Chem.* **1998**: 561–3.
54. Yoshida H, Bogaki M, Nakamura S, et al. Nucleotide sequence and characterization of the *S. aureus* *norA* gene, which confers resistance to quinolones. *J Bacteriol.* **1990**: 6942–9.
55. Kaatz GW, Seo SM. Inducible *NorA*-mediated multidrug resistance in *S. aureus*. *Antimicrob Agents Chemother.* **1995**: 2650–5.
56. Kaatz GW, Seo SM. Mechanisms of fluoroquinolone resistance in genetically related strains of *S. aureus*. *Antimicrob Agents Chemother.* **1997**: 2733–7.
57. Couto I, Costa SS, Viveiros M, et al. Efflux-mediated response of *Staphylococcus aureus* exposed to ethidium bromide. *J Antimicrob Chemother.* **2008**:504–13.



58. Kaatz GW, Seo SM, O'Brien L, et al. Evidence for the existence of a multidrug efflux pump transporter distinct from NorA in *Staphylococcus aureus*. *Antimicrob Agents Chemother*. **2000**: 1404–6.
59. Truong-Bolduc QC, Dunman PM, Strahilevitz J, et al. MgrA is a multiple regulator of two new efflux pumps in *S. aureus*. *J Bacteriol*. **2005**: 2395–405.
60. Truong-Bolduc QC, Strahilevitz J, Hooper DC. NorC, a new efflux pump regulated by MgrA of *S. aureus*. *Antimicrob Agents Chemother*. **2006**: 1104–7.
61. Truong-Bolduc QC, Bolduc GR, Okumura R, et al. Implication of the NorB efflux pump in the adaptation of *S. aureus* to growth at acid pH and in resistance to moxifloxacin. *Antimicrob Agents Chemother*. **2011**: 3214–9.
62. Truong-Bolduc QC, Dunman PM, Eidem T, et al. Transcriptional profiling analysis of the global regulator NorG, a GntR-like protein of *S. aureus*. *J Bacteriol*. **2011**: 6207–14.
63. Kaatz GW, McAleese F, Seo SM. Multidrug resistance in *S. aureus* due to overexpression of a novel multidrug and toxin extrusion (MATE) transport protein. *Antimicrob Agents Chemother*. **2005**: 1857–64.
64. Kaatz GW, McAleese F, Seo SM. Multidrug resistance in *S. aureus* due to overexpression of a novel multidrug and toxin extrusion (MATE) transport protein. *Agents Chemother Antimicrob*. **2005**: 1857–64.
65. Huang J, O'Toole PW, Shen W, et al. Novel chromosomally encoded multidrug efflux transporter MdeA in *S. aureus*. *Antimicrob Agents Chemother*. **2004**: 909–17.
66. Narui K, Noguchi N, Wakasugi K, et al. Cloning and characterization of a novel chromosomal drug efflux gene in *S. aureus*. *Biol Pharm Bull*. **2002**: 1533–6.
67. Schmitz F-J, Fluit AC, Lückefahr M, et al. The effect of reserpine, an inhibitor of multidrug efflux pumps, on the in-vitro activities of ciprofloxacin, sparfloxacin and moxifloxacin against clinical iso-lates of *S. aureus*. *J Antimicrob Chemother*. **1998**: 807–10.

68. Frempong-Manso E, Raygada JL, DeMarco CE, et al. Inability of a reserpine-based screen to identify strains overexpressing efflux pump genes in clinical isolates of *S. aureus*. *Int J Antimicrob Agents*. **2009**: 360–3.
69. Costa SS, Falcão C, Viveiros M, et al. Exploring the contribution of efflux on the resistance to fluoroquinolones in clinical isolates of *S. aureus*. *BMC Microbiol*. **2011**: 229–241.
70. Martins M, Viveiros M, Couto I, et al. Identification of efflux pump-mediated multidrug-resistant bacteria. Ethidium Bromide-Agar Cartwheel Method. *In Vivo*. **2011**:171–8.
71. Gillespie SH, McHugh TD, Viveiros M, Rodrigues L, Martins M, et al. In Evaluation of efflux activity of bacteria by a semi-automated fluorometric system. New York: Humana Press; Antibiotic Resistance Protocols; 2010: 159–72.
72. Newman, D. J., Cragg, G. M. & Snader, K. M. Natural products as a source of new drugs over the period 1981–2002. *J. Nat. Prod*. **2003**: 19-34.
73. Chanda S, Rakholiva K. Indian Combination therapy: Synergism between natural plant extracts and antibiotics against infections diseases. Science against Microbial Pathogens: Communicating Current Research and Technological Advances, I. Spain: Formatex Research Center, **2011**: 520-529.
74. Projan, S. J. Infectious diseases in the 21st century: increasing threats, fewer new treatments and a premium on prevention. *Cur. Opin. Pharmacol*. **2003**: 457–458.
75. Projan S. J. Why is big pharma getting out of antibacterial drug discovery? *Cur. Opin. Microbiol*. **2003**: 427–30.
76. Chanda S, Rakholiva K. Indian Combination therapy: Synergism between natural plant extracts and antibiotics against infections diseases. Science against Microbial Pathogens: Communicating Current Research and Technological Advances, I. Spain: Formatex Research Center, **2011**: 520-529.
77. Novick R. Properties of cryptic high-frequency transducing phage of *S. aureus*. *Virology* **1967**: 155-166.
78. H. Wagner, G. U.-M., Synergy research: Approaching a new generation of phytopharmaceuticals. *Phytomedicine* **2009**: 97-110.

79. Greco WR, Bravo G, Parsons JC. The search for synergy: a critical Review from response surface perspective. *Pharmacol Rev* **1995**: 331–85.
80. Victor Lorian, M. D., *Antibiotics in Laboratory Medicine*. Fifth ed.; Lippincott Williams & Wilkins: New York, **2005**.
81. Dennis McKenna, K. J., Kerry Hughes, Sheila Humprey, *Botanical Medicines: The Desk Reference for Major Herbal Supplements*. 2 ed.; Haworth Herbal Press: New York, **2002**.
82. Lesley Braun, M. C., *Herbs & Natural Supplements: An evidence-based guide*. 3 ed.; Churchill Livingstone Elsevier: Australia, **2010**.
83. Moerman, D., *Native American Medicinal Plants An Ethnobotanical Dictionary*. Timber Press: Portland, **2009**
84. Chi-Li Kuo, C.-W. C., Tsung-Yun Liu, The Anti-inflammatory potential of berberine in vitro and in vivo. *Cancer Letters* **2004**: 127-137.
85. Jacquelyn R. Villinski, E. R. D., Hee-Byung Chai, John M. Pezzuto, Cindy K. Angerhofer, Stefan Gafner, Antibacterial activity and alkaloid content of *Berberis thunbergii*, *Berberis vulgaris* and *Hydrastis canadensis*. *Pharmaceutical Biology* **2003**: 551-557.
86. Bannerman JE. Goldenseal in world trade: pressures and potentials. *HerbalAgram* **1997**: 251-53.
87. Wagner H, Ulrich-Merzenich G. Synergy research: approaching a new generation of phytopharmaceuticals. *Phytomedicine* **2009**: 97-110.
88. Blumenthal M. Herb market levels after five years of boom. *Herbalgram* **1999**: 64-65
89. Upton R. Goldenseal root *Hydrastis canadensis*; Standards of analysis, quality control, and therapeutics. Santa Cruz: American Herbal Pharmacopocia **2001**.
90. Cech RA. Making plant medicine. Williams: Horizon Herbs; **2000**: 276.

91. No author. Methods for dilution antimicrobial susceptibility tests for bacteria that grow aerobically; approved standard, Vol. 26, 7<sup>th</sup> edition. Wayne: Clinical and Laboratory Standards Institute; **2006**: M7-A70.
92. Eliopolous GM, Moellering RC. Antimicrobial combinations. In: Lorian V, editor. Antibiotics in laboratory medicine. Baltimore, MD: Williams and Wilkins; **1996**: 330-396.
93. Paulsen, I. T. Multidrug efflux pumps and resistance regulation and evolution. *Current Opinion Microbiology*. **2003**: 6, 446-451.
94. McKeegan, K.S. & Walmsley, A. R. Structure and function of efflux pumps that confer to resistance to drugs. *Biochemistry Journal* **2003**: 313-338.
95. Ian T. Paulsen, M. H. B., Ronald A. Skurray, Proton-Dependent Multidrug Efflux Systems. *Microbiological Reviews* **1996**: 575-608.
96. Ian T. Paulsen, M. H. B., Ronald A. Skurray, Proton-Dependent Multidrug Efflux Systems. *Microbiological Reviews* **1996**: 575-608.
97. Carmen E. Demarco, L. A. C., Emmanuel Frempong-Manso, Susan M. Seo, Tinevimbo A. A. Jaravaza, and Glenn W. Kaatz, Efflux-Related Resistance to Norfloxacin, Dyes, and Biocides in Bloodstream Isolates of *Staphylococcus aureus*. *Antimicrobial Agents and Chemotherapy* **2007**: 3235-3239.
98. Carmen E. Demarco, L. A. C., Emmanuel Frempong-Manso, Susan M. Seo, Tinevimbo A. A. Jaravaza, and Glenn W. Kaatz, Efflux-Related Resistance to Norfloxacin, Dyes, and Biocides in Bloodstream Isolates of *Staphylococcus aureus*. *Antimicrobial Agents and Chemotherapy* **2007**: 3235-3239.
99. Marcin Kolaczowski, A. K., Frank R. Stermitz, Modulation of the Antifungal Activity of New Medicinal Plant Extracts Active on *Candida glabrata* by the Major Transporters and Regulators of the Pleiotropic Drug-Resistance Network in *Saccharomyces cerevisiae*. *Microbial Drug Resistance* **2009**: 11-17.
100. Ettefagh, K. A.; Burns, J. T.; Junio, H. A.; Kaatz, G. W.; Cech, N. B., Goldenseal (*Hydrastis canadensis* L.) Extracts Synergistically Enhance the Antibacterial Activity of Berberine via Efflux Pump Inhibition. *Planta Medica* **2011**: 835-840.

101. Weijia Kong, J. W., Parveen Abidi, Meihong Lin, Satoru Inaba, Cong Li, Yanling Wang, Zizheng Wang, Shuyi Si, Huaining Pan, Shukui Wang, Jingdan Wu, Zhuorong Li, Jingwen Liu, Jiang-Dong Jiang, Berberine is a Novel Cholesterol-140 Lowering Drug Working through a Unique Mechanism Distinct from Statins. *Nature Medicine* **2004**: 1344-1352.
102. Parveen Abidi, W. C., Fredric B. Kraemer, Hai Li, Jingwen Liu, The medicinal plant goldenseal is a natural LDL-lowering agent with multiple bioactive components and new action mechanisms. *Journal of Lipid Research* **2006**: 2134-2147.
103. Parveen Abidi, W. C., Fredric B. Kraemer, Hai Li, Jingwen Liu, The medicinal plant goldenseal is a natural LDL-lowering agent with multiple bioactive components and new action mechanisms. *Journal of Lipid Research* **2006**: 2134-2147.
104. Parveen Abidi, W. C., Fredric B. Kraemer, Hai Li, Jingwen Liu, The medicinal plant goldenseal is a natural LDL-lowering agent with multiple bioactive components and new action mechanisms. *Journal of Lipid Research* **2006**: 2134-2147.
105. Frank R. Stermitz, P. L., Jeanne N. Tawara, Lauren A. Zenemicz, Kim Lewia, Synergy in a medicinal plant: Antibimicrobial action of berberine potentiated by 5'-methoxyhydnocarpin, a multi-drug pump inhibitor. *Proceedings of the National Academy of Sciences* **2000**: 1433-1437.
106. Junio, H. A.; Sy-Cordero, A. A.; Etefagh, K. A.; Burns, J. T.; Micko, K. T.; Graf, T. N.; Richter, S. J.; Cannon, R. E.; Oberlies, N. H.; Cech, N. B., Synergy-Directed Fractionation of Botanical Medicines: A Case Study with Goldenseal (*Hydrastis canadensis*). *Journal of Natural Products* **2011**: 1621-1629.
107. Jefferson KK, Goldmann DA, Pier GB. Use of confocal microscopy to analyze the rate of vancomycin penetration through *S. aureus* biofilms. *Antimicrob Agents Chemother.* **2005**: 2467-73.
108. Jefferson KK, Goldmann DA, Pier GB. Use of confocal microscopy to analyze the rate of vancomycin penetration through *S. aureus* biofilms. *Antimicrob Agents Chemother.* **2005**: 2467-73.
109. Etefagh, K. A.; Burns, J. T.; Junio, H. A.; Kaatz, G. W.; Cech, N. B., Goldenseal (*Hydrastis canadensis* L.) Extracts Synergistically Enhance the Antibacterial Activity of Berberine via Efflux Pump Inhibition. *Planta Medica* **2011**: 835-840.

110. Couto I, Costa SS, Viveiros M, et al. Efflux-mediated response of *Staphylococcus aureus* exposed to ethidium bromide. *J Antimicrob Chemother.* **2008**: 504–13.
111. Frank R. Stermitz, P. L., Jeanne N. Tawara, Lauren A. Zenemicz, Kim Lewia, Synergy in a medicinal plant: Antibimicrobial action of berberine potentiated by 5'-methoxyhydnocarpin, a multi-drug pump inhibitor. *Proceedings of the National Academy of Sciences*, **2000**: 1433-1437.
112. Junio, H. A.; Sy-Cordero, A. A.; Etefagh, K. A.; Burns, J. T.; Micko, K. T.; Graf, T. N.; Richter, S. J.; Cannon, R. E.; Oberlies, N. H.; Cech, N. B., Synergy-Directed Fractionation of Botanical Medicines: A Case Study with Goldenseal (*Hydrastis canadensis*). *Journal of Natural Products* **2011**: 1621-1629.
113. Etefagh, K. A.; Burns, J. T.; Junio, H. A.; Kaatz, G. W.; Cech, N. B., Goldenseal (*Hydrastis canadensis* L.) Extracts Synergistically Enhance the Antibacterial Activity of Berberine via Efflux Pump Inhibition. *Planta Medica* **2011**: 835-840.
114. Junio, H. A.; Sy-Cordero, A. A.; Etefagh, K. A.; Burns, J. T.; Micko, K. T.; Graf, T. N.; Richter, S. J.; Cannon, R. E.; Oberlies, N. H.; Cech, N. B., Synergy-Directed Fractionation of Botanical Medicines: A Case Study with Goldenseal (*Hydrastis canadensis*). *Journal of Natural Products* **2011**, 74, (7), 1621-1629.
115. Richards MJ, Edwards JR, Culver DH, Gaynes RP Nosocomial infections in medical intensive care units in the United States. *Crit Care Med* **1999**: 887–92.
116. R.M. Klevens, M.A. Morrison, J. Nadle, S. Petit, K. Gershman, S. Ray, L.H. Harrison, R. Lynfield, G. Dumyati, J.M. Townes, A.S. Craig, E.R. Zell, G.E. Fosheim, L.K. McDougal, R.B. Carey, S.K. Fridkin, *J. Am. Med. Assoc.* **2007**: 1763.
117. H.F. Chambers, F.R. Deleo, *Nat. Rev. Microbiol.* **2007**: 629.
118. B.T. Tsuji, M.J. Rybak, C.M. Cheung, M. Amjad, G.W. Kaatz, *Diagn. Microbiol. Infect. Dis.* **2007**: 41.
119. Thoendel, M.; Kavanaugh, J. S.; Flack, C. E.; Horswill, A. R., Peptide signaling in the staphylococci. *Chem Rev* **2011**: 117-51.
120. Thoendel, M.; Kavanaugh, J. S.; Flack, C. E.; Horswill, A. R., Peptide signaling in the staphylococci. *Chem Rev* **2011**: 117-51.

121. Hiyas A. Junio<sup>1</sup>, Daniel A. Todd<sup>1</sup>, Keivan A. Etefagh<sup>1</sup>, Brandie M. Ehrmann<sup>1</sup>, Jeffrey S. Kavanaugh<sup>2</sup>, Alexander R. Horswill<sup>2</sup>, and Nadja B. Cech<sup>1</sup> Quantitative Analysis of Autoinducing Peptide I (AIP I) from *Staphylococcus aureus* Cultures using UPLC-HRMS. *Journal of Chrom B.* **2013**: 7-12.
122. Cech, N. B.; Junio, H. A.; Ackermann, L. W.; Kavanaugh, J. S.; Horswill, A. R., Quorum Quenching and Antimicrobial Activity of Goldenseal (*Hydrastis canadensis*) against Methicillin-Resistant *S. aureus* (MRSA). *Planta Medica* **2012**, 78 (14), 1556-1561.
123. Mario Figueroa,<sup>†</sup> Alan K. Jarmusch,<sup>‡</sup> Huzefa Raja,<sup>†</sup> Tamam El-Elimat,<sup>†</sup> Jeffrey S. Kavanaugh,<sup>§</sup> Alexander R. Horswill,<sup>§</sup> R. Graham Cooks,<sup>‡</sup> Nadja B. Cech,<sup>†</sup> and Nicholas H. Oberlies<sup>\*,†</sup> **Fungal Blood: Chemistry, Ambient Mass Spectrometry Imaging by DESI-MS and Quorum Sensing Inhibition of *S. aureus* by the Guttations of a *Penicillium* sp. (G85)** *ACS Chemical Biology* In preparation.
124. Cech, N. B.; Junio, H. A.; Ackermann, L. W.; Kavanaugh, J. S.; Horswill, A. R., Quorum Quenching and Antimicrobial Activity of Goldenseal (*Hydrastis canadensis*) against Methicillin-Resistant *S. aureus* (MRSA). *Planta Medica* **2012**: 1556-1561.
125. The *Dictionary of Natural Products* (DNP). [dnp.chemnetbase.com](http://dnp.chemnetbase.com). Accessed May 2013.